Durham E-Theses

Electrochemical methods for the dechlorination and detection of chilorinated ethenes

Wylie, Lisa A.

ELECTROCHEMICAL METHODS FOR THE DECHLORINATION AND DETECTION OF CHLORINATED ETHENES

LISA A. WYLIE

Thesis submitted as part of the requirement for the degree of Ph.D

UNIVERSITY OF DURHAM
DEPARTMENT OF CHEMISTRY
JANUARY 2003

ELECTROCHEMICAL METHODS FOR THE DECHLORINATION AND DETECTION OF CHLORINATED ETHENES

Lisa A. Wylie

Chlorinated ethenes in the environment are dechlorinated by accepting electrons from electron donors found in nature. Such reductive dechlorination forms the basis of this research into remediation and detection of these compounds in the environment.

The reducing abilities of one of the strongest electron donors known, tetrakis(dimethylamino)ethylene (TDAE), were used to abiotically simulate reductive dechlorination. TDAE was found to form an electron donor-acceptor complex with tetrachloroethene, and to very rapidly reduce trichloroethene and *cis*-dichloroethene via removal of the most positive chlorine.

Microbiological studies of bacteria utilising chlorinated ethenes in their metabolic systems established that Vitamin B_{12} (cyanocobalamin) is of great importance to the dechlorination process, acting as a cofactor for the organism's dehalogenase enzyme. The dechlorination mechanism involves cobalt (I) as the active transition metal in extremely reducing conditions. A series of analytical experiments were undertaken to establish the reductive capability of cobalt (I), both in a simple cobalt salt and in vitamin B12, under reducing conditions. Molasses was used as a hydrogen source and an electron donor in simulation of the biotic process. Results indicate that Vitamin B_{12} is more successful at dechlorination than simple cobalt salts, but neither system presents an ideal method for commercial dechlorination based on current experimental process.

Remediation of environmental tetra- and trichloroethene contamination would be improved by the development of on-line sensors. Glutathione, an intracellular sulfhydryl tripeptide comprising glutamyl, cysteinyl, and glycinyl, bonds with alkyl halides via the thiol group in its cysteine moeity, and displays characteristic redox behaviour, presenting an ideal prospective system for development of a relevant biosensor. Potentiometric and amperometric studies have been carried out to determine the efficacy of the proposed system; results indicate that response to and selectivity for alkyl halides at environmental concentrations can be achieved.

Declaration

The work described herein was carried out in the Department of Chemistry at the University of Durham between October 1999 and September 2002. All the work is my own, unless stated to the contrary, and it has not been submitted for a degree at this or any other university.

Statement of copyright

"Few can foresee whither their road will lead them, till they come to its end."

Legolas Greenleaf, in J.R.R. Tolkien's The Lord of the Rings.

TABLE OF CONTENTS

List of Abbreviations

AE	Auxiliary Electrode
ATP	Adenosine Triphosphate
BBPA	Bis-(1-butylpentyl)adipate
c-DCE	*cis*-Dichloroethene
CE	Capillary Electrophoresis
CV	Cyclic Voltammetry
DPV	Differential Pulse Voltammetry
GR	Glutathione Reductase
GSH	Glutathione (reduced form)
GSSG	Glutathione (oxidised form)
HPCE	High Performance Capillary Electrophoresis
HPLC	High Performance Liquid Chromatography
KTPB	Potassium tetrakis-3,5-bis(trifluoromethyl)phenyl borate
NAD^+	Nicotinamide Adenine Dinucleotide (oxidised)
NADH	Nicotinamide Adenine Dinucleotide (reduced)
NADP	Nicotinamide Adenine Dinucleotide Phosphate (oxidised)
NADPH	Nicotinamide Adenine Dinucleotide Phosphate (reduced)
PCE	Tetra (per) chloroethene
RDE	Rotating Disk Electrode
RE	Reference Electrode
TPAB	Tetrabutylammonium perchlorate
TCE	Trichloroethene
TCNQ	Tetracyanoquinodimethane
TDAE	Tetrakis(dimethylamino)ethylene
t-DCE	*trans*-Dichloroethene
TTF	Tetrathiafulvalene
UV-vis	Ultra Violet – visible light spectroscopy
WE	Working electrode.

List of Illustrations

2

3

5

List of Tables

Acknowledgements

Firstly, I would like to thank my supervisor, Ritu Kataky, for her help, her support and her endless patience with a geologist in a lab-coat. *Dhanyabad.*

Thanks to EPSRC for funding this research.

I thank Professor R.D. Chambers for his helpful insights into TDAE reaction mechanisms.

A big thank you to Dave Bryant, who sorted out some rather niggling mass spec for me.

I'd like to thank the British Council for the opportunity to study for a time in Warsaw University, and Professor Marek Trojanwicz and Dr. Ewa Pobozy for their kindness in making sure I wanted for nothing during my stay.

I am indebted to Dr. Stephanie Blair, Aileen Congreve, Kelly Flook, and Dr. Suzy Kean for being my chemistry teachers, and helping me time and again with the building blocks of practical chemistry. Without their guidance, this could not have been accomplished. Thanks for your patience with my myriad 'stupid questions.'

Mum and Dad, thank you for being prepared, as always, to back me up in whatever crackpot scheme I embark upon. Your love and support give me the courage to take the leap, knowing that if I fall you'll catch me, and there's nothing I can't accomplish with that knowledge. All my love and lots of my gratitude.

Finally, I'd like to thank Alistair, Audrey, Corran, Gill, Kelly, Nik, Simon A, Shelley, Suzy and the Gradsoc hockey and netball gals for their friendship throughout the last three years – their company has been my deliverance, on many occasions, from the burdens of disappointment, self-doubt, and the thousand and one little niggles that go hand-in-glove with research projects. My round, I think.

CHAPTER 1

Introduction

PART 1 – Environmental Pollution by Chlorinated Ethenes

1.1 Industrial Usage of chlorinated aliphatic hydrocarbons

Tetrachloroethene (PCE) and Trichloroethene (TCE) (Fig 1.1) are common industrial solvents used principally as cleaning fluids in the textiles[1,2] and aircraft manufacture and maintenance industries. Trichloroethylene is also used as a chain transfer agent for the production of polyvinyl chloride[2]. Consequently their production ranges into hundreds of millions of pounds (273 million pounds of PCE were produced in the USA in 1993, and 170 million pounds of TCE in 1986[1,2]).

Figure 1.1 The chlorinated ethenes tetrachloroethene and trichloroethene

1.2 Release of chlorinated ethenes to the sub-surface environment

Contamination of groundwater by TCE was first detected in the 1970's[3]. By 1997, US EPA surveys revealed that at least 861 of the 1,428 National Priorities List (NPL) Sites (judged the most seriously contaminated sites within the US) were contaminated with TCE[4]; PCE had been identified in 771 sites[5].

Release of these pollutants to the groundwater environment is predominantly caused in two ways. Firstly, by leaching from old landfill disposal sites. With

11

increasingly strict legislation on pollution (such as the Environment Act 1995 in the UK) coming into effect within the last decade, introducing the requirement to dispose of waste in licensed landfill sites which are properly engineered against leakage, the majority of current contamination is most likely to stem from accidental spills and leaks during use.

1.3 Toxicological effects of TCE and PCE

1.3.1 PCE

The Agency for Toxic Substances and Disease Registry (ATSDR) toxicological profile for PCE[1] lists the following effects:

Acute exposure to PCE in high concentrations can cause death through excessive depression of the respiratory centre or fatal cardiac arrhythmia (PCE is a cardiac epinephrine sensitizer).

Occupational exposure could not be linked to increased mortality in workers due to lack of control studies for alcohol and tobacco. Similarly, while there is evidence for a synergistic effect with smoking in terms of developing cancer, no significant link could be established

1.3.2 TCE

The ATSDR toxicological profile for TCE[2] lists the following effects:

Acute exposure to TCE (in high concentrations) has been shown to cause Central Nervous system depression, drowsiness, headache and nausea. Prolonged exposure to high concentrations (given in reports as greater than $10.9g/m^3$) may cause hepatic or respiratory failure, which may result in coma or death[6].

Occupational exposure (76 – 464mg/m^3) can result in hepatic cancers (EPA) and damage to the liver parenchyma[7]. Neurological disorders have also been observed, such as decreased appetite, insomnia, ataxia, vertigo and short-term memory loss[2].

TCE has recently been classified as likely to cause Cancer within the EU, although literature studies suggest that it is its equivalent epoxide[8], formed as a metabolic breakdown step, which is the cause of TCE's attributed carcinogenicity. Incidence of specific cancers associated with textile workers[2] demonstrates a statistical link, if not a causal one.

1.4 The Groundwater Environment

1.4.1 The Earth's water budget and the hydrological cycle

Approximately 97% of the Earth's water budget is accounted for in the oceans; saline solution unsuitable for human consumption. The remaining 3% is termed 'fresh water', and it is upon this 3% that the sustenance of land life depends. However, further limitations apply – it is estimated that of that 3%, the majority of fresh water (66%, or 2% of the planetary total) is locked into the polar ice caps, and is therefore inaccessible. In essence, we may consider that approximately 1% of the total water present on the planet is available for utilisation[9].

This 1% is the component of the water supply involved in the hydrological cycle (Fig. 1.2), the huge environmental systems which govern the distribution of water between the land and the oceans. These cycles operate on a vast scale; within them, much smaller 'local' systems are in operation, such as the run-off to rivers, or the infiltration of rainfall to groundwater.

Figure 1.2. The Hydrological Cycle

The Hydrological Cycle

Condensation

Precipitation on land

Evaporation from precipitation

Evaporation from land

Evapo-transpiration

Surface Runoff

from water surface

from vegetation

from soil

from resevoir

water table

Infiltration

subsurface flow

surface overflow

Evaporation from ocean

groundwater outflow

ocean

Percolation (deep)

saltwater intrusion

1.4.2 Groundwater

Groundwater is, put simply, water that flows beneath the surface of the land.
Precipitation infiltrates the ground via the soil, filling up any vacant pores/cavities
in the soil layer and in any permeable rocks such as sandstone or limestone
(aquifers), creating large underground flow systems, which can be considered for
the purposes of consumption as subterranean reservoirs. Groundwater accounts
for 0.6 of the 1% available fresh water budget.

1.4.3 The water table

One of the most important features of a groundwater system in terms of pollution is the Water Table. This is the surface at which the pore water pressure is equal to the atmospheric pressure; above this the pores in the rock/soil are vacant. (Fig 1.3)

Figure 1.3. The Water Table.

Ground Surface

Vadose (Unsaturated) Zone

Water Table

Saturated Zone

Soil

Sandstone (Aquifer)

Clay (impermeable)
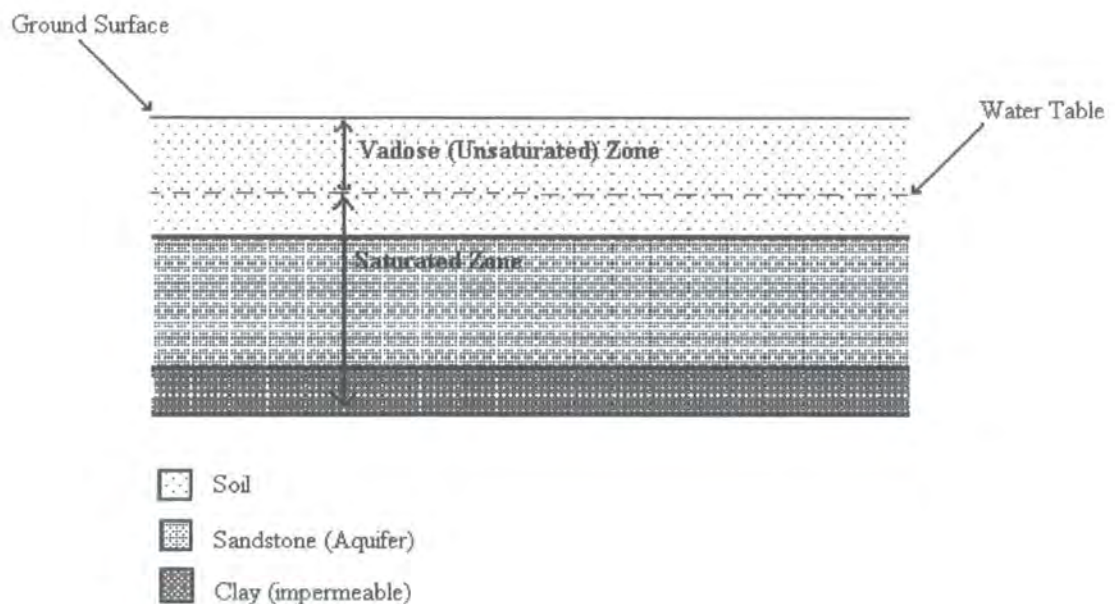
Above the water table, the pores are filled with air, and this section is referred to as the *Vadose* or unsaturated zone, which extends to the surface. Typically, this is a few metres in depth.

However, it is important to note that the depth of the water table *varies with climatic conditions.* If precipitation is persistently heavy, the pores fill up more rapidly than the groundwater can flow and the water table rises, saturating the vadose zone. This rise and fall of the water surface level can result in pollutants being washed into the groundwater.

1.5 Contaminant Pathways

The evaluation of the risk of pollution posing a threat to public welfare is a complex process with many parameters, including toxicity, spatial location, potential exposure methods and chronologies, and chemical 'lifetime' in the environment. However, at its most basic level, assuming some set degree of toxicity, it can be considered analogous to a 'fire triangle'; three components without any one of which it can be reasonably assumed there is no risk of harm. These components can be termed the source, pathway, and target.

Source: the actual introduction of the pollutant to the environment.

Pathway: the route within the environment the pollutant takes to allow exposure to the target.

Target: the person/object that is at risk of harm from the pollutant.

If, for example, TCE contamination is defined in these terms, the source is accidental spillage/poor disposal of solvents from the textile and metal industries, and the target is the public (leaving aside the workforce who by the nature of their employment see a degree of occupational exposure). The pathway is the interconnected network of aquifers from which 35% of the public water supply in England and Wales is drawn[10].

1.6 Contaminant Plumes

As has been noted above, the majority of chlorinated solvent pollution sources are spillages or dumping from industries. When the solvents are introduced to the

environment, they percolate down through the unsaturated zone, and into the groundwater.

Chlorinated solvents are Non-Aqueous Phase Liquids (NAPL's), sparingly soluble in water, and thus the pollutants do not disperse evenly through out the local aquifer system; they collect into pools within the aquifer, frequently becoming absorbed onto the rock/soil matrix. As both PCE and TCE are more dense than water, they tend to sink to the base of the aquifer. Over time, slow dissolution of the solvent occurs, producing a contaminant 'plume' in the downstream direction of the aquifer (Fig.1.4)

Figure 1.4. Development of a contaminant plume over time.
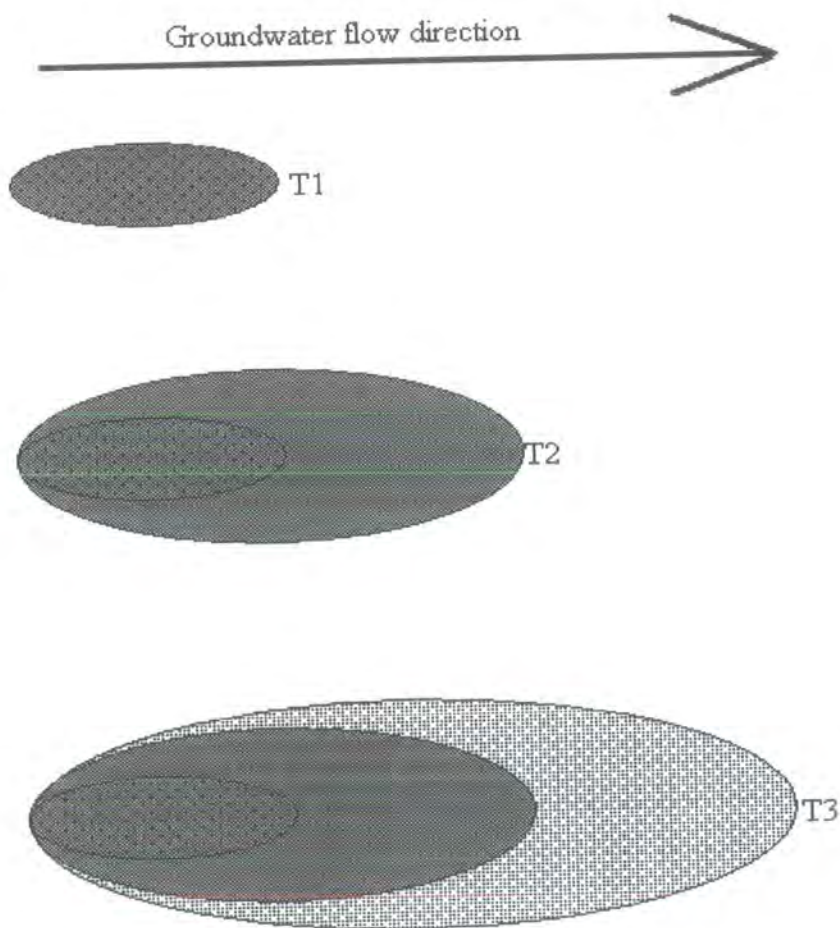
It follows that the further from the point source of contamination, the lower the concentration as the polluted water mixes with fresh water further downstream; contaminant plumes are mapped by defining lines of equal concentration of contaminant in groundwater [11].

1.7 Remediation of Chlorinated Solvent Pollution

Remediation, in engineering terms, is the process of removing the risk of harm from a pollution scenario. Again, in basic terms, there are three principal ways of achieving this. Firstly, and usually most easily, is removal of the source, where the actual pollutant is cut off from the environment. This is generally either achieved by physical relocation, or chemical reaction to render the pollutant inert. The second method is to block the pathway, e.g. by building an impermeable concrete barrier to cut off flow. The third, only employed for those cases deemed impossible to remediate (such as radiation) is to remove the target, relocate the people or objects which may be affected.

In realistic terms, while any one of these methods is equally effective, economics and practicality have directed most research towards chemical and biological clean-up of pollution sources for the following reasons:

1) They present relatively cheap *in situ* alternatives to prohibitively expensive physical removal;

2) The pollutants are broken down into non-toxic by products, rather than being moved to another location;

3) The method allows the site and any existing infrastructure to remain in use throughout.

In environmental engineering, Remediation by Natural Attenuation (RNA) is a standard practice for clean-up at large numbers of chlorinated ethene contaminated sites. Where the chlorinated ethene is a co-contaminant with some suitable organic compound that can act as a substrate, particularly BTEX

(Benzene, Toluene, Ethyl-benzene and Xylene) fuels, the pollutants are left to biodegrade via reductive dechlorination (Fig 1.5). It has been noted, however, that the primary drawback to allowing reductive dechlorination to proceed naturally in the environment is the long time-scale. Another serious consideration is the fact that as the reductive dechlorination process is rate limited at its final step, vinyl chloride to ethene, reductive dechlorination can lead to accumulation of vinyl chloride in the contaminated site, effectively increasing the contamination of the site.

Therefore, it follows that the two main thrusts of research into reductive dechlorination focus on detection of target chlorinated compounds and their daughter compounds in the sub-surface, and enhancement of dechlorination to overcome the problems of incomplete reactions.

Figure 1.5. Reductive dechlorination pathways of tetra- and trichloroethene.
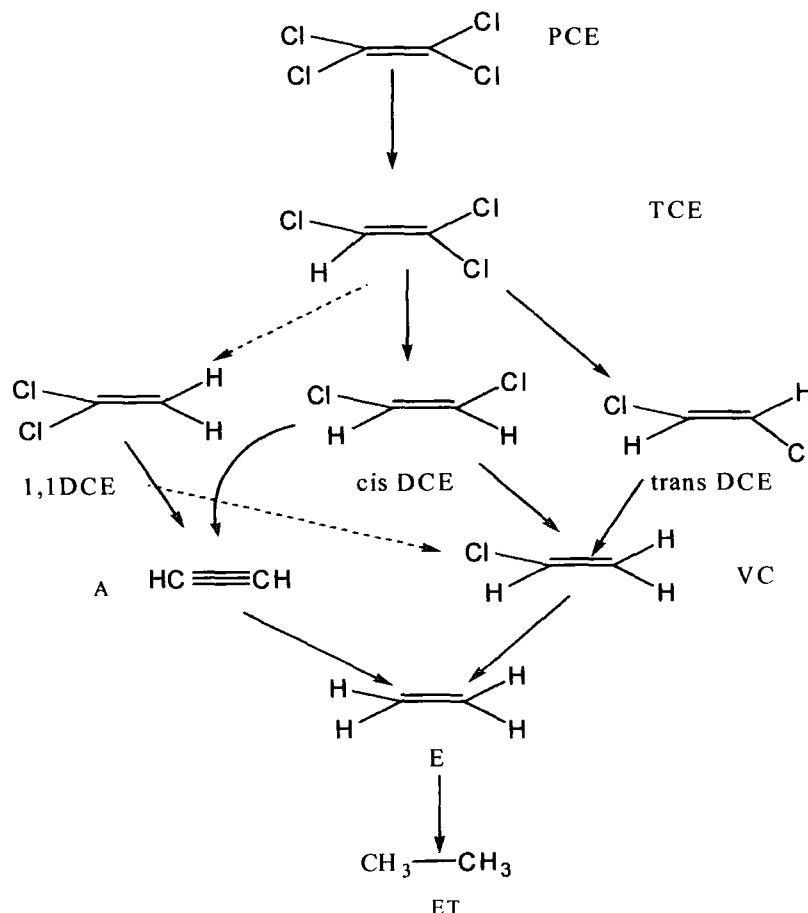
The ongoing research into optimisation of remediation technology has two targets; to reduce the overall time-scale, and overcome the problems posed by the rate-limited dechlorination reaction. To do this, mechanistic studies are required. If the processes of natural dechlorination are understood, it then becomes possible to develop external assistance, through actual enhancement and close monitoring techniques. Electrochemical techniques offer intriguing possibilities for advancement of both actual remediation and detection methods in this field.

PART 2 – General Electrochemistry

1.8 Introduction

Electrochemistry can be defined as "the science of the interaction of phases containing ions and phases containing electrons."[12] It has a long but sporadic history, beginning with Galvani's observations of electrical effects in 1791 and compounded by Faraday and Grove in the 1830's. The principal work on electrochemistry was done by Nernst and Ostwald in the late 19th century, and there followed a fairly quiescent period until the 1950's, since when improvements in instrumentation and experimental control have allowed the discipline to flourish.

1.9 General Electrochemical Principles

Electrochemistry is fundamentally an interfacial process, dealing with the movement of charge across interfaces (most commonly between an electrode and a electrolyte). The processes that occur at interfaces can be categorised as either Faradaic or non-Faradaic. Faradaic processes are those which are governed by Faraday's Laws, such that the quantity of chemical reaction at the electrode is proportional to the quantity of electricity (current) applied. Non-Faradaic processes, including adsorption and desorption, do not obey this law.

1.9.1 Non-Faradaic processes

An electrode-solution interface behaves like a capacitor, accumulating charge. At a given potential, ϕ_M, a charge q_M (an excess or deficiency of electrons) will exist in the metal, and a charge q_S will exist in the surrounding solution (an excess of anions or cations close to the electrode). At all times $q_M = -q_S$, and these values may be expressed as charge densities thus:

$$\sigma = \frac{q}{A}$$

(1)

where A = area (mm^2).

The arrangement of charged species and oriented dipoles at a solution electrode interface is termed the electrical double layer (Figure 1.6). The structure is important to electrochemistry, as it can affect the rates of electron processes.

Figure 1.6. The electrical double layer formed at a solution-electrode interface
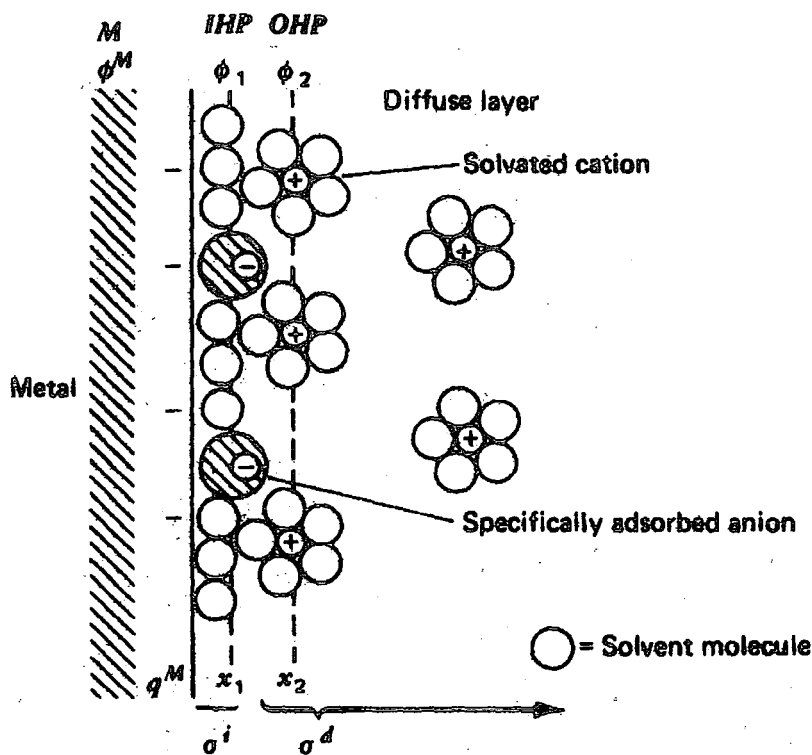
where IHP = Inner Helmholtz Plane
OHP = Outer Helmholtz Plane
ϕ_M = Electrostatic potential at the metal
ϕ_1 = Electrostatic potential at the IHP
ϕ_2 = Electrostatic potential at the OHP
X_1 = distance to the IHP

22

X_2 = distance to the OHP

σ^i = charge density of the inner layer of specifically adsorbed ions

σ^d = charge density of the diffuse layer

The thickness of the diffuse layer is dependent on the ionic concentration of the solution (a concentration greater than 10^{-2} mol dm^{-3} will give a diffuse layer thickness of less than 100Å).

Because of this phenomenon, at a given potential the electrode-solution interface will have a capacitance, C_d, which cannot be neglected when considering electrode behaviour.

1.9.2 . Faradaic processes: Electrode potentials

When the metal wire is introduced to a beaker containing salts of two metal ions (e.g. Fe^{2+} and Fe^{3+}) equilibrium is quickly established at the surface of the wire thus:

$$Fe^{3+} \text{(aq)} + e^- \text{(metal)} \rightleftharpoons Fe^{2+} \text{(aq)} \qquad (2)$$
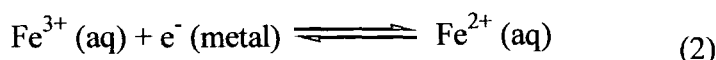
Both reactions occur at the same rate, with the wire acting as both sink and source for electrons. Both reactions involve the transfer of electrons between phases (the metal and the solution) and therefore there will be a net electrical charge on each phase, complementary to one another in order to maintain neutrality.

In terms of electrochemistry, the relative charges on the phases and hence the direction favoured by equilibrium are unimportant. The key issue is that the difference in charge between the phases causes a potential difference to exist. The potential difference varies with changing concentration of the ion species, and can be expressed as:

$$\phi_M - \phi_S = \text{constant} - \frac{RT}{F}\ln\left\{\frac{[Fe^{2+}]}{[Fe^{3+}]}\right\} \qquad (3)$$

This is a simplified expression of the Nernst Equation, where;

R = the gas constant (8.313 J K^{-1} mol^{-1})

T = absolute temperature (K)

F = Faraday's Constant (96487 C mol^{-1})

1.10. Thermodynamic equilibrium and the Nernst Equation

In an ideal solution at equilibrium, where the Gibbs Free Energy of the reaction is at a minimum, reactants and products must have equal chemical potentials, i.e.

$$\mu_A = \mu_B \qquad (4)$$

where

$$\mu_A = \mu_A^0 + RT\ln[A] \qquad (5)$$

and

$$\mu_B = \mu_B^0 + RT\ln[B] \qquad (6)$$

for a single phase aqueous equilibrium, where μ_n^0 is the standard chemical potential of the species.

However, because electrode equilibria involve charged particle transfer, electrical energy must be considered along with chemical energy. Therefore, the electrochemical potential of species A can be written as:

$$\overline{\mu_A} = \mu_A + z_A F\phi \qquad (7)$$

24

where $z_A F \phi$ refers to the electrical energy of species A. z_A is the ionic charge, F is the Faraday constant, and ϕ is the potential of the phase the species is present in.

Applied to the example of the $Fe^{2+}/^{3+}$ system:

$$\left(\mu_{Fe^{3+}} + 3F\phi_S\right) + \left(\mu_{e^-} - F\phi_M\right) = \left(\mu_{Fe^{2+}} + 2F\phi_S\right) \tag{8}$$

which rearranges to give:

$$F\left(\phi_M - \phi_S\right) = \mu_{Fe^{3+}} + \mu_{e^-} - \mu_{Fe^{2+}} \tag{9}$$

and thus:

$$\phi_M - \phi_S = \Delta\phi^0 - \frac{RT}{F}\ln\left\{\frac{\left[Fe^{2+}\right]}{\left[Fe^{3+}\right]}\right\} \tag{10}$$

where $\Delta\phi^0$ = change in standard potential.

This is the Nernst equation expressed for a single phase boundary, provided that

$$\Delta\phi^0 = \frac{1}{F}\left(\mu^0_{Fe^{3+}} + \mu^0_{e-} - \mu^0_{Fe^{2+}}\right) \tag{11}$$

remains constant. Since the μ^0_n terms are standard chemical potentials (for Fe^{3+}, an electron, and Fe2+ in this example), $\Delta\phi^0$ is constant in this case.

For non-ideal systems, such as electrolytes, it is more appropriate to use the activity, a, of a species rather than its concentration, to give the general form of the equation.

$$\phi_M - \phi_S = \Delta\phi^0 - \frac{RT}{F}\ln\left\{\frac{\left[a_A^{vA}, a_B^{vB}...\right]}{\left[a_C^{vC}, a_D^{vD}...\right]}\right\} \tag{12}$$

25

where a_N^{vN} is the activity of a given species.

Electrode potentials, then, form the basis for all types of electrochemical methods, which can be divided into two main categories; potentiometric methods, in which the measurement of the potential of a system is done at zero current, and voltammetric methods, where current is applied to a system across a range of potentials and the effects are monitored.

1.11. Use of Reference Electrodes

While the potential of a given interface can be theoretically predicted, according to Equation 12, it is impossible to measure an absolute value with only one electrode – a second electrode must be added. However, this electrode will also experience a potential change as it is introduced, and any voltmeter connected to the system will read the difference between the potential drops of the electrodes, and not the interface.

A way to rectify this problem is by employing a reference electrode. The reference electrode maintains a constant potential change across the solution interface, i.e. for a two-electrode system:

$$E = (\phi_M - \phi_S) + \text{constant} \tag{13}$$

Hence, any change in E reflects a change at the interface of interest.

Since a reference electrode must have a fixed potential, two conclusions can be drawn:

(1) That the chemical composition of the electrode and the solution to which it is directly exposed must also be fixed. Implied in this statement

is that a current cannot be passed through the reference electrode as it would result in concentration changes to the species which determine the equilibrium

and

(2) There is a need for fast electrode kinetics to allow a rapid thermodynamic equilibrium.

A two-electrode system is suitable for applications such as potentiometry, where no current is applied between the electrodes, but it does not suffice for voltammetric methods. In voltammetry, a three-electrode system is employed, which will be dealt with in a later section.

1.11.1 The Standard Hydrogen Electrode (SHE)

The SHE is the designated reference electrode for reporting Standard Electrode Potentials (E^0) (the potential of a half-cell reaction measured against the SHE at 298K, 1 mol dm^{-3} concentration and 1 atm pressure). Its half-cell reaction is

$$H^+ (aq) + e- \rightleftharpoons 1/2\ H_2\ (g) \tag{14}$$
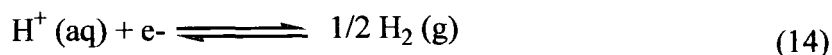
and by convention is defined as having an absolute potential of zero.

1.12. Electrochemical cells

Electrochemical cells are made up of two half cells, termed the right hand electrode (RHE) and the left-hand electrode (LHE). The overall cell reaction is represented as:

$$E_{cell} = E^o_{right} - E^o_{left} \qquad (15)$$

where E_{cell} is the overall cell potential, and E^o_{right} and E^o_{left} are the Standard Electrode Potentials of the half-cell reactions. By IUPAC conventions, the positive electrode in the cell is designated as the RHE. For example, in a cell consisting of one silver electrode and one copper electrode, the formal cell reaction is:

$$Cu(s) + 2Ag^+ \rightleftharpoons Cu^{2+} + 2Ag(s) \qquad (16)$$
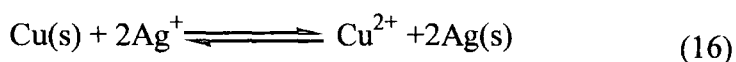
and E_{cell} is given by:

$$E_{cell} = E^o_{(Ag/Ag^+)} - E^o_{(Cu/Cu^{2+})} \qquad (17)$$

For the formal cell reaction:

$$\sum_i n_i R_i \rightarrow \sum_j n_j P_j \qquad (18)$$

where R_i represents the reaction species, P_j the product species and n_i/n_j their stoichiometric coefficients, the Nernst Equation is:

$$E_{cell} = E^0_{cell} + \frac{RT}{F} \ln \frac{\prod a_{R_i}^{n_i}}{\prod a_{P_j}^{n_j}} \qquad (19)$$

where $\prod a_{R_i}^{n_i}$ is the product of the activities of the reactants and $\prod a_{P_i}^{n_i}$ the product of the activities of the products.

1.13. Cell Resistance, Ohmic Drop and the Three-Electrode cell

As was mentioned section 1.10, a major requirement for a reference electrode is that no current may pass through it. In practical terms, for potentiometric measurements this is not an issue, but voltammetric methods (or electrolysis) rely on the passage of current applied from an external source. When an externally applied potential, E_a, passes through a reference electrode, the electrode experiences a voltage drop equal to iR_S (in accordance with Ohm's law), where R_S is the solution resistance between the electrodes and i is the current flowing through the cell. Thus the cell potential is:

$$E_a = E_w - iR_S \tag{20}$$

meaning that the potential at the working electrode (E_w) is not the potential that the operator desires.

While this effect can be avoided by a careful choice of background solutions (electrolytes) with low R_S values, in practice this is not always possible, especially in situations where non-aqueous solvents are employed.

A more practical solution is the introduction of a third counter or auxiliary electrode. Current is passed between the auxiliary and working electrodes, but the potential of the working electrode is measured with respect to the reference electrode which is connected through a high impedance voltmeter to ensure a negligible current passes through (Fig. 1.7).

Figure 1.7. A three electrode system connected to a potentiostat.
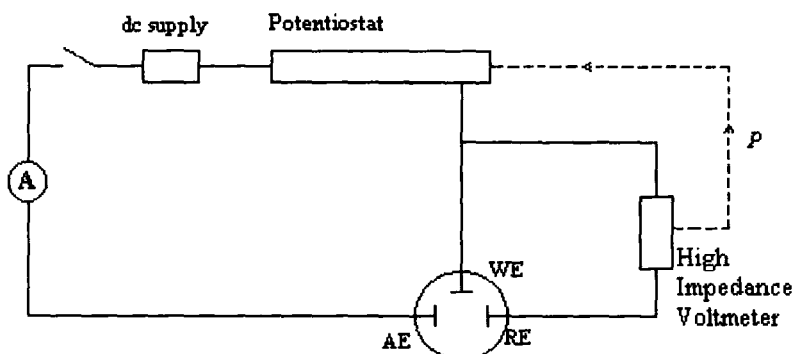
1.14. Silver/Silver Chloride Reference electrodes

There are many types of reference electrode, each with characteristics which make them suitable for certain studies but not others. In this thesis, all amperometric studies reported were carried out using an Ag/AgCl reference electrode.

The potential defining equilibrium of the electrode is:

$$AgCl(s) + e^- \rightleftharpoons Ag(s) + Cl^- \qquad (21)$$
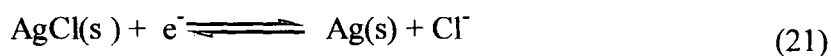
The electrical response is:

$$E(AgCl, Ag) = E^0(AgCl, Ag) + \left(\frac{RT}{F}\right)\ln\left\{\frac{1}{a}(Cl^-)\right\} \qquad (22)$$

and the Standard Electrode Potential of the system is 0.222V with respect to SHE, at atmospheric pressure and 298K. A schematic is shown below (Fig. 1.8).

Figure 1.8. Schematic of a silver/silver chloride reference electrode.

Silver Wire

Silver Chloride Coating

KCl solution - [C] constant

Glass Frit
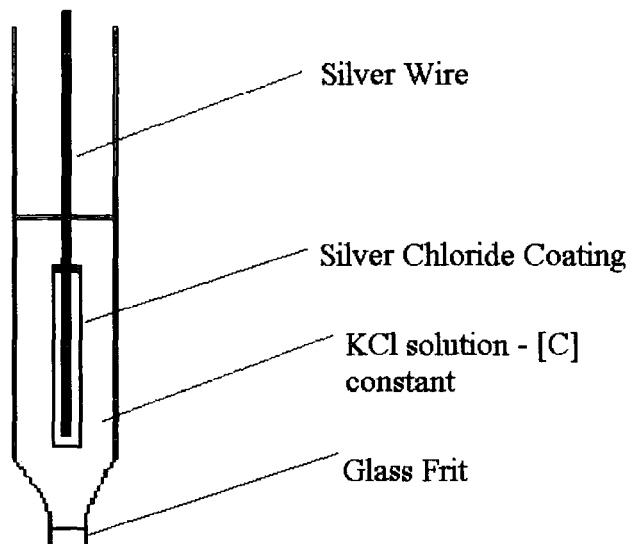
1.15. Electrode Kinetics

1.15.1 General Rate Constants

Consider the general reaction:

$$O_{(aq)} + e^-_{(m)} \underset{k_{ox}}{\overset{k_{red}}{\rightleftharpoons}} R_{(aq)} \tag{23}$$

where O is converted to R (and vice versa) by a single electron transfer. If the total current, i, flowing in the cell is given by:

$$i = i_{red} + i_{ox} \tag{24}$$

where

$$i_{red} = FAk_{red}[O]_0 \tag{25}$$

and

$$i_{ox} = FAk_{ox}[R]_0 \tag{26}$$

then

$$i = FA\left(k_{ox}[R]_0 - k_{red}[O]_0\right) \tag{27}$$

where F = Faraday's constant

A = Area of the electrode (mm^2)

k_{ox} = rate constant of oxidation reaction

k_{red} = rate constant of reduction reaction

O_0 = initial concentration of oxidised species

R_0 = initial concentration of reduced species

If electron transfer is assumed to be analogous to chemical rate processes, transition state theory expresses the rate of the reduction reaction, k_{red}, as:

$$k_{red} = A \exp\left\{\frac{-\Delta G_{red}^*}{RT}\right\} \tag{28}$$

where ΔG^* is the free energy of activation, and A is the frequency factor accounting for the collision rate of the electroactive molecules and the electrode surface. Similarly:

$$k_{ox} = A \exp\left\{\frac{-\Delta G_{ox}^*}{RT}\right\} \tag{29}$$

However, electrochemical reactions are affected by the interfacial potential. If the reaction

$$Fe^{3+}{}_{(aq)} + e^-{}_{(m)} \rightleftharpoons Fe^{2+}{}_{(aq)} \tag{30}$$
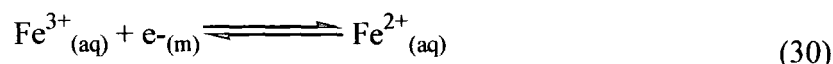
is occurring at an electrode, the free energy of the reactants is:

$$G_{Fe^{3+}} = \text{constant} + 2F\phi_S - F(\phi_M - \phi_S) \tag{31}$$

and the free energy of the products is:

$$G_{Fe^{2+}} = \text{constant'} + 2F\phi_S \tag{32}$$

The transition state is inferred as intermediate, thus:

$$G^* = \text{constant''} + 2F\phi_S - (1-\alpha)F(\phi_M - \phi_S) \tag{33}$$

Where the value of α ($0 < \alpha < 1$) reflects the transition state's sensitivity to the potential drop $\Delta\phi_{M|S}$.

1.15.2 Overpotential

If a potential, E, is applied to a cell, and $E = E_e$ (the equilibrium potential) then no current will flow. Therefore, for electrolysis to occur, a potential different in value to the E_e of the reaction should be applied to drive the electrode reaction. The excess potential ($E-E_e$) is termed the overpotential.

33

If k_{red} and k_{ox} depend on the overpotential applied to a two or three-electrode cell, then:

$$k_{red} = A \exp\left(\frac{\Delta G_{red}^*}{RT}\right) \exp\left(\frac{-\alpha F \eta}{RT}\right)$$ (34)

$$k_{ox} = A \exp\left(\frac{\Delta G_{ox}^*}{RT}\right) \exp\left(\frac{(1-\alpha)F \eta}{RT}\right)$$ (35)

where η = overpotential

$$\Delta G_{red}^* = \Delta G_0^* + \alpha F \left(E_e - E^0\right)$$ (36)

$$\Delta G_{ox}^* = \Delta G_0^* - (1-\alpha)F \left(E_e - E^0\right)$$ (37)

Since for any given reaction all the parameters of the first term are constant, equations 34 and 35 simplify to:

$$k_{red} = k_{red}^0 \exp\left(\frac{-\alpha F \eta}{RT}\right)$$ (38)

$$k_{ox} = k_{ox}^0 \exp\left(\frac{(1-\alpha)F \eta}{RT}\right)$$ (39)

Substituting into equation 27 gives the relationship for the net current, i, flowing at the electrode (the Butler-Volmer equation).

$$i = i_0 \left(\frac{[R]_0}{[R]_{bulk}} \exp\left\{\frac{(1-\alpha)F \eta}{RT}\right\} - \frac{[O]_0}{[O]_{bulk}} \exp\left\{\frac{-\alpha F \eta}{RT}\right\}\right)$$ (40)

1.16. Mass Transport Effects

As has been discussed so far, electrode potential and ion activity are important parameters in reactions at interfacial surfaces. A third key parameter is mass transport effects; the transport of materials between the electrode and the bulk solution. Mass Transport can be subdivided into three categories; diffusion, convection and migration.

1.16.1 Diffusion

Diffusion arises from uneven concentration distributions, and acts to homogenize the bulk solution composition.

The rate of diffusion at a certain point is dependent upon the local concentration gradient, and is given by Fick's first law of diffusion.

$$j = -D_B \frac{\partial [B]}{\partial x} \qquad (41)$$

where j = diffusional flux

D_B = diffusion coefficient

B = concentration of reactant species (Fig. 1.9)

Figure 1.9. Diffusion approaching an electrode surface
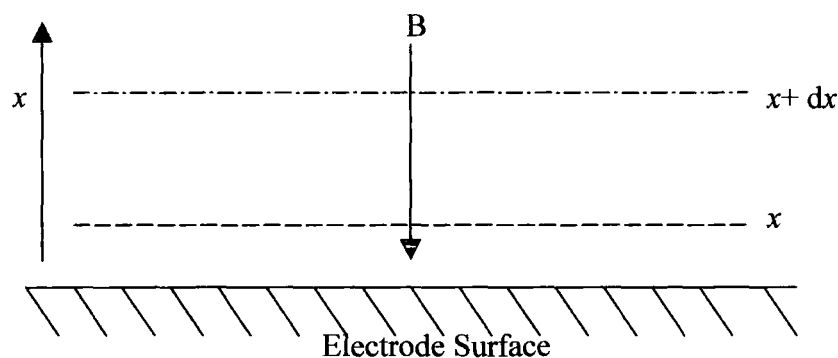
However, in electrochemistry it is important to consider diffusion at a point close to the electron gradient *over time*. In Fig 1.9, if there is a variation in the flux of B entering the area through x and leaving through $x + dx$ in a time interval dt, then Fick's second law applies.

$$\frac{\partial [B]}{\partial t} = D_B \left(\frac{\partial^2 [B]}{\partial x^2} \right)$$

(42)

1.16.1.1. Nernst Diffusion Layer

If a potential is applied to an electrode so as to oxidise or reduce a species in a solution, a concentration gradient exists between the electrode and the bulk solution, perpendicular to the electrode surface. The gradient forces a flux of species from the solution to flow towards the electrode, building up a diffusion layer close to the electrode interface. Theoretically, during electrolysis, this layer should expand until it exhausts all the reactive species present, but due to mixing and natural convection in the solution the layer has a limiting, steady-state thickness, under which transport within the layer takes place by diffusion alone. The width of the diffusion layer (δ) was estimated by Nernst by extrapolating the linear plot of concentration vs. distance from the electrode up to a concentration equal to that of the bulk solution (Fig.1.10). Typically, δ is circa 0.05cm in normal experimental conditions.

Figure 1.10. Plot of reactant concentration versus distance from the electrode surface
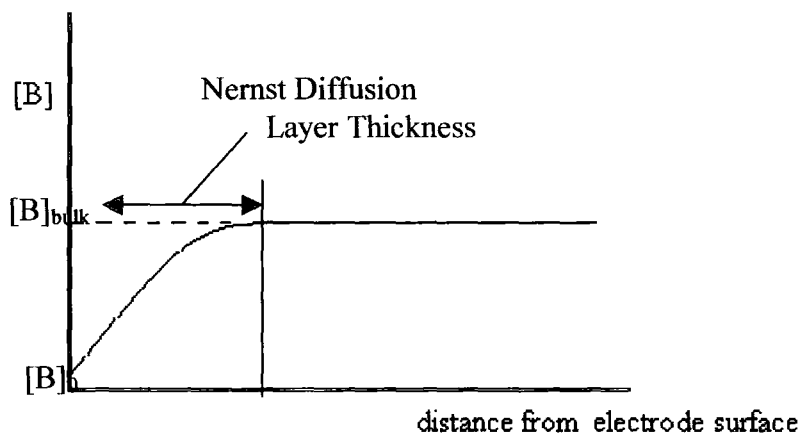
This approach allows the calculation of the current flowing.

$$\frac{i}{FA} = j = D_B \frac{[B]_{bulk} - [B]_0}{\delta} \tag{43}$$

B_0 (the concentration at the electrode surface) is determined by the electrode potential; in the above example a highly oxidising potential is represented, so B_0 is almost zero.

1.16.2. Convection

Convection may arise naturally in a solution through heat and density gradients. In a given solution, heat gradients may be generated by the endo-/exothermicity of the reaction process, and density can be affected by local concentrations of products with densities different to those of the bulk solution and reactants. Such natural convection is undesirable due to its unpredictable nature.

Forced convection such as gas bubbling or stirring is usually introduced to experiments of longer than 20 seconds duration. This overwhelms any natural convection in the cell, allowing reproducible results to be measured. In experiments which require strict control of mass transport, a hydrodynamic electrode such as the Rotating Disk Electrode is usually employed. Hydrodynamic electrodes produce predictable patterns of convection, allowing calculations of diffusion to be made.

1.16.3. Migration

The change in electrode potential across a solution/electrode interface ($\Delta\phi$ m|s) gives rise to an electric field ($d\phi/d\chi$) capable of exerting an electrostatic force on charged particles in the interfacial region, giving rise to ion attraction and repulsion.

1.16.3.1 Background electrolyte

Experimentally, migration, like natural convection, is undesirable, and to countermand it, a background electrolyte is added to solutions. A chemically and electrochemically inert salt such as KCl is an example, and is usually used in high excess concentrations (0.1 mol dm^{-3} or greater is typical). The quantities of background ions maintaining the electroneutrality throughout the bulk solution are so large that the slight perturbation caused by the electrode reaction is masked, allowing migration effects to be ignored.

Further advantages of background electrolytes are:

1)   They increase the solution conductivity; the bulk of the current can flow through the background electrolyte, lowering the R_S value.

2)   The high concentration compresses the electrical double layer to c. 20Å, reducing the magnitude of the electric field.

3)   The high excess concentration means that the ionic strength of the solution is effectively constant, and thus the activity coefficient of the reagents will be constant.

1.17. Electrochemical Methods

1.17.1. Cyclic Voltammetry

Cyclic Voltammetry (CV) is a controlled potential sweep technique which is used to scan a region of potential and observe the resulting current. A potentiostat applies a triangular waveform as the potential of the working electrode (WE) of an electrochemical cell, sweeping from a (usually negative) start potential to a vertex, then returning at a constant scan rate, υ (where $\upsilon = |dE/dt|$). The driving of the electrode to more positive potentials causes an oxidation current to flow from the cell solution to the electrode. Conversely, driving the electrode to more negative potentials causes a reducing current to flow from the electrode to the solution.

When the potential of the system reaches the standard potential, E^0, of the species present in the solution, the oxidation of the species begins to occur at the electrode surface, causing an increase in observed current. This causes a local change in species concentration, and consequently, a concentration gradient develops. Diffusion draws more of the electroactive species to the electrode surface, allowing the reaction to continue until depletion of the species in solution causes the current to decrease, or the electrode potential moves beyond that of the oxidation. On the reverse sweep of the cycle (providing the reaction is reversible), the oxidised form of the species derived from the forward sweep is readily available for reduction at the standard potential, and has a like effect on the current.

CV can provide information on the reversibility of a reaction simply from the shape of the current-potential curve (voltammogram) derived (Fig. 1.11).

Figure 1.11. Example Voltammogram of a reversible system (adapted from reference 13.)
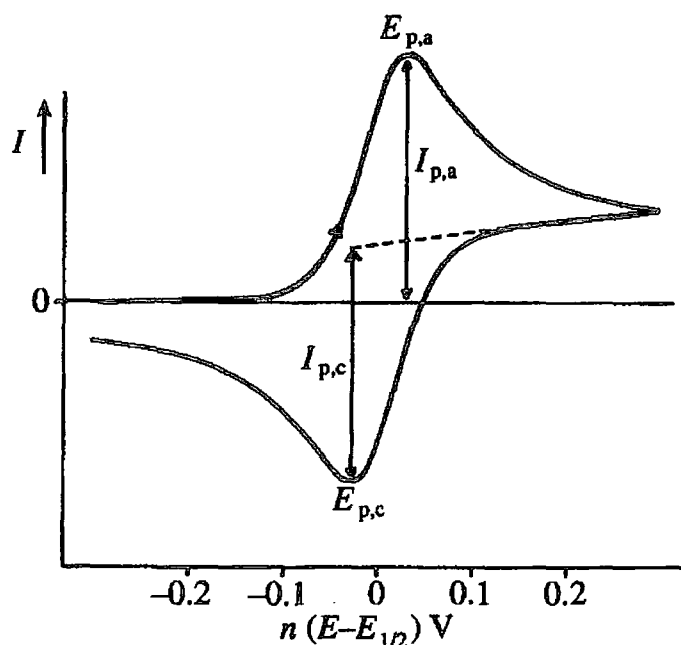
In reversible reactions the product of the oxidation on the positive sweep is reduced when the scan direction is reversed. The diagnostic criteria for a reversible system are:

1) That the peak current, i_{pa}, is proportional to the square root of the scan rate, according to the Ilkovic Equation;

$$i_{pa} = 2.69 \times 10^5 \, n^{3/2} A D_B^{1/2} [B]_\infty v^{1/2} \quad (44)$$

Where i_{pa} = peak anodic current (A)

n = no. of electrons

A= area of electrode (mm^2)

D_B = diffusion coefficient (cm^2 s^{-1})

B = reactant species (mmol dm^{-3})

v = Scan rate (V s^{-1})

2) E_p, the peak potential, is independent of scan rate.

3) The separation of the oxidised and reduced peaks, should have the Nernstian value, 59mV.

Irreversible reactions exhibit only one oxidation/reduction peak in a voltammogram, and E_p varies with scan rate. Quasi-reversible systems display reverse peaks which are much smaller than their forward counterparts: reaction rate constants can be deduced from their peak separation.

1.17.2 Rotating Disk Electrode Voltammetry

Hydrodynamic electrodes are used to implement a controlled mass transport regime in a system by forcing a specific convection pattern in the cell. This allows a known and controllable manner of transporting species to and from the electrode surface. Equations that define the understood convection can then be used to make predictions about diffusion at the electrode surface and comparisons with actual experimental data.

The Rotating Disk Electrode (RDE) is an example of such an electrode. It consists of a small disc of electrode material (e.g. platinum) embedded in a larger cylinder of non-reactive material such as Teflon, connected to a motor which rotates it at speed designated by the user, termed the angular velocity, ω (in Hertz). It is more common to measure the electrode rotation in revolutions per minute (r.p.m.), and the two are linked by the equation:

41

$$\omega = \left(2\Pi\big/_{60}\right)f'$$

(45)

where ω = angular velocity (Hz)

f' = revolutions per minute

When the electrode is rotated, it pulls the solution towards its surface in a specific manner. The solution is drawn vertically up towards the electrode surface, and thrown outwards radially. At the electrode surface, the velocity of the solution normal to the surface is 0, and increases with distance until it reaches a limiting value in the bulk solution. Therefore we can say that the importance of convection decreases as the electrode surface is approached. Immediately adjacent to the electrode surface, if there is no flow normal to the electrode, there exists a layer, thickness δ, where only rotational movement is occurring. For the purposes of analysis, this layer is assumed to be convection free, that is, mass transport in the layer is totally controlled by diffusion.

In electrolysis, electroactive material needs to be at the electrode surface for reactions to occur, therefore the largest observed current will be constrained by the rate of transport of those materials to the electrode. If the potential of the WE is increased, and the surface concentration of the electroactive species is zero (i.e. all material transported to the surface reacts immediately), the limiting current of the system is reached.

Under these conditions, the Levich equation states that:

$$i_L = 0.62nF\omega^{1/2}v^{1/6}D^{2/3}c_0$$

(46)

Where i_L = limiting current (A)

n = number of electrons transferred

F = Faraday's constant (C mol^{-1})

ω = angular velocity (Hz)

v = kinematic viscosity ($m^2 s^{-1}$)

D = diffusion coefficient ($cm^2 s^{-1}$)

c_o = concentration of reactive species (mol dm^{-3})

Since the limiting current can be read directly from the voltammograms produced, and all the other parameters are known to the experimentalist, the equation can be used to calculate the diffusion coefficient, D.

1.17.3. Differential Pulse Voltammetry

CV and RDE Voltammetry are potential sweep techniques, varying the potential of a system continuously. Another type of technique is potential step voltammetry, where the potential is instantaneously changed from an initial value to one of interest. The Faradaic response to this 'step' is a pulse of current, which decays with time as the electroactive species near the electrode is used up. The non-Faradaic response from double layer charging is a small capacitive current.

In Differential Pulse Voltammetry (DPV), the potential waveform applied can be visualised as a series of pulses overlaid on a potential staircase (Fig 1.12).

Figure 1.12. Differential Pulse Waveform (adapted from reference 13).
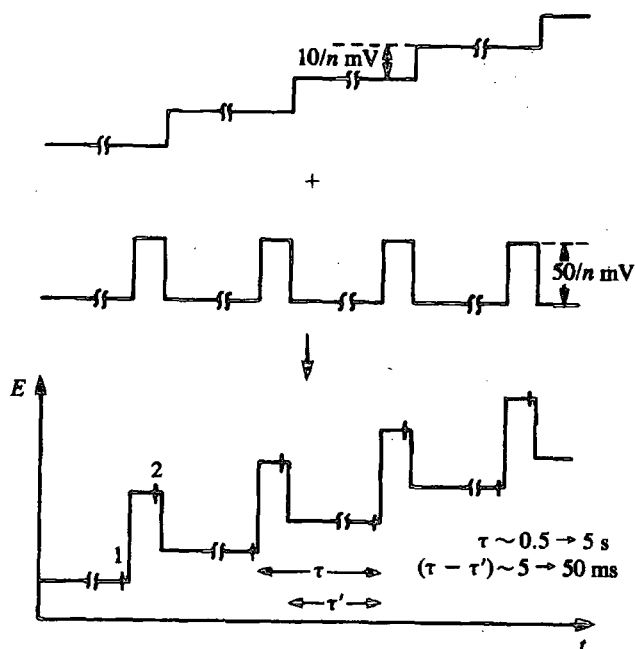
Subtracting i_1 from i_2 cancels out any interference from capacitive current, thus making the technique extremely sensitive; its detection limit is typically around 10^{-7} mol dm^{-3}. A typical DPV voltammogram is shown below (Fig.1.13).

Figure 1.13. Typical DPV response curve (adapted from reference.13).

$$\Delta I = I(2) - I(1)$$
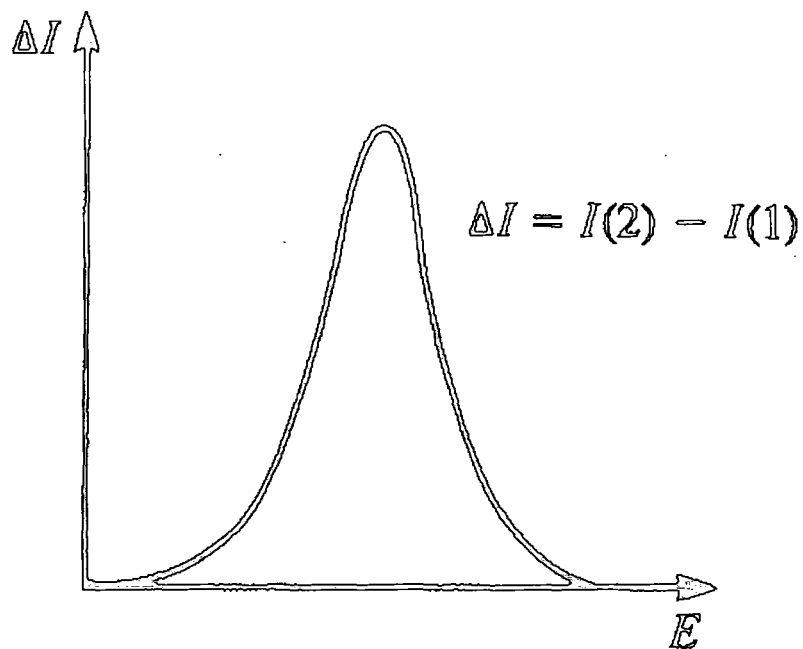
REFERENCES

1. ATSDR Toxicological Profile for Tetrachloroethylene,
http://www.atsdr.cdc.gov/toxprofiles/tp18.pdf. Accessed 27/08/02.

2. ATSDR Toxicological Profile for Trichloroethylene,
http://www.atsdr.cdc.gov/toxprofiles/tp19.pdf. Accessed 27/08/02.

3. Schollhorn, A., Savary, C., Stucki, G., and Hanselmann, K.W., *Wat. Res.*, 1997,
31, 1275 – 1282.

4. Agency for Toxic Substances and Disease Registry (ATSDR) Public Health
Statement for Trichloroethylene,
http://www.atsdr.cdc.gov/toxprofiles/phs19.html. Accessed 27/08/2002.

5. ATSDR Public Health Statement for Tetrachloroethylene,
http://www.atsdr.cdc.gov/toxprofiles/phs18.html. Accessed 27/08/2002.

6. Defaulque, F.J., *Clin. Pharmacol. Ther.*, 1961, **2**, 665-688.

7. International Agency for Research on Cancer. Overall evaluations of
carcinogenicity: an updating of IARC monographs volumes 1-42, Lyon, **1987**, pp
364 – 366.

8. Bolt, H.M., Laib, R.J., and Filser, J.G., *Biochem. Pharmacol.*, 1982, **31**, pp1-4.

9. Press, F. and Siever, R., *Understanding Earth*, Freeman and Company, New
York,**1994**, 252.

10. British Geological Survey – Hydrogeology - Groundwater Pollution website,
http://www.bgs.ac.uk/hydrogeology/PollProb.htm. Accessed 27/08/02

11. Wiedemeier, T., Rifai, H., Newell, C., and Wilson, T., *Natural Attenuation of
Fuels and Chlorinated Solvents in the Subsurface*, John Wiley and Sons Inc., New
York, **1999**, pp 27 – 31.

12. Hibbert, D.B., *Introduction to Electrochemistry*, MacMillan Press, London,
1993, 1.

13. Brett, C.M.A., and Brett, A.M.O., *Electroanalysis*, Oxford University Press,
Oxford, **1998**, 51-57.

CHAPTER 2

The Abiotic Reaction Mechanism of Reductive Dechlorination

2.1 Introduction

Reductive dechlorination of PCE and TCE in biotic systems relies on the use of chlorinated ethenes as electron acceptor in metabolic or co-metabolic processes. Therefore, to determine an abiotic reaction mechanism for the dechlorination process through electrochemical study, a strong electron donor was chosen. Tetrakis(dimethylamino)ethylene was selected, as its extremely negative oxidation potential (-0.75V) indicates a strong electron donor character.

2.2 Literature Review – Tetrakis(dimethylamino)ethylene

Tetrakis(dimethylamino)ethylene (TDAE) (Fig 2.1) was the first tetraaminoethylene to be discovered, during work by Pruett et al.[1] in 1950 on the reactions of polyfluoro olefins with primary and secondary amines; the product of reacting dimethylamine on trifluorochloroethylene. They describe the product as being "strongly luminescent in contact with air," and also its reaction with oxygen to form a white solid, but made no further investigation. Indeed, further work on tetraaminoethylenes did not occur until 1960, when Wanzlick et al.[2] reported a second member of the class (1,1',3,3',-tetraphenyl-2,2'-biimidazolidinylidene) and by 1968 over thirty compounds had been isolated and studied. TDAE remains one of the simplest.

Figure 2.1. Tetrakis(dimethylamino)ethylene.
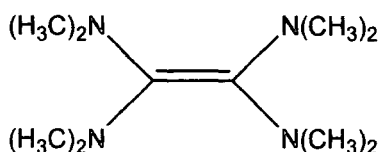
Tetraaminoethylenes are strong organic electron donors; their participation in reactions involves either giving up electrons to an oxidising agent, or sharing them with an acid (acid-base reaction). The luminescence in the presence of air/reaction with oxygen indicates that TDAE is capable of auto oxidation[3,4]. Oxidising agents which remove two electrons include carbon tetrachloride[5] and dinitrogen tetroxide[6], producing the $TDAE^{2+}$ (octamethyloxamidinium) radical dication. In his review, Wiberg[7] postulates that the ease with which the TDAE molecule gives up two electrons is because the four amine groups stabilise the positive charge by partially transferring their free electron pairs onto the carbon atoms. Work by King[8] on the reactivity of TDAE with metal carbonyls demonstrated TDAE's operation as a 2-electron reducing agent and not as a Lewis base (typical for amines). King's work revealed that TDAE's reactions with the carbonyls of vanadium and cobalt are unique amongst amines in that they produce a metal carbonyl anion salt with a metal-free cation $(TDAE^{2+})$, as opposed to the normal metal-containing amine cation $[M^{II}(base)_6]^{2+}$, where M= Co or V, and base = amine used in reaction. This behaviour characterises TDAE's behaviour as a 2-electron reducing agent.

Production of the dication radical was shown to be a two-step reaction in work by Kuwata and Geske[9]. Polarography demonstrated a two-step oxidation, at half-wave potentials of -0.75 and –0.61V vs. SCE in an acetonitrile and tetrabutylammonium perchlorate background. This result was confirmed by Burkholder et al.[10] in their study thirty-four years later, where potentials of -0.78 and –0.61V vs. SCE were reported, working in an acetonitrile and tetraethylammonium fluoroborate background. The extremely negative potentials

of the system presented the first quantitative expression of TDAE's electron donor characteristics; in fact, the potential of the first oxidative step is comparable to the standard potential of zinc ($Zn \rightarrow Zn^{2+} + 2e$; $E_0 = -0.76V$).

The polarography studies done by Kuwata and Geske were followed by controlled potential electrolysis of a TDAE solution at $-0.7V$. This produced a strongly orange-coloured solution that, when examined using ESR, displayed an absorption maximum at 385nm due to the presence of the $TDAE^+$ radical cation: thus, the two-step oxidation elucidated by cyclic voltammetry can be explained as follows.

$$E_0\ ^-0.75V \qquad TDAE \rightarrow TDAE^+$$
$$E_0\ ^-0.61V \qquad TDAE^+ \rightarrow TDAE^{2+}$$

When TDAE is reacted with organic molecules with an oxidation potential lower than that of its chemical counterpart $TCNE^5$, complete electron transfer gives way to the formation of donor-acceptor complexes[11]. Such is the strength of TDAE as a donor it can complex even weak electron acceptors, including tetrachloroethene (PCE)[7].

Work by Wiberg and Buchler[5] demonstrated the removal of chlorine atoms from carbon tetrachloride in organic solvents via the reaction

$$TDAE + CX_4 \longrightarrow TDAE^{2+}X^-CX_3^-\ \tag{1}$$
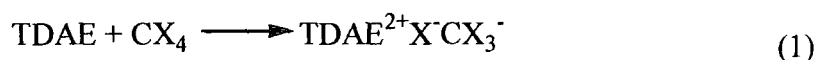
When X= Halogen, the product of the reaction is unstable and loses a halide ion to form CX_2. In the case X=Cl, therefore:

$$TDAE + 2CCl_4 \longrightarrow TDAE(Cl_2) + 2CHCl_3 + ? \tag{2}$$

where ? represents unidentified minor products.

Further study by Carpenter[12] showed that reactions with polyhalogenated molecules may proceed in two ways, 1) by replacement of a single halogen with hydrogen, and 2) by removal of two vicinal halogens to form alkenes. Carpenter also discovered that the more positive a halogen, the easier it is for TDAE to remove. More recent work by Chambers *et al.*[13], Briscoe *et al.*[14] and Burkholder *et al.*[15] has utilised TDAE as a defluorinating agent.

In summation, TDAE presents an ideal candidate with which to conduct electrochemical investigations into the dehalogenation of chlorinated ethenes; its abilities as a strong electron donor, defined electrochemical behaviour and documented capability to remove halogen atoms from molecules present a well understood platform from which to commence further study.

2.3 Experimental

2.3.1 Materials

HPLC grade Acetonitrile was obtained from Riedel de Haen (Poole, Dorset, UK). TDAE, 2-Chlorophenol, c-DCE and t-DCE were purchased from Sigma-Aldrich (Poole, Dorset, UK). PCE and TBAP were obtained from Fluka (Gillingham, Dorset, UK) and TCE was from BDH Laboratory supplies (Poole, Dorset, UK).

2.3.2. Methods

Cyclic Voltammetry [CV] and Rotating Disc Electrode Voltammetry [RDE] were used to elucidate the mechanisms of abiotic dechlorination of chlorinated ethenes in a strongly reducing environment.

The experiments were conducted on an EG&G PARC Model 273 Potentiostat/Galvanostat. Computer control and data storage were achieved using EG&G PARC Model 270 Research Electrochemistry software. All analytes were dissolved in a background electrolyte of 0.01mol dm^{-3} TBAP in acetonitrile, at an equivalent concentration to that of the TBAP (0.01mol dm^{-3}); where more than one analyte is present the molar ratio is 1:1. Acetonitrile was used as the solvent since both TDAE and the chlorinated ethenes have very limited solubility in water.

For CV, the electrodes were mounted in a circular Teflon cap, and placed in a cylindrical cell (length 65mm, diameter 20mm). The auxiliary electrode (AE) was made of platinum foil, area 1cm^2, connected to copper wire and mounted in a glass body, and was made by the Departmental glassblowers. The working electrode (WE) was made of glassy carbon and purchased from BAS (West Lafayette, IN, USA). The reference electrode (RE) was a non-aqueous silver/silver chloride electrode, self-assembly kit, also purchased from BAS. The

cell was filled with 10ml of the desired analyte solution, which was stirred
continuously using a magnetic stirrer bar, and purged with nitrogen. The cell
assembly was placed inside a Faraday cage to eliminate interference. All
measurements were carried out at 298K.

For RDE voltammetry, a specially constructed cell was employed (Fig.2.2). A
Luggin probe was used to take measurements as close to the surface of the
working electrode as possible, and a frit was positioned between the working and
auxiliary electrode compartments to prevent contamination of the solution by
electrolysis products. The working electrode used was an EG&G PARC Model
616 Rotating Disk Electrode. The electrode disc was platinum, diameter 4mm;
CE and RE were previously described. Again, all measurements were recorded
inside a Faraday cage, at 298K.

Figure 2.2. Cell design for RDE voltammetry
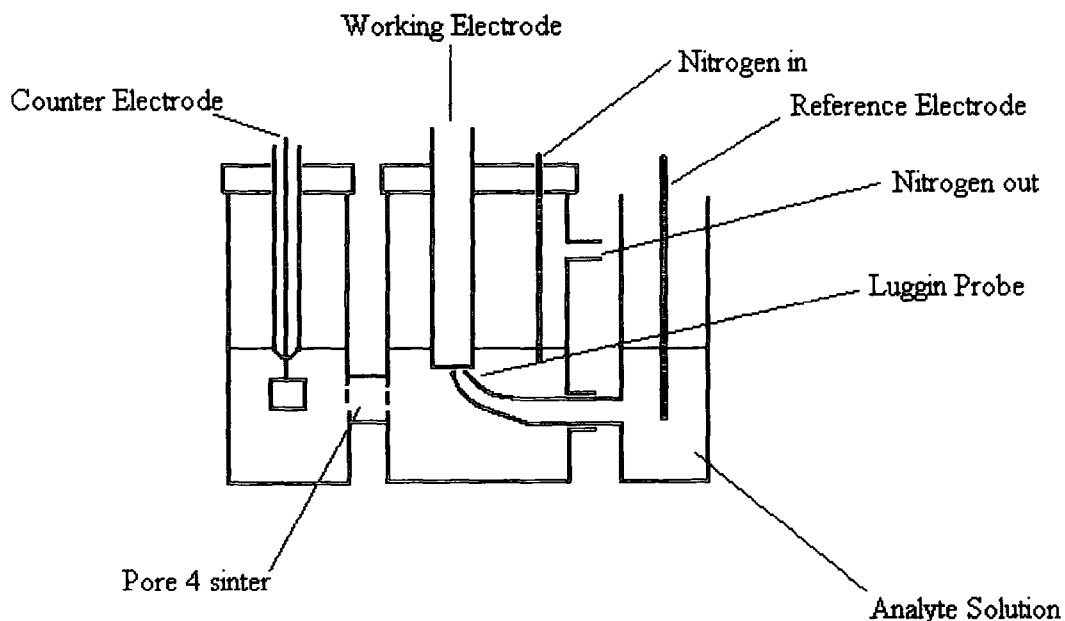
2.3.3 UV-Vis Spectroscopy and Chloride Analysis

A Pharmacia Biotech Ultrospec 4000 UV/Visible photospectrometer was used for UV-vis spectroscopy, using quartz cells with a path length of 1cm. Aliquots of analyte mixtures were examined prior to and after RDE voltammetry to monitor the degradation of colour in the solutions. With fresh, coloured solutions, a one in four dilution strategy was employed, as the intensity of the colour was found to be swamping the detector.

Chloride analysis of the samples was performed by the Analytical Services Division of the Department, utilising ion exchange chromatography. The experiments were carried out on a Dionex (Sunnyvale, CA, USA) DX-120 Ion Chromatograph with an electron capture detector. The eluent was 3mmol dm^{-3} NaOH.

2.4 Results and Discussion

2.4.1 Cyclic Voltammetry

2.4.1.1 Cyclic Voltammetry of TDAE

Cyclic voltammetry of a freshly prepared, coloured TDAE solution in acetonitrile (background electrolyte 0.01 mol dm^{-3} TBAP) showed a reversible two-step oxidation at -0.59V and -0.38V vs. Ag$^+$/AgCl (Fig. 2.3), or -0.81V and -0.60V vs SCE. The oxidations indicate the formation of the dication radical, TDAE^{2+}, as illustrated in the voltammogram below (Fig. 2.4). These values correspond reasonably well to previously published results; Kuwata and Geske[9] reported values of -0.75V and -0.61V vs. SCE (in acetonitrile, electrolyte 0.1mol dm^{-3} tetraethylammonium perchlorate), and Burkholder et al[10] found similar values of -0.78V and -0.61V vs. SCE (in acetonitrile, electrolyte 0.1 dm^{-3} Et$_4$NBF$_4$). The very slow scan rate at which the voltammetry was conducted reflects the slow kinetics of the reaction; with faster scan rates, the two-step oxidation was seen as a single reversible peak.

Figure 2.3. Voltammogram of TDAE, Scan rate 20mV s^{-1}.
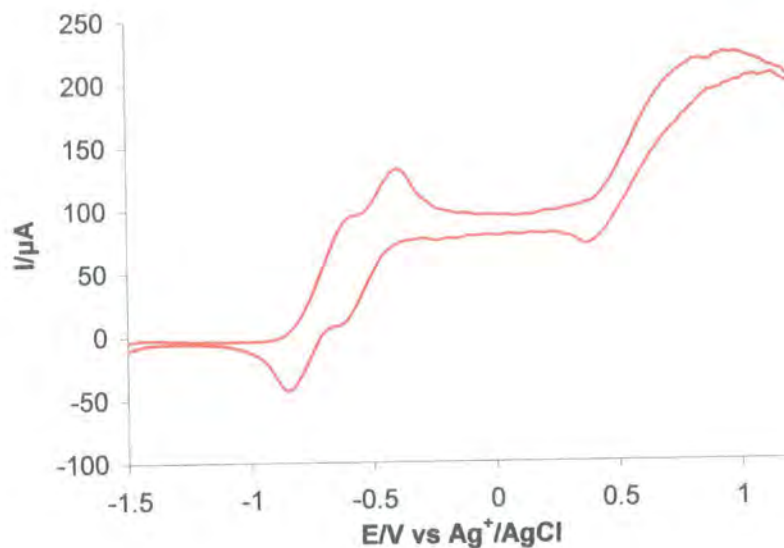
Figure 2.4. Formation of the TDAE radical dication, TDAE^{2+}.
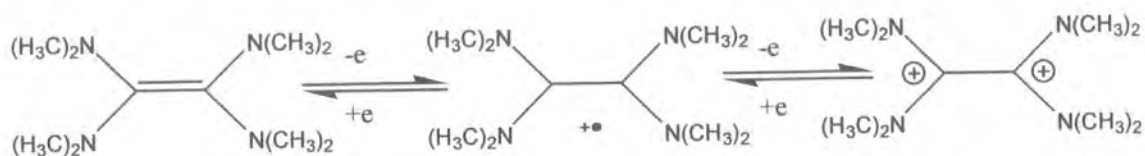
A further, irreversible, oxidation peak, observed at 0.88V, is due to formation of higher oxidation products. During sample preparation it was found that the addition of TDAE to acetonitrile produced a strong orange colour, which degraded over time to a colourless solution. This process is hastened by the application of oxidative potentials, or indeed kinetic energy, to the solution. (see Table 2.1). This is due to the autooxidation of TDAE, a phenomenon investigated by Urry et al.[3] Figure 2.5 below shows the oxidation products elucidated by that study; the oxidation peak at 0.88V reflects their formation.

Table 2.1. Auto oxidation times for TDAE under varying experimental conditions.

Analyte	Time for colour change (left standing)	Time for colour change (under electrolysis)	Time for colour change (under RDE stirring)
TDAE	1 hour	1 hour	10 minutes
TDAE + PCE	1.3 hours	1 hour	10 minutes
TDAE + TCE	1.3 hours	1 hour	10 minutes
TDAE + c-DCE	4 hours+	1 hour	10 minutes
TDAE + T-DCE	4 hours	1 hour	10 minutes

Figure 2.5. Oxidation of TDAE to tetramethylurea or tetramethyloxamide.
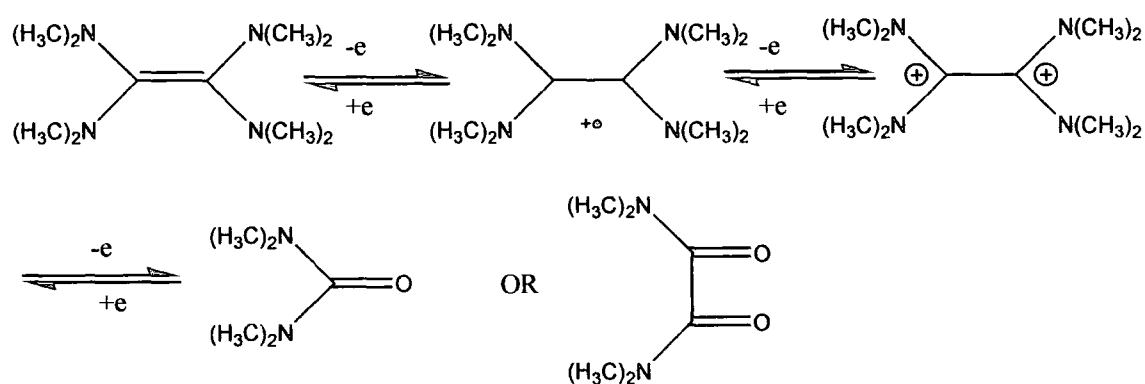
After one hour, the solution became colourless, and a different pattern of reduction was observed (Fig. 2.6). The two-step oxidation is no longer discernable, although the final oxidation persists, suggesting that all of the TDAE has been converted to its fully oxidised form.

Figure 2.6. Voltammogram of colourless TDAE solution. Scan rate 100mV s⁻¹.
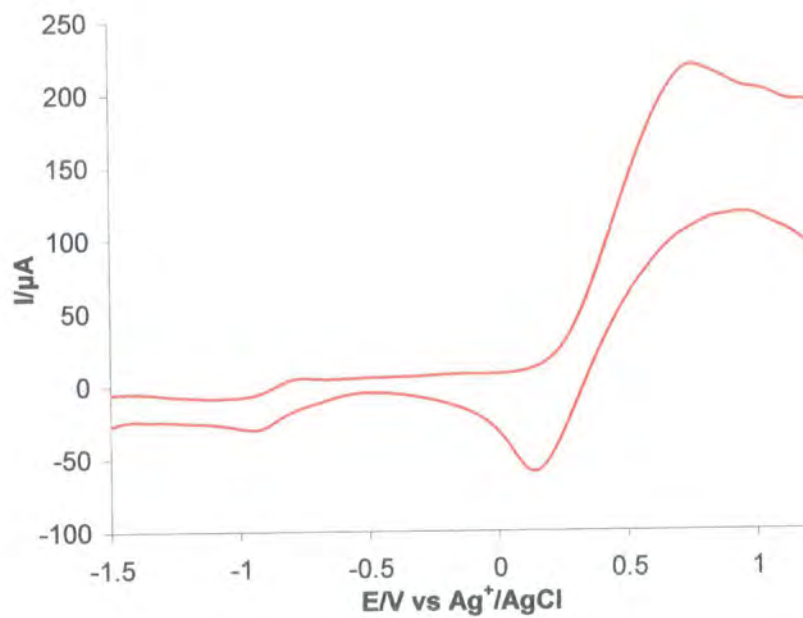
2.4.1.2 Cyclic Voltammetry of TDAE and Chlorinated Ethenes

The addition of chlorinated ethenes to a freshly prepared solution of TDAE had an electrocatalytic effect (Fig. 2.7) on the production of $TDAE^{2+}$. The application of a potential lowers the activation energy of the oxidation shown in Figure 2.4 above, allowing the formation of $TDAE^{2+}$ at much faster rates. When the chlorinated ethenes are added to the solution, the activation energy drops even further; the extremely positive redox potential ($E^0_{PCE/TCE} = 0.576V$) of the chlorinated ethenes makes the reaction thermodynamically favourable. Hence a catalysis of the reaction is seen, according to the scheme shown in Figure 2.8; this is reflected in the voltammogram's greatly increased peak current and steep slopes. The magnitude of the effect varied with differently substituted ethenes: greatest in the presence of c-DCE > PCE > TCE. The t-DCE showed practically no deviation from the voltammogram of pure TDAE (Fig. 2.9).

Figure 2.7. Voltammograms showing the catalytic reaction of TDAE with the chlorinated ethenes PCE, TCE, and c-DCE. Scan rate 20mV s^{-1}.
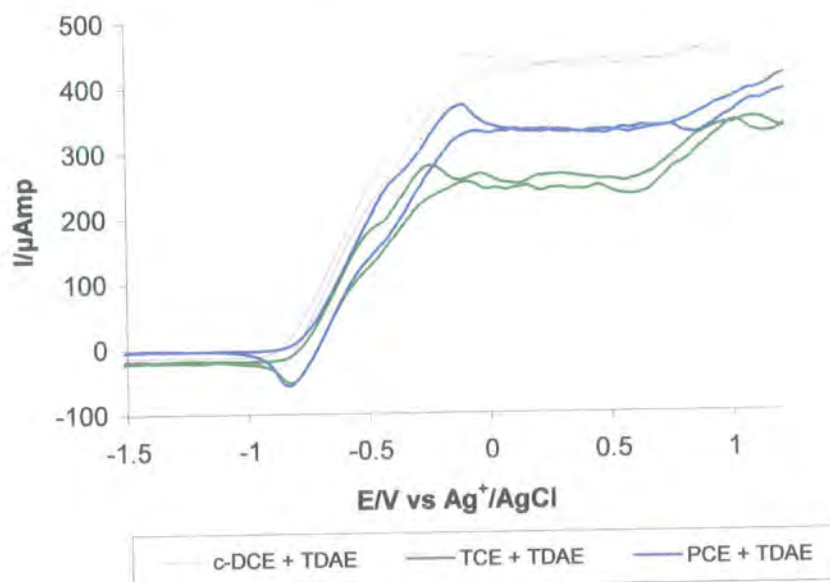
Figure 2.8. Scheme for TDAE/chlorinated ethene reaction.
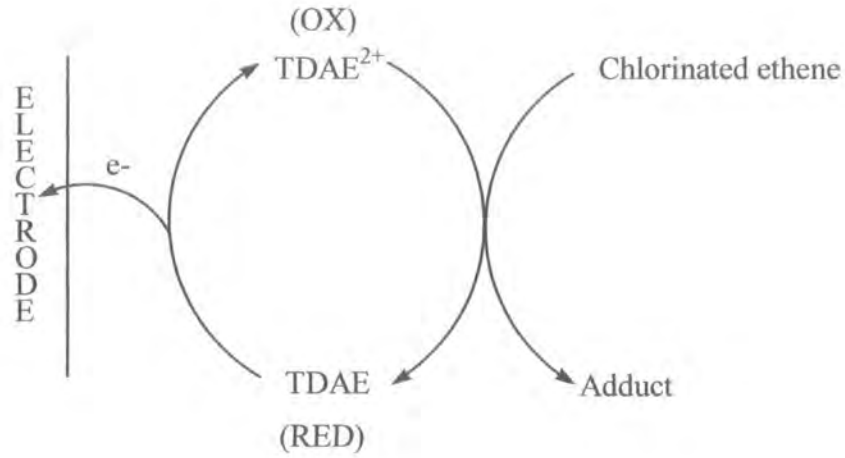
Figure 2.9. trans-Dichloroethene produces virtually no deviance from the voltammogram of TDAE. Scan rate 20mV s^{-1}.
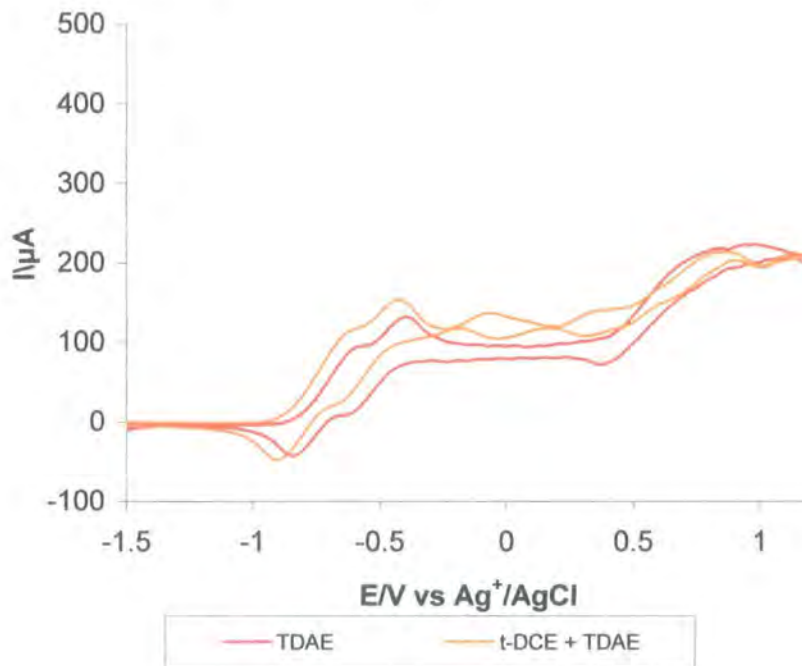
Once the solutions have aged and become colourless, the electrocatalytic effect is no longer observed (as demonstrated in Figures 2.10 and 2.11).

Figure 2.10. Comparison of coloured and colourless solutions of TDAE.
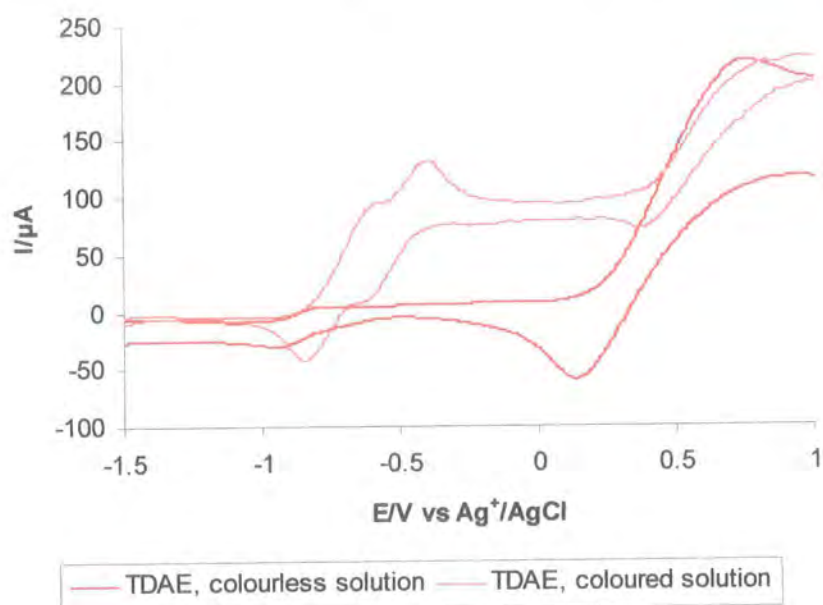
Figure 2.11. Voltammograms of TDAE and chlorinated ethenes in aged, colourless solutions.

a) PCE and TCE
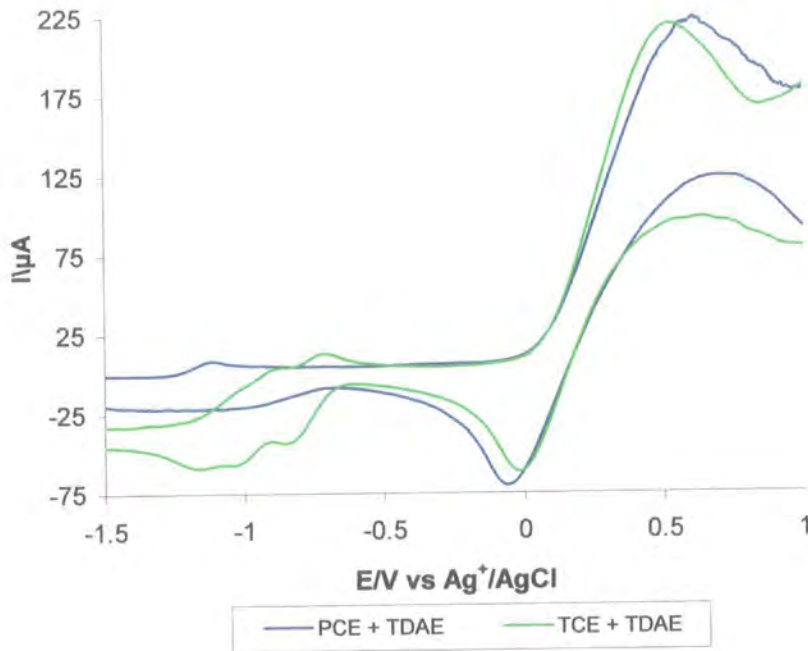
b) t-DCE and c-DCE
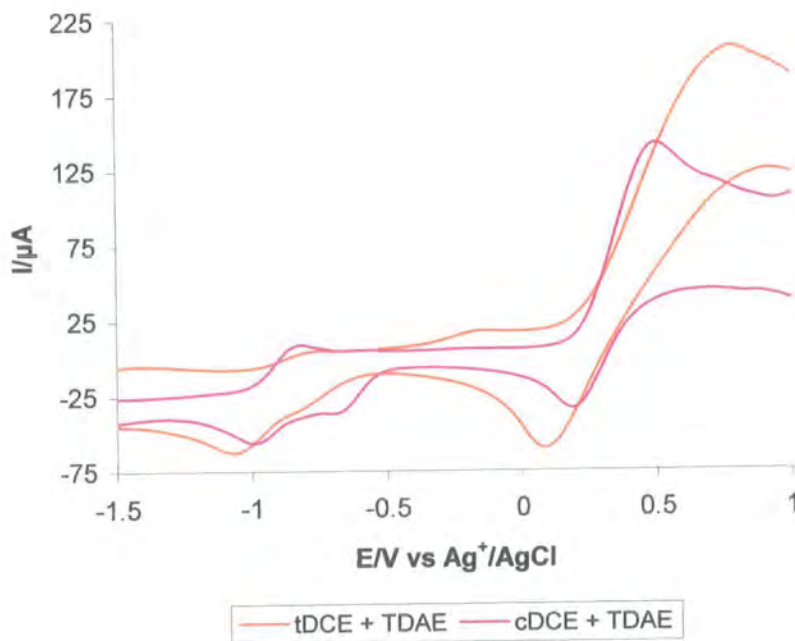
With TCE, three reductions are seen (Fig 2.12), at potentials –0.86V, -1.04V, and –1.19V. C-DCE shows two reductions at –0.69V and –1V. PCE shows no additional reductions. Again, the t-DCE displays no deviation from the voltammogram of the TDAE.

Figure 2.12. Reduction of TCE and c-DCE in aged TDAE solutions, compared to TDAE. Scan Rate 100mV s^{-1}.
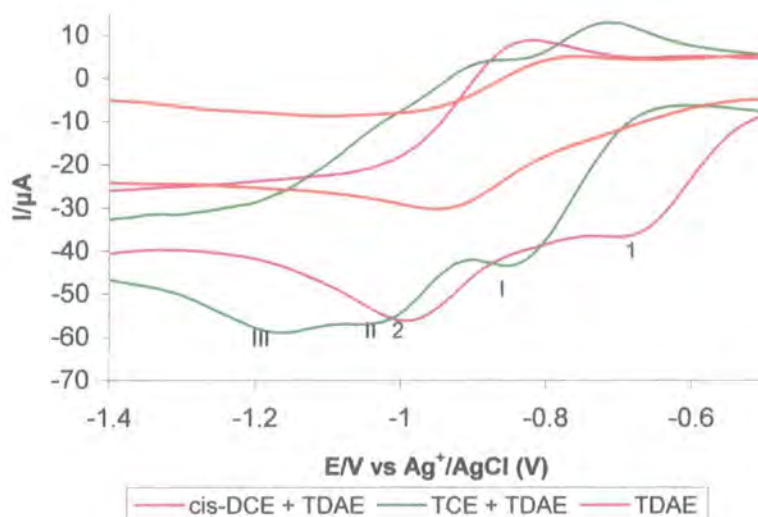
2.4.2 Rotating Disc Electrode Voltammetry

Steady state RDE voltammetry measurements were performed in order to ascertain whether or not adduct formation was occurring. RDE provides data on the oxidative processes occurring during the reaction only. The coloured solutions produced a suite of voltammograms as shown below.

Figure 2.13. RDE voltammograms of coloured TDAE/chlorinated ethene solutions.
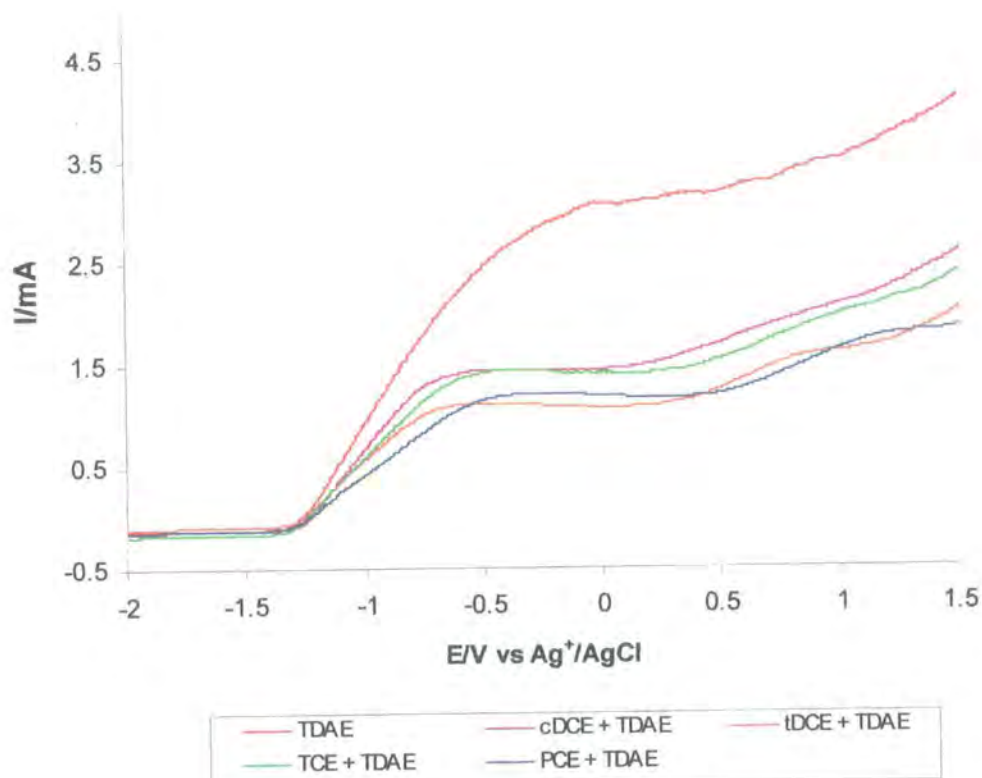
It can be seen from the figure that a much higher current is being produced under RDE than in the cyclic voltammograms previously displayed. This is due to the greater proportion of the solution being drawn to the electrode and reacting, and the much higher kinetic energy of the voltammetric technique. Peak currents and potentials are given in Table 2.2.

Table 2.2. Limiting currents and potentials determined by RDE Voltammetry of fresh TDAE/Chlorinated Ethene solutions.

Analyte	I_L (mA)	E_L (V vs. Ag^+/AgCl)
TDAE	3.1	-0.05
PCE/TDAE	1.2	-0.36
TCE/TDAE	1.4	-0.47
c-DCE/TDAE	1.3	-0.57
t-DCE/TDAE	1.0	-0.6

The single step in the voltammogram around the mean E_p value indicates that the kinetics of the two-step oxidation are slow; with increasing energy in the system the intermediate step is not seen. The high peak current of the TDAE voltammogram reflects the increased amount of oxidation to $TDAE^{2+}$ taking place. The peak currents for the TCE and c-DCE mixtures are slightly higher than those of PCE and t-DCE, suggesting that the reactions of TCE and c-DCE with TDAE are progressing more rapidly.

Diffusion coefficients calculated from the limiting current readings using the Levich equation,

$$i_L = 0.62nF\omega^{1/2}v^{1/6}D^{2/3}c_0 \qquad (3)$$

give direct evidence of adduct formation (Table 2.3). The diffusion coefficient of TDAE, 1.23×10^{-4} cm^2/s, is notably higher than those of the chlorinated solvent mixtures, and the TCE and c-DCE mixtures' coefficients (2.28×10^{-5} cm^2/s) are significantly greater than those of PCE (1.70×10^{-5} cm^2/s) and t-DCE (1.55×10^{-5} cm^2/s). The intermediate diffusion coefficients of TCE and c-DCE demonstrate complexation between them and the TDAE at these oxidation potentials.

Table 2.3. Diffusion coefficients derived from RDE voltammetry using the Levich equation.

Analyte Mixture	Diffusion Coefficient, D (as calculated by Levich equation) (cm^2/s)
TDAE	1.23×10^{-4}
c-DCE + TDAE	2.28×10^{-5}
t-DCE + TDAE	1.55×10^{-5}
TCE	2.28×10^{-5}
PCE	1.70×10^{-5}

The aged, colourless solutions of TDAE and chlorinated ethenes show very different voltammograms, as shown in figure 2.14. As was observed in the cyclic voltammograms, the oxidation at the negative potential is no longer taking place, and a different oxidation can be seen at approximately 0.9V vs. $Ag^+/AgCl$, with TDAE, PCE, TCE and c-DCE. This is the autooxidation of TDAE, which again supports the cyclic voltammetry data. The limiting current is less in all cases except that of c-DCE (Table 2.4). The t-DCE voltammogram displays no evidence of reaction.

Figure 2.14. RDE voltammograms of colourless TDAE/chlorinated ethenes.
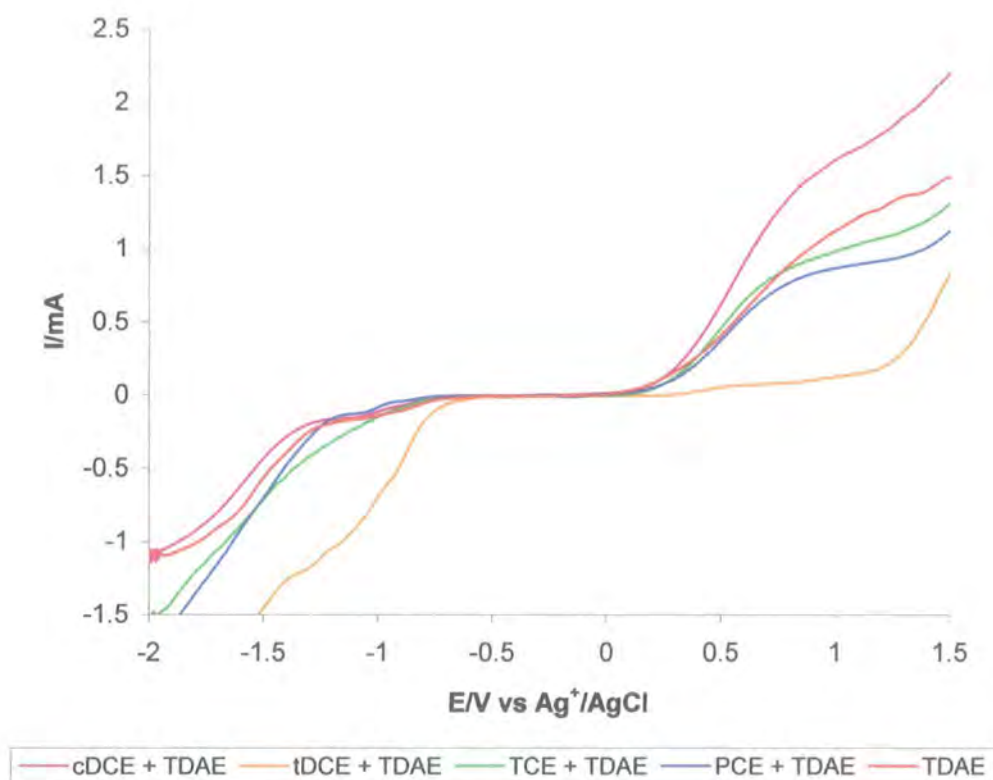
Table 2.4. Limiting currents and potentials determined by RDE Voltammetry of aged TDAE/Chlorinated Ethene solutions.

Analyte	I_L (mA)	E_L (V vs. Ag^+/AgCl)
TDAE	1.20	1.08
PCE/TDAE	0.82	0.88
TCE/TDAE	0.96	0.85
c-DCE/TDAE	1.63	1.01
t-DCE/TDAE	N/A	N/A

2.4.3 Ion Exchange Chromatography

Samples of all chlorinated solvents mixed with TDAE were submitted for ion chromatographic analysis after being left to react together (*i.e*. PCE reacting with TDAE *etc*.) for 24 hours. Results revealed a stoichiometric ratio of chloride ions (3:2) was being produced during the reactions of TCE and c-DCE (see Table 2.5). Examination of PCE showed very little chloride formation, corroborating previous arguments for the formation of a donor-acceptor complex[7]. T-DCE produced less than 1ppm chloride, therefore it can be concluded that no reaction between t-DCE and TDAE is occurring.

Table 2.5. Chloride formation in analyte solutions.

Analyte Mixture	Chloride content (ppm)
PCE/TDAE (colourless)	2.0
TCE/TDAE (colourless)	31.3
Cis-DCE/TDAE (colourless)	19.0
trans-DCE/TDAE (colourless)	0.88

This evidence clearly demonstrates the dechlorination of both the c-DCE and the TCE by TDAE. The three to two stoichiometric ratio of the chloride content shows that when the TCE reacts, three chlorides are removed from the chlorinated ethene molecule, and when the c-DCE reacts, two chlorides are removed. The lack of reaction by t-DCE presents further evidence for the evaporation of t-DCE from solution before any dechlorination process can occur.

2.4.4 UV-vis Spectroscopy

Fresh solutions analysed prior to RDE voltammetry showed an absorbance peak at 391nm (Fig 2.15). This is consistent with results published by Kuwata and Geske[9], which describe an intense absorption maximum at wavelength 385nm, and that peak was confirmed by electron spin resonance spectroscopy as corresponding to the formation of the $TDAE^+$ cation radical. The increased initial absorbance values (see Table 2.6) in the presence of the chlorinated ethenes PCE, TCE and c-DCE suggests that the presence of the chlorinated ethenes is enhancing the production of the radical cation, which correlates with the catalytic behaviour seen in the electrochemical studies.

Figure 2.15. UV Spectra of TDAE/Chlorinated Ethene solutions prior to RDE voltammetry.
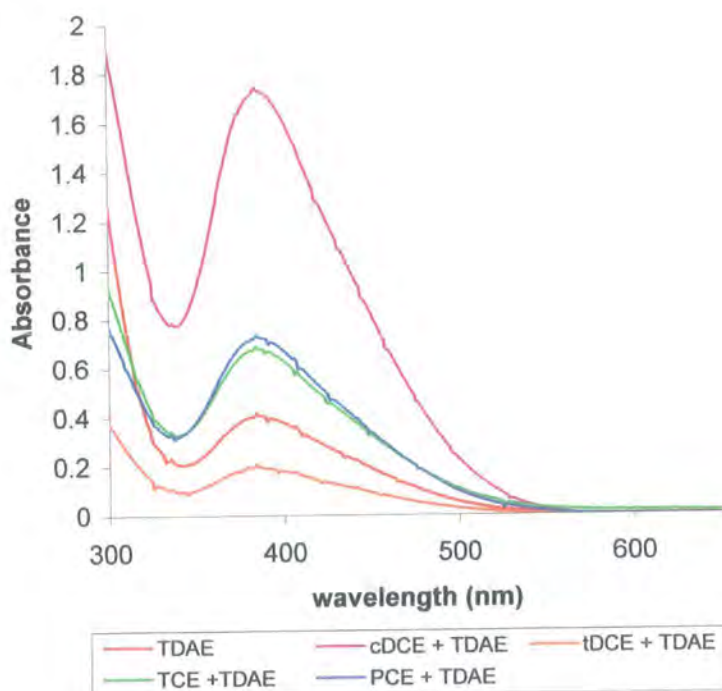
$TDAE^+$ is formed as an intermediate step in the oxidation of TDAE to $TDAE^{2+}$. Therefore as the production of $TDAE^{2+}$ goes to completion, the absorbance at this wavelength would be expected to drop. Examination of the solutions after being

subjected to RDE showed this to be the case (Fig 2.16). The order of decrease in absorbance observed when chlorinated ethenes were added was as follows: c-DCE > PCE > TCE. (Fig 2.17), and is quantified in Table 2.4. Of all the mixtures, t-DCE/TDAE alone displayed an increase in absorbance, which may be due to experimental error.

Figure 2.16. Contrast in Absorbance of TDAE pre and post RDE voltammetry.
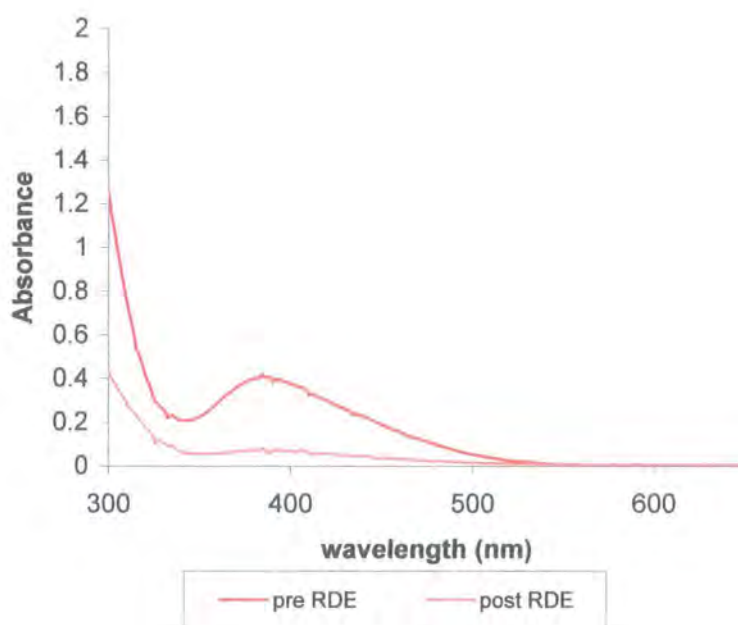
Table 2.6. Change in Absorbance displayed by TDAE/chlorinated ethene solutions.

Reactant Mixture	Pre-RDE Absorbance (A)	Post-RDE Absorbance (A)	ΔA
TDAE	0.405	0.052	-0.353
PCE/TDAE	0.722	0.211	-0.511
TCE/TDAE	0.661	0.266	-0.395
c-DCE/TDAE	1.723	0.794	-0.929
t-DCE/TDAE	0.192	0.567	+0.375

Figure 2.17. UV Spectra of TDAE/Chlorinated Ethene solutions post RDE voltammetry.
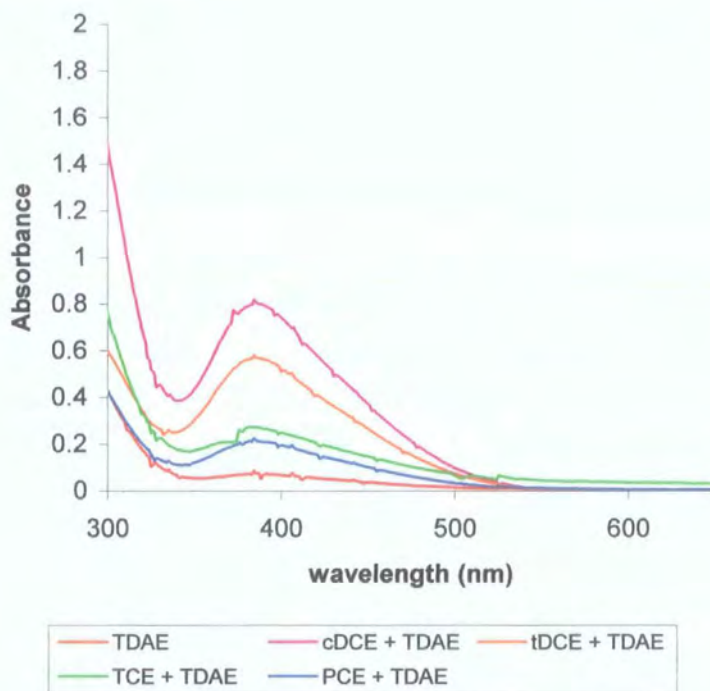
On the basis of the UV-vis data, fresh samples of the TDAE/chlorinated ethene solutions were submitted for ^{1}H NMR monitoring over the course of the dechlorination reaction. Unfortunately however, the spectra obtained were so complex as to be inconclusive.

2.5 Conclusions

TDAE demonstrated a two-step oxidation under voltammetric examination that corresponds well to previously published work. The data obtained suggests, however, that the reactions taking place when TDAE is added to the different chlorinated ethenes are not uniform.

PCE/TDAE, TCE/TDAE and c-DCE/TDAE all display markedly altered voltammograms from that of the simple TDAE; t-DCE does not. This would suggest two possibilities;

1) That the dechlorination of t-DCE occurs almost instantaneously; the voltammogram seen under electrochemical investigation would then show only residual TDAE.

2) The volatile nature of t-DCE has caused it to evaporate from the solution prior to any electrochemical examination.

The latter would seem to be more likely, and we can therefore conclude that t-DCE may not be of concern as a groundwater pollutant[16].

If a reaction is occurring between t-DCE and TDAE, then the reactions of c-DCE, PCE and TCE with TDAE are kinetically slower. Their electronegativity lowers the activation energy barrier, and combined with the electrode potential produces an electrocatalytic effect on $TDAE^{2+}$ production, as evidenced by the high current and steep peaks of the cyclic voltammograms.

The diffusion coefficients calculated for c-DCE and TCE mixtures with TDAE indicate complexation between the TDAE and the chlorinated ethenes. The stoichiometric ratio of chloride ions produced and the 3:2 ratio of reductions shown in their respective voltammograms (Figure 2.11), together with this evidence of complexation, is confirmation that a dechlorination reaction is taking

71

place between TCE/c-DCE and TDAE. The lack of reaction displayed by PCE under electrochemically reducing conditions, its lower diffusion coefficient, and lack of chloride production conforms to the published formation of a donor-acceptor complex between PCE and TDAE[7].

Based on the above evidence, and work by Carpenter[12] and Chambers *et al.* with TDAE and fluorinated compounds[17], the dechlorination reaction probably proceeds via the removal of the most positive halogen first. The mechanism for the dechlorination of TCE is shown below (Fig. 2.18).

The reaction mechanism of abiotic dechlorination of chlorinated ethenes where the chlorinated ethenes are present as an electron acceptor has been elucidated. This study will serve as a useful model for investigation of an environmentally viable abiotic dechlorination methods.

Figure 2.18. Reaction mechanism of TCE dechlorination.
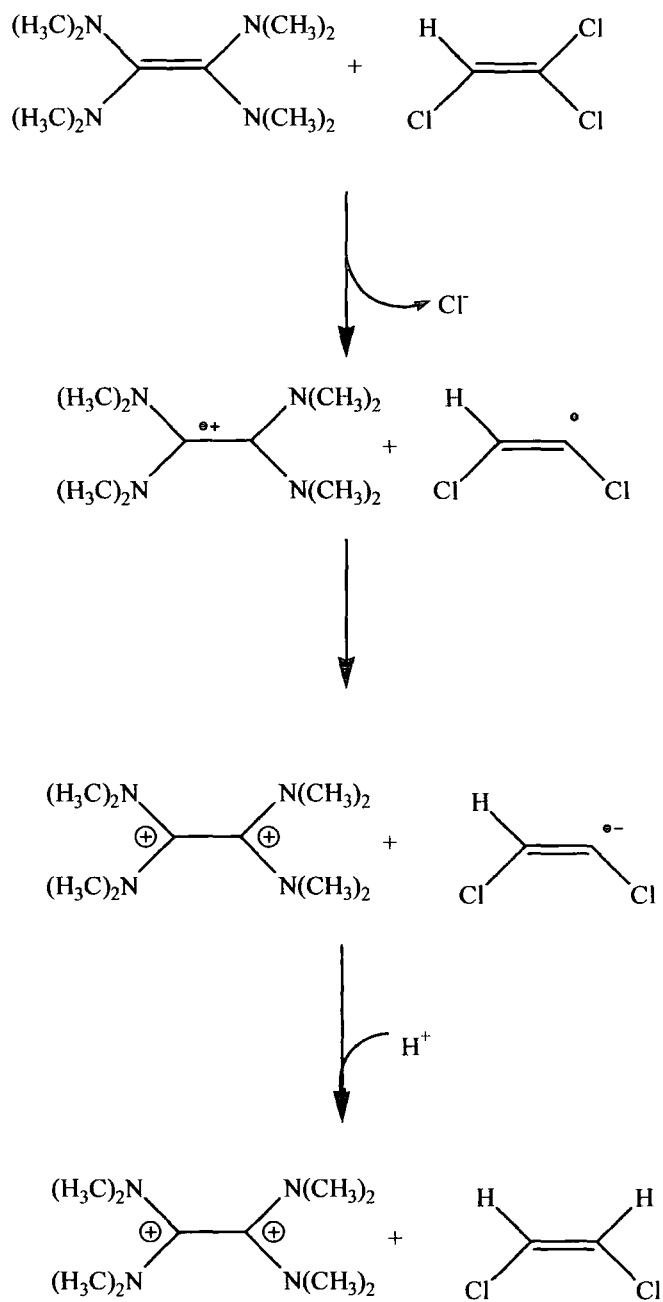
REFERENCES

1. Pruett, R.L., Barr, J.T., Rapp, K.E., Bahner, C.T., Gibson, J.D., and Lafferty Jr., R.H., *J. Amer. Chem. Soc.,* **1950**, 72, 3646.

2. Wanzlick, H.-W., and Schikora, E., *Angew. Chem.,* **1960**, 72, 494.

3. Urry, W.H., and Sheeto, J., *Photochem. Photobiol.,* **1965**, 4, 1067.

4. Fletcher, A.N., and Heller, C.A., *J. Phys. Chem.,* **1967**, 71, 1507.

5. Wiberg, N., and Buchler, J.W., *Chem. Ber.,* **1963**, 96, 3223.

6. Thun, W.E., *J. Org. Chem.,* **1967**, 32, 503.

7. Wiberg, N., *Angew. Chem. Internat. Edit.,* **1968**, 7, 766.

8. King, R.B., *Inorg. Chem.,* **1965**, 4, 1518.

9. Kuwata, K., and Geske, D.H., *J. Amer. Chem. Soc.,* **1964**, 86, 2101.

10. Burkholder, C., Dolbier Jr., W.R., and Médebielle, M., *J. Org. Chem.,* **1998**, 63, 5385.

11. Briegleb. G. Elektronen-Donator-Acceptor-Komplexe. Springer, Berlin, 1961

12. Carpenter, W., *J. Org. Chem.,* **1965**, 30, 3082.

13. Chambers, R.D., Nishimura, S., and Sandford, G., *J. Fluorine Chem.,* **1998**, 91, 63.

14. Briscoe, M.W., Chambers, R.D., Mullins, S.J., Nakamura, T., Vaughan, J.F.S. and Drakesmith, F.G., *J. Chem. Soc. Perkin Trans. 1,* **1994**, 3115.

15. Burkholder, C., Dolbier Jr., W.R., and Médebielle, M, *Tetrahedron Lett.,* **1997**, 38, 821.

16. Wiedemeier, T., Rifai, H., Newell, C., and Wilson, T., *Natural Attenuation of Fuels and Chlorinated Solvents in the Subsurface*, John Wiley and Sons Inc., New York, **1999.**

17. Chambers, R.D., Gray, W.K., Kom, S.R., *Tetrahedron,* **1995**, 51, 13167 – 13176.

CHAPTER 3
Corrinoids and cobalt:
a viable abiotic alternative?

CHAPTER 3

Corrinoids and cobalt: a viable abiotic alternative?

3.1 Introduction

As was discussed in the Introduction, one of the major directions in which research into reductive dechlorination is leading is artificial enhancement of the existing biotic processes. Since studies of TDAE have shown that an abiotic system utilising a strong electron donor is capable of reductively dechlorinating PCE and TCE under anaerobic conditions, the next step in devising a suitable remediation augmentation is to isolate a donor which is 'environmentally friendly', i.e. a compound which presents little or no toxicological threat.

Since natural ecosystems have proved to be successful in producing dechlorinating methods, the best course would be to investigate their biochemistry to determine whether or not a biomimetic technique could be designed to achieve the same effect.

3.2 Literature Review

3.2.1 Microbial activity and its effect on chlorinated ethene pollution.

As a general consideration, it can be stated that the incidence of chlorinated ethenes in the environment is roughly determined (not taking into consideration the initial spillage) by their sensitivity to biodegradation or transformation by microbial organisms. More specifically, the determination rests with anaerobic organisms; aerobic bacteria are incapable of degrading PCE[1] (the standard potentials of the chlorinated ethenes are too high to be easily oxidised).

CHAPTER 3
Corrinoids and cobalt:
a viable abiotic alternative?

A great deal of study into the dechlorination of chlorinated molecules (alkenes and aromatics) by anaerobic bacteria has been carried out. Initial work showed that mixed cultures of anaerobic bacteria are capable of dehalogenating chlorinated pollutants in contaminated industrial sites[2]; sulphate-reducing[3,4,5], methanogenic and acetogenic[1] bacteria all have the ability to reductively dechlorinate molecules as a co-metabolic process, incidental to their primary metabolic functions. Laboratory work by Boopathy and Peters[6] demonstrated complete conversion of TCE to ethene by a mixed consortium of bacteria. Reductive dehalogenation is mostly favoured in methanogenic and sulphate reducing conditions[7,8].

A fundamental principle of ecological diversification is that environmental pressure (for example, competition between organisms for nutrients or living space) will drive species to specialise in an available 'niche'. As a consequence of chlorinated compound contamination, the evolution of dehalorespiratory species of bacteria has occurred. As noted by Holliger et al.[9] during their isolation of the *dehalobacter restrictus* bacterium, PCE and TCE are strictly anthropogenic chemicals. Their presence in the environment is solely a function of human activity; hence their development is limited to the last fifty years.

The first species of bacteria capable of dechlorination to be isolated (in 1990) was *Desulfomonile tiedjei*, which dehalogenates chlorinated aromatics such as 3-chlorobenzoate[10], which was followed by Freedman and Gosset's work on the dechlorination of dichloromethane (DCM), showing that dechlorination was occurring in different reducing conditions and was not therefore attributable (in this case) to methanogenic bacteria[11]. By 1998, six strains of bacteria with the ability to use PCE or TCE as an electron acceptor had been isolated; the best known of these are *Dehalospirillum multivorans* and *Dehalobacter restrictus*.

The process termed 'halorespiration' makes use of chlorinated ethenes by employing them as electron acceptors, and utilising the energy generated to

CHAPTER 3
Corrinoids and cobalt:
a viable abiotic alternative?

synthesise Adenosine Triphosphate (ATP); chlorinated compounds are known to be better oxidants than nitrates[12]. The positive redox potential of the PCE/TCE couple (0.576V)[13] means that the reaction

$$R\text{---}Cl + 2[H] \rightarrow R\text{---}H + H^+ + Cl^-$$
(1)
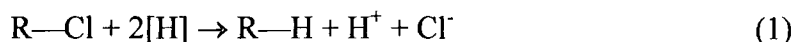
is thermodynamically favourable.

3.2.2 Electron donors and the role of hydrogen

"Complete conversion, when it is found, probably depends critically on the availability of an electron donor source to perform the key functions of: (1) supporting growth of methanogenic or sulphate-reducing microbial communities that produce strongly reducing conditions; and (2) providing hydrogen or other direct electron donor for use by the dehalogenating bacteria." J.F. Ferguson and J.M.H Pietari.[8]

If chlorinated ethenes are critical to microbial growth as electron acceptors, equally important to an organism's metabolism is the growth substrate; the electron donor. Common electron donors for microbial systems include dihydrogen, formate and acetate[14]. Considering the two most common dehalorespiratory bacteria, *d. multivorans* is capable of using any of the substrates mentioned above; conversely, *d. restrictus* will thrive only with dihydrogen as its donor. Ballapragada *et al.* demonstrated a Michaelis-Menten relationship between hydrogen partial pressure (substrate concentration) and dechlorination[15]. The Michaelis-Menten relationship is expressed as:

$$V_0 = \frac{V_{max}[S]}{K_m + [S]}$$
(2)

CHAPTER 3
Corrinoids and cobalt:
a viable abiotic alternative?

for the reaction

$$E + S \underset{k_2}{\overset{k_1}{\rightleftharpoons}} ES \xrightarrow{k_3} E + P$$

(3)
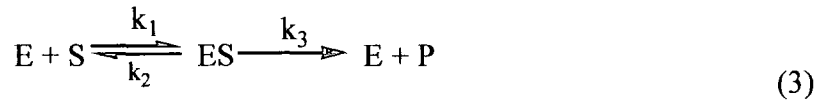
where E = Enzyme

S = Substrate

P = Product

V_0 = initial reaction rate

V_{max} = maximum reaction rate

$K_m = k_2 + k_3/k_1$ = the Michaelis constant.

If an enzyme system is said to demonstrate a Michaelis-Menten relationship, K_m is equal to the substrate concentration, [S], at which the reaction rate is half its maximal value.

Dehalorespiratory bacteria are not the sole consumers of hydrogen in anaerobic environments, which raises the issue of competition for nutrients, most usually with methanogenic organisms. Smatlak et al.[16] noted "inexplicable" variations in dechlorination rates at different field sites with similar anaerobic conditions. Comparing this to Ballapragada's observations of variance in dechlorination rate with reducing conditions[15], it can be deduced that competition is as important a factor in dechlorination as the correct anoxic conditions.

Smatlak et al.'s study suggested that as competition increased, methanogenic bacteria tended to benefit. It demonstrated that the half velocity constant for dechlorination, with H_2 as the substrate, was considerably lower than that of methanogenesis, i.e. that dechlorinating bacteria require a much lower level of H_2 than methanogens, and suggested that fermentation of other electron donors such as ethanol or butyrate to give a consistent, low-concentration feed of hydrogen might promote more effective dechlorination. This observation was confirmed by

CHAPTER 3
Corrinoids and cobalt:
a viable abiotic alternative?

Carr and Hughes'[17] work on mixed culture dechlorination. Yang and McCarty[7], as well as confirming effective dechlorination at low H_2 levels, found that electron acceptors each have a unique "threshold concentration" of hydrogen; this may be of use in defining reducing conditions at a given site[18].

3.2.3 Enzyme chemistry

Biologically, the key component in microbial reductive dehalogenation is the intracellular enzyme dehydrogenase. The first example of these enzymes was reported by Neumann et al. in 1994[19]; a tetrachloroethene dehalogenase isolated from *D. multivorans*. Other early isolates have been reported[20, 21, 22], for both chlorinated ethenes and aromatics: Holliger *et al.* provide a complete listing in his review of bacterial reductive dechlorination[23].

Neumann *et al.*'s[19] study of a PCE dehalogenase purified from *Dehalospirillum multivorans* provides clear evidence for the presence of a corrinoid (a cobalt metal-centred stable macrocycle) coenzyme, having noted that their utilisation in previous studies on reductive dechlorination of haloalkanes[24] (using titanium (III) citrate as an electron donor)[25] had shown successful dechlorination. An extract of isolated PCE dehalogenase was pre-treated with titanium (III) citrate, then reacted with PCE. The reaction was then subjected to the addition of propyl iodide, since "Corrinoid enzymes are known to be inactivated by alkyl halides such as propyl iodide exclusively when the cobalt is in the reduced state Co (I); the inactivation is reversed by illumination."[19] Propyl iodide was found to reduce the activity of the PCE dehalogenase to 10%, and the lost activity was completely restored by light, therefore it can be concluded that dehalogenation by the enzyme is attributable to the presence of the corrinoid (cobalamin). The requirement for pre-treatment with the reducing agent Ti(III) citrate shows that the natural state of the corrinoid in the enzyme is its oxidised form; this was confirmed by the enzyme's

CHAPTER 3
Corrinoids and cobalt:
a viable abiotic alternative?

inhibition in the presence of cyanide. Work by Christiansen *et al.* confirmed the corrinoid presence in dehalorespiratory bacteria using UV spectroscopy[22].

Holliger *et al.*'s review divulges that of nine isolated bacterial species capable of reducing PCE, eight (including *dehalospirillum multivorans*) contain a corrinoid cofactor. Further investigation[19, 26] led to the proposal of the theoretical reaction mechanism shown below as the likely method of dehalogenation (Fig. 3.1).

Figure 3.1. Proposed dehalogenation method for PCE dehalogenase corrinoid.
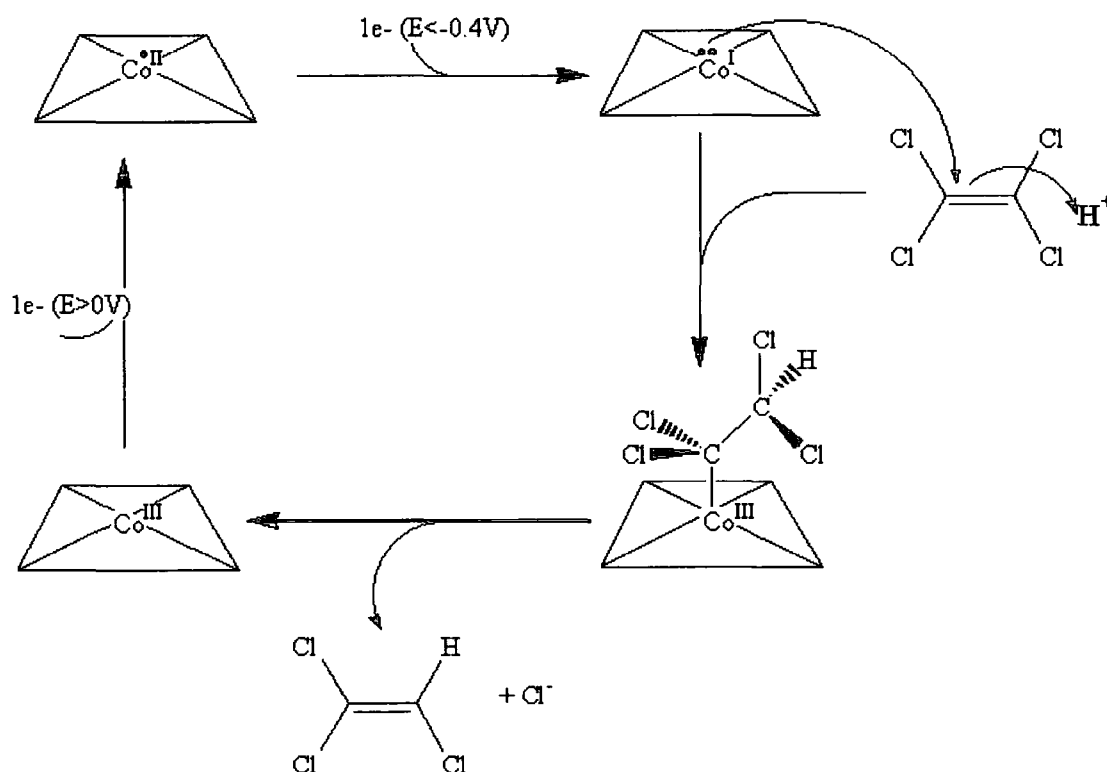
Later work by Holliger *et al.*[27] and Glod *et al.*[28] provided experimental evidence for a different mechanism. A one-electron transfer from the reduced cob(I)alamin to the PCE produces a chloride anion, which is eliminated to yield a trichloroethenyl radical that combines with a H-radical to give TCE (Fig. 3.2).

CHAPTER 3
Corrinoids and cobalt:
a viable abiotic alternative?

Figure 3.2. One electron transfer mechanism for dechlorination.
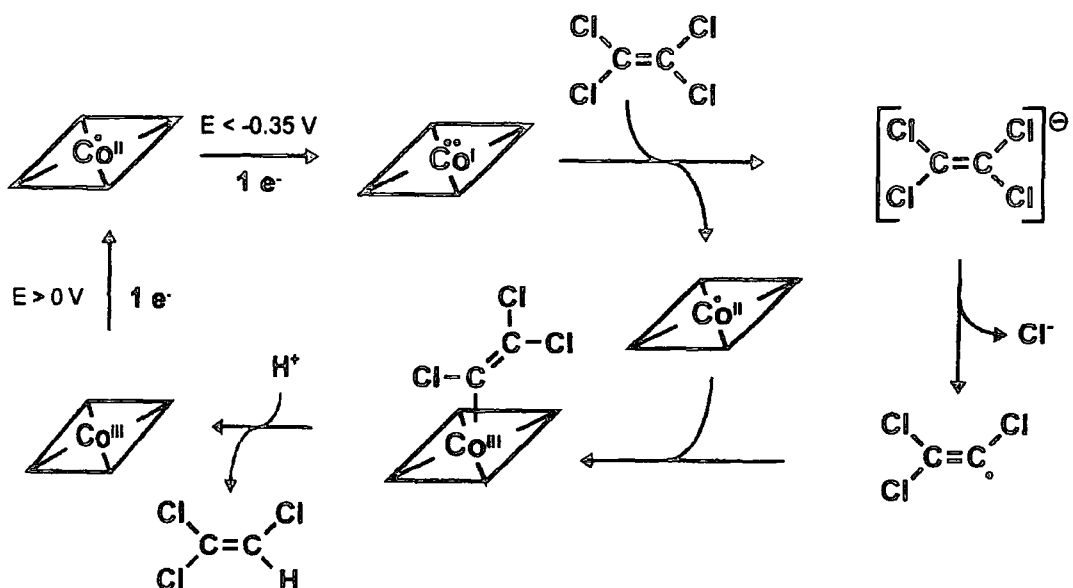
3.2.4. Reductive dehalogenation by cyanocobalamin (Vitamin B_{12})

Vitamin B_{12} (Fig. 3.3) is a corrinoid molecule similar to the cofactor present in dehalorespiratory bacteria. As such, and based on the successful corrinoid-catalysed dechlorination of chloroalkanes, it would be reasonable to assume that Vitamin B_{12} would similarly be able to reductively dechlorinate chlorinated ethenes. The first study on B_{12} in this capacity was done by Gantzer and Wackett[29]. Utilising titanium (III) citrate as an electron donor, they found that reacting Vitamin B_{12} with PCE led to the stoichiometric formation of TCE, and reaction of Vitamin B_{12} and TCE produced a stoichiometric concentration of DCE (with >90% forming as the *cis*- isomer). The absence of either Ti(III) citrate or Vitamin B_{12} resulted in failure to react, and from this it was concluded that the so-called 'super-reduction' of cobalt to the Co(I) state was necessary for the reaction to occur. The reaction rate for the dechlorination proved to be much slower than that of the enzyme-catalysed reactions.

CHAPTER 3
Corrinoids and cobalt:
a viable abiotic alternative?

Figure 3.3. Vitamin B_{12} (cyanocobalamin)
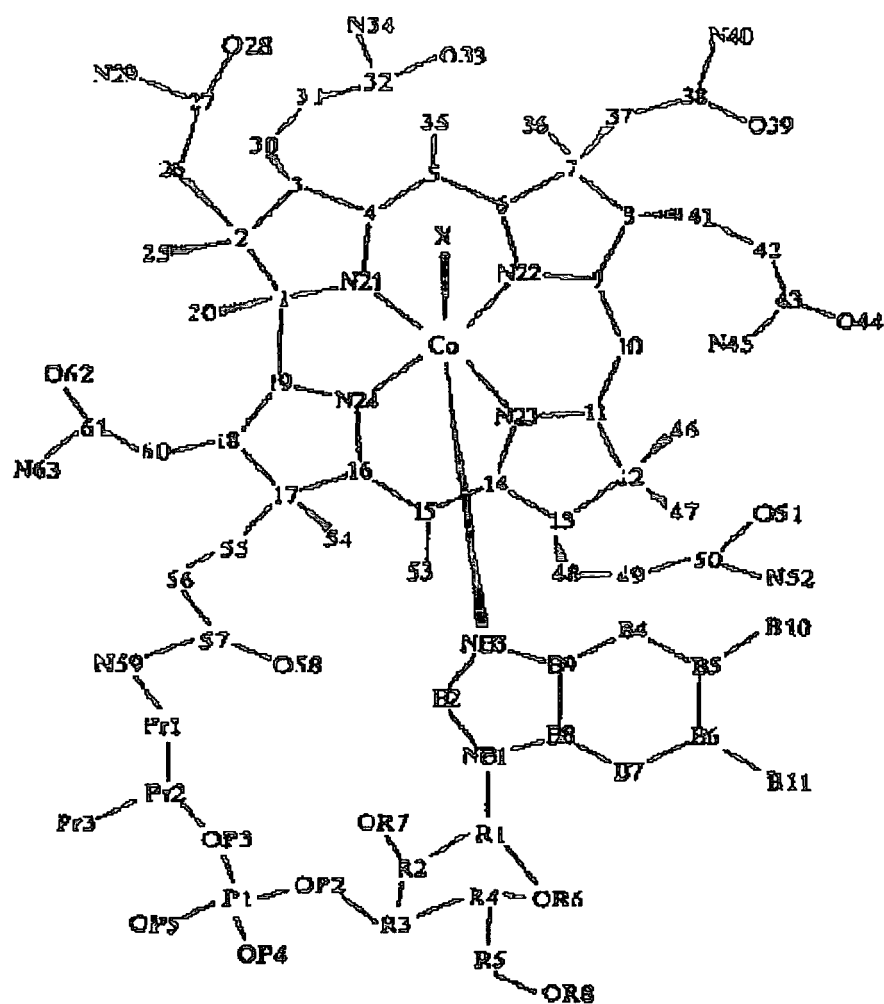
Later work by Shey and Van der Donk[30] focused on the mechanistic aspects of the reaction, and determined that the first step of the reaction pathway for Vitamin B_{12} dechlorination is the catalytic one-electron transfer from Vitamin B_{12} to PCE, as shown above for the enzyme cofactor.

CHAPTER 3
Corrinoids and cobalt:
a viable abiotic alternative?

3.2.5 Transition metals and electrochemical reduction

Super-reduced corrinoids are known to be very strong nucleophiles, however very negative conditions are required for such reduction.

$$E^0[\text{Co}^{+/2+}] = -606\text{mV} \tag{4}$$

While addition of Ti(III) citrate to a reaction mixture can produce the required reducing conditions, in terms of methods applicable to actual remediation the introduction of further anthropogenic chemicals to the system is undesirable. Electrochemical methods offer a 'cleaner' means to a highly reducing environment, and investigations of its use in conjunction with transition metals as electron donors are numerous in existing literature.

Early work on the subject was done by Norton[31] and Geoly[32], who showed that dechlorination of polychlorinated phenols could be achieved by passing an electric current through solutions. Most published work has focused on the transformation of chloroaromatics, particularly pentachlorophenol, utilising bulk electrolysis methods.

The proposal that metallic iron filings could be used for reductive dechlorination of pollutants in groundwater[33] was the beginning of research into transition metal-enhanced dechlorination. Work by Weathers et al.[34] described the use of zero valent iron to assist the reductive dechlorination of chlorinated aliphatic hydrocarbons, through hydrogen production, in reactor experiments, and has led to further investigation of electrochemically-assisted systems. Farrell et al.[35] investigated the efficacy of a reactor dechlorination system for PCE and TCE, in conjunction with an amperometric study which employed zero valent iron aggregate and wire electrodes. Their findings suggested different methods of dechlorination acted on the chlorinated solvents. PCE was found to reduce by direct electron transfer, and TCE by reaction with atomic hydrogen released by

CHAPTER 3
Corrinoids and cobalt:
a viable abiotic alternative?

iron corrosion. In another study, Farrell and Li[36] investigated the effect of palidized-iron cathodes on dechlorination of TCE and carbon tetrachloride, reporting a half-life of 9.4 minutes for TCE in the reactor, with the primary products being ethene and ethane, and less than 2% chlorinated reaction by-products. The addition of palladium as an electrocatalyst increased reaction rates by a factor of three. Again, the mechanism of TCE reduction is suggested to be indirect, via atomic hydrogen.

Other work in the area has been undertaken examining the use of a zinc cathode to reduce pentachlorophenol (PCP) by bulk electrolysis. Lin and Tseng[37] showed that PCP could be reduced to less chlorinated phenols, using hydrogen as a catalyst, but at concentrations too high for environmental application.

Work with modified carbon electrodes in the field of electrochemical dechlorination is limited to chloroaromatic molecules. Transition metals, however, continue to play a critical role in investigations in this area, as they are employed to modify the carbon electrodes. Carbon-felt electrodes modified with palladium were reported as successful in dechlorinating chlorinated aromatic compounds[38, 39, 40]. Hydrogen is reported to have an enhancing effect on dechlorination, and palladium's catalytic effect on the process is attributed to its ability to absorb hydrogen into its lattice[38, 39]. Dabo et al[41] reported similar success with palladium and rhodium modified reticulated vitreous carbon electrodes.

CHAPTER 3
Corrinoids and cobalt:
a viable abiotic alternative?

3.2.6. Conclusion

From the above findings, it was concluded that an environmentally acceptable electrochemical method might be rendered by the use of a cobalt compound/corrinoid in conjunction with potentiostatic control to produce the extremely negative potential conditions necessary to reduce the metal to its Co^+ state.

CHAPTER 3
Corrinoids and cobalt:
a viable abiotic alternative?

3.3 Experimental

3.3.1 Materials

Cobalt (II) chloride hexahydrate was supplied by Janssen Chemicals (Belgium). Unrefined cane molasses sugar was purchased from a local retailer. All aqueous samples were made up using de-ionised water (Purite filtration system). Glucose, fructose, sucrose, PCE, c-DCE t-DCE, and Vitamin B_{12} were purchased from Sigma-Aldrich (Poole, Dorset, UK). Trichloroethene (TCE), potassium nitrate (KNO_3), and potassium chloride (KCl) were from BDH (Lutterworth, Leics, UK).

3.3.1.1 Composition of Molasses

In this study, we chose to use molasses, previously studied by Boopathy et al[42], as the substrate for bacterial growth. It meets the criteria of a substrate on several levels;

- It can ferment to produce a mixture of other substrates such as methanol and lactate
- It can be broken down to pyruvate through glycolysis by bacteria (pyruvate is known to be an effective electron donor for PCE)[12].
- It can act as a source for hydrogen,
- It supplies nutrients for bacterial growth.

Molasses is a by-product of the sugar refining process, and is predominantly a mixture of carbohydrates. Compositions vary with sugar cane type, provenance, and molasses type (e.g. edible molasses has a higher sucrose: reducing sugars ratio than has blackstrap, the final industrial residue). Typical carbohydrate compositions are summarised in the table below.

86

CHAPTER 3
Corrinoids and cobalt:
a viable abiotic alternative?

Table 3.1 Typical compositions of molasses cane sugar residue[43].

Component	% present in molasses
Sucrose	35 – 50
Reducing Sugars (Glucose + Fructose)	20 - 35
Sugar breakdown products	10
Nitrogen	1
Non-nitrogenous acids	8
Vitamins	Trace
Inorganic components (carbonate ash)	14

3.3.2 Methods

3.3.2.1 Cyclic Voltammetry

All Cyclic Voltammetry was carried out under anaerobic conditions, using a three-electrode cell set-up and potentiostat as previously described (Chapter 2). The cell was placed in a Faraday cage to limit interference. The RE was Ag/AgCl, the AE was platinum, and the WE was either platinum or glass carbon. Cobalt (II) chloride, chlorinated ethenes and molasses were all used at a concentration of 0.01mol dm^{-3}: Vitamin B_{12}, due to its documented catalytic nature and high molecular weight, was used at a concentration of 0.001mol dm^{-3}. 0.1mol dm^{-3} KCl was used as the background electrolyte except in pH dependent experiments, where the buffer salts fulfilled the capacity. For pH dependent experiments phosphate buffer (Na_2HPO_4: NaH_2PO_4) was used for pH ≤ 7.5; carbonate buffer (Na_2HCO_3: $NaHCO_3$) was used for pH > 7.5.

Voltammetric scans were run from $-1.5V$ to $1.5V$, the maximum range permitted by the background electrolyte's voltage window (Figure 3.4 [the reductive peak seen at 0.34V is due to impurities in the KCl salt]). The extremely negative initial

CHAPTER 3
Corrinoids and cobalt:
a viable abiotic alternative?

potential was utilised to ensure that cobalt was present in its super-reduced, Co(I), state.

Figure 3.4. Voltage window of 0.1mol dm^{-3} KCl$_{(aq)}$ electrolyte, glassy carbon electrode.
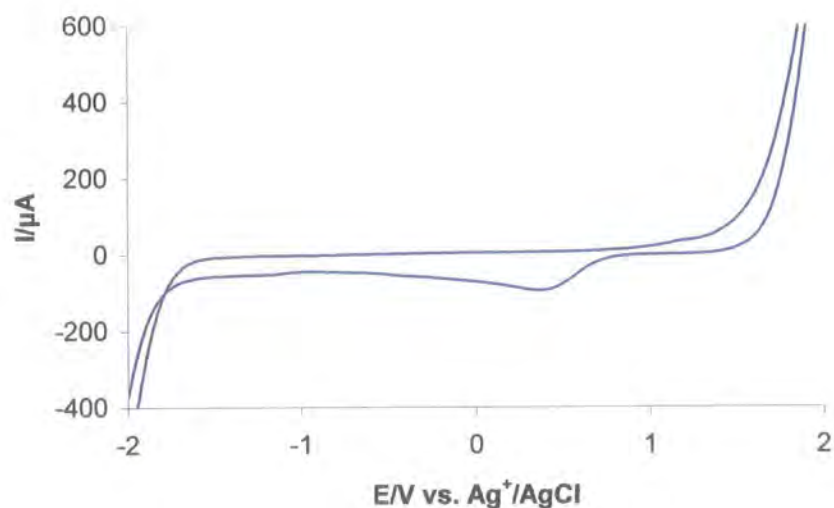
3.3.2.2 Rotating Disk Voltammetry

The RDE Voltammetry set up was as previously described. All analytes and concentrations are identical to those for CV (0.01mol dm^{-3} cobalt(II) chloride, chlorinated ethenes and carbohydrates, 0.001mol dm^{-3} Vitamin B$_{12}$).

3.3.2.3 Controlled Potential Electrolysis

Controlled potential electrolysis (or potentiostatic coulometry) is a technique which relies upon the passage of a known quantity of electricity through a solution. The charge passed, Q, drives the desired reaction. The potential of the system is held at a value which ensures that the reaction will occur (usually

CHAPTER 3
Corrinoids and cobalt:
a viable abiotic alternative?

slightly positive or negative of the E^0 of the electroactive species, depending on which way the reaction is to progress).

As the electroactive species is consumed, the current will decay exponentially, i.e.

$$I_t = I_0 \exp(-pt) \qquad (5)$$

where p = constant

I_t = current at time t

I_0 = initial current

t = time

Thus Q_t, the charge at a given time t, is given by:

$$Q_t = \int_0^t I_t dt = Q_\infty (1 - \exp[-pt]) \qquad (6)$$

which solves to:

$$Q_t = I_0/p - I_t/p \qquad (7)$$

Q_∞ is the charge passed after all the electroactive species in the solution are consumed, and is given by:

$$Q_\infty = nFVc \qquad (8)$$

where n = number of electrons

F = Faraday's constant

V = volume of electrolyte (dm^{-3})

c = concentration of electrolyte (mol dm^{-3})

Hence, since n and F are known constants, the amount of material produced is related to Q without need for any calibration. This simplicity makes controlled potential electrolysis an attractive analytical technique.

In this case, the purpose of the experiment was to monitor chloride production, as opposed to the reduction of Co(II) to Co(I), therefore a simple programmable

CHAPTER 3
Corrinoids and cobalt:
a viable abiotic alternative?

current source was employed to accomplish the electrolysis; the potentiostatic control common to coulometric analysis could be dispensed with.

Controlled potential electrolysis was carried out in a cell purchased from BAS (West Lafayette, IN, USA). An example is shown in Figure 3.5. The WE was reticulated vitreous carbon mesh, and the AE was a platinum coil. The reference electrode was a BAS aqueous $Ag^+/AgCl$ electrode. The RE was isolated from the cell by a potassium nitrate salt bridge to prevent leaching of chloride from the inner filling solution, which could lead to false chloride concentration readings. For the same reason, the background electrolyte was 0.1mol dm^{-3} KNO_3. The solution was stirred continuously by magnetic stirrer, and purged continuously with argon. The potential set for the electrolysis was $-2V$ vs. Ag/AgCl, in order to maintain the metal's redox state as Co(I).

Figure 3.5. Bulk electrolysis cell.

CHAPTER 3
Corrinoids and cobalt:
a viable abiotic alternative?
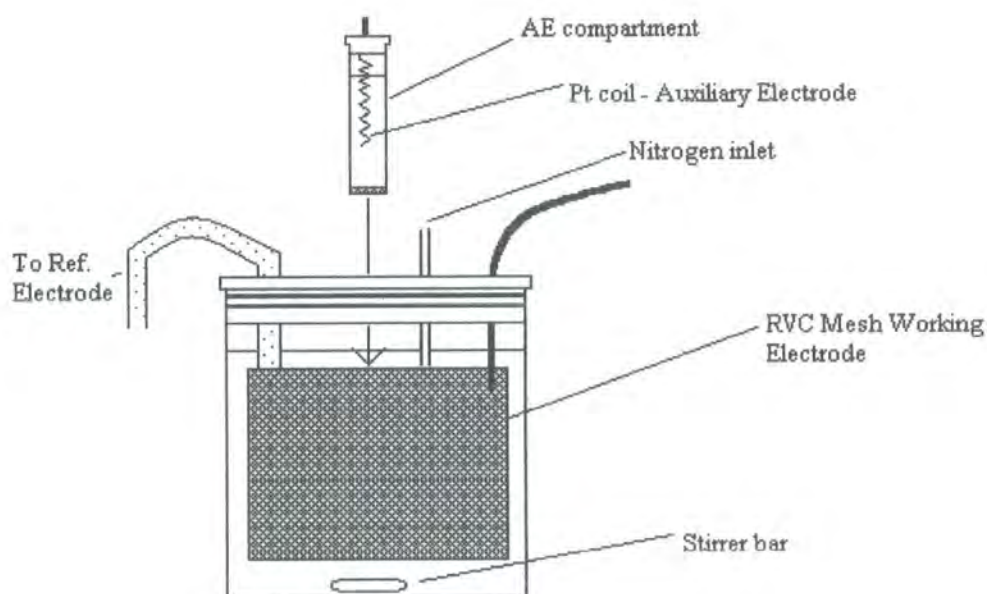
The potential was applied and maintained by a Keithley 224 programmable current/voltage source.

Measurements were taken on an hourly basis using UV-vis spectroscopy, and pre and post experimental samples were submitted to the department's Analytical services division for chloride analysis via Ion Exchange Chromatography (carried out on a Dionex (Sunnyvale, CA, USA) DX-120 Ion Chromatograph). UV-vis measurements were taken in quartz cells of path length 1cm. The experiments were run for eight hours.

3.3.2.4 Continuous voltammetric monitoring experimental

Long term monitoring was carried out in specially designed cells (see Fig 3.6) manufactured by the departmental glassblowers. 150ml of aqueous analyte solution was placed in the cells. The gas in and gas out ports were sealed with butyl rubber septa and aluminium crimp caps. The electrodes (Platinum AE, Glassy Carbon WE) were introduced through the Teflon cap, and any gaps were then sealed using Dow Corning silicone sealant. The O-rings on the cap provide the cell seal, which was reinforced with Parafilm. Then the entire system was purged with nitrogen via the septa-sealed gas ports (to simulate anaerobic conditions), and connected to the potentiostat. Four cells were prepared, all linked to the same remote reference electrode via saturated KNO_3 salt bridges[1]. The cells were designated as follows:

1. The Control cell. $0.01 mol\, dm^{-3}$ PCE, and $0.01 mol\, dm^{-3}$ molasses, in the background electrolyte ($0.1 mol\, dm^{-3}$ KNO_3). Molasses was chosen as the substrate. No reducing agent was introduced.

2. The Cobalt (II) Chloride cell. $Co(II)Cl_2$ was introduced to the substrate solution at $0.1 mol\, dm^{-3}$.

---

[1] Salt bridge composition – $2.5 mol\, dm^{-3}$ (saturated) KNO_3 in Agar solution (3.5g/100ml)

CHAPTER 3
Corrinoids and cobalt:
a viable abiotic alternative?

3. The Vitamin B_{12} cell, containing $0.001 mol\ dm^{-3}$ Vitamin B_{12} in the substrate solution

4. The Bacterial cell. 10ml of a culture of *Dehalobacter Restrictus* was added to the substrate solution. The culture was introduced to the cell after purging and sealing, as the bacteria is an anaerobic species. Purging of the cell was carried out once a week to remove any build up of noxious gases (e.g. CO).

The experiment was run for 57 days. A Cyclic Voltammetry sweep was performed daily, from $-1.5V$ to $2V$, at a scan rate of 100mV/s. The long term monitoring experiment is controlled by a Perkin Elmer (Wellesley, MA, USA) VMP Multichannel Potentiostat; hence, all four cells can be measured simultaneously.

Figure 3.6. Multipotentiostat experimental cell

CHAPTER 3
Corrinoids and cobalt:
a viable abiotic alternative?
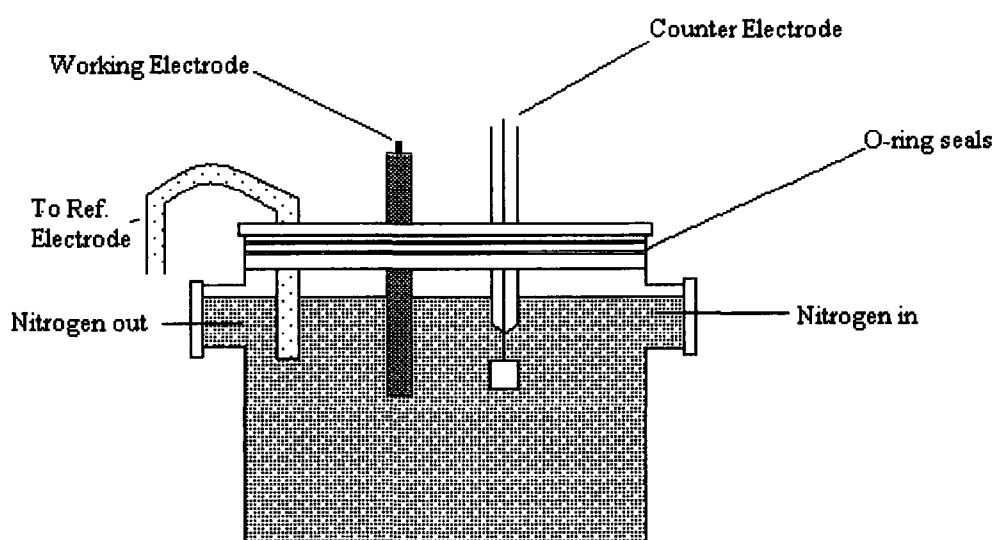
3.3.2.5. Preparation of bacterial culture, *dehalobacter restrictus*

3.3.2.5.1. Materials

A freeze-dried culture of the bacterial strain dehalobacter restrictus was obtained from the DSMZ (Braunschweig, Germany). Resazurin, peptone, pantothenic acid and all other vitamin solution chemicals were purchased from Sigma-Aldrich (Poole, Dorset, UK). All other chemicals were stock chemicals in the laboratory. Deionised (Purite) water was used in all preparations.

3.2.2.5.2. Preparation of nutrient media

Solution A – 0.0037 mol dm^{-3} potassium hydrogen phosphate, 0.0014mol dm^{-3} sodium dihydrogen phosphate, 1.9×10^{-6} mol dm^{-3} resazurin, 0.1

gram/litre peptone, and 0.0056 mol dm^{-3} sodium acetate, in 1 litre deionised water. Boiled and then cooled under nitrogen. Sealed to retain anoxic atmosphere.

Solution B – 100ml water, 0.0034mol dm^{-3} ammonium carbonate, flushed with nitrogen for 30 minutes.

Solution C – 7.4×10-4mol dm^{-3} calcium chloride dihydrate, and 0.05×10^{-4} mol dm^{-3} magnesium chloride hexahydrate, in 10ml deionised water. Flush with nitrogen gas for 20 minutes then seal.

Solution D - 10ml 7.7 mol dm^{-3} hydrochloric acid, 9.2×10^{-3} mol dm^{-3} anhydrous ferric chloride, 0.5×10^{-3} mol dm^{-3} manganese chloride tetrahydrate, 0.1×10^{-3} mol dm^{-3} boric acid, 0.7×10^{-3}

CHAPTER 3
Corrinoids and cobalt:
a viable abiotic alternative?

mol dm^{-3} cobalt (II) chloride, 1×10^{-5} mol dm^{-3} copper (II) chloride dihydrate, and 0.1×10^{-3} mol dm^{-3} nickel (II) chloride. Add 990ml water, then take 10 ml of solution, add 5mg ferric chloride and 0.1mg aluminium chloride, purge with nitrogen, and seal.

Solution E -   A vitamin solution. 2mg biotin, 2mg folic acid, 10mg pyridoxine hydrochloride, 5mg thiamine hydrochloride dihydrate, 5mg riboflavin, 5mg nicotinic acid, 5mg D-Ca-pantothenic acid, 0.1mg Vitamin B$_{12}$, 5mg p-aminobenzoic acid and 5mg lipoic acid, dissolved in 1 litre of water, flushed with nitrogen and sealed.

Solution G -   45 ml hexadecane and 5ml tetrachloroethene, flushed with nitrogen and sealed.

3.3.2.5.3. Culture preparation

To prepare the culture, 90ml of Solution A was transferred to a cell culture flask under nitrogen, and purged thoroughly for twenty minutes. To this, 10ml solution B, 1ml solution C, 0.1ml Solution D, and 1ml Solution E were added. The mixture was then purged again with nitrogen for a further ten minutes.
Once the solution was de-oxygenated, the dried bacterial sample supplied by DSMZ was introduced. The pellet was re-hydrated in its vial using 1ml of the prepared solution. This was then purged with nitrogen, sealed, and gently agitated. Then the culture was mixed in a sterilised Pasteur pipette and quickly transferred to the cell culture flask. To complete the medium, 1.5ml of Solution G was introduced, and the whole culture was purged with nitrogen for ten minutes.

CHAPTER 3
Corrinoids and cobalt:
a viable abiotic alternative?

The flask was then sealed, wrapped in tin foil, and stored in the dark at approximately 298K.

Plate counts (see Appendix 1) were developed in an attempt to ascertain the growth rate of the species, but oxygen contamination of the plates led to growth being suppressed; no consistency of data could be achieved.

CHAPTER 3
Corrinoids and cobalt:
a viable abiotic alternative?

3.4 Results and Discussion

3.4.1. Cyclic Voltammetry of Cobalt(II) Chloride and Chlorinated Ethenes

To investigate the effect of the oxidation state of cobalt on dechlorination, a simple cobalt salt, Cobalt(II) chloride was utilised, in a background electrolyte of 0.1 mol dm^{-3} KCl. The voltammogram below represents its electrochemical behaviour.

Figure 3.7. Voltammogram of Cobalt(II) chloride, at a platinum WE.
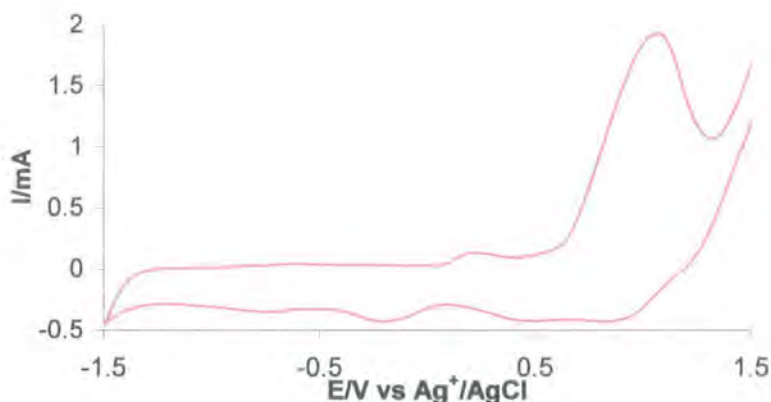
The voltammogram shows an oxidation at 1.1V, and a small reduction at – 0.25V. The oxidation corresponds approximately to the standard potential of the Co^{2+}/Co^{3+} couple, 1.45V vs. SCE (1.67V vs. Ag/AgCl). The introduction of TCE to the solution did not alter the shape of the voltammogram produced (Fig. 3.8.). A reduction in current was observed due to the increase in solution resistance on addition of TCE.

CHAPTER 3
Corrinoids and cobalt:
a viable abiotic alternative?

Figure 3.8. Voltammogram of Cobalt(II) Chloride and TCE (green trace), comparison to Cobalt(II) chloride (pink trace), at a platinum WE.
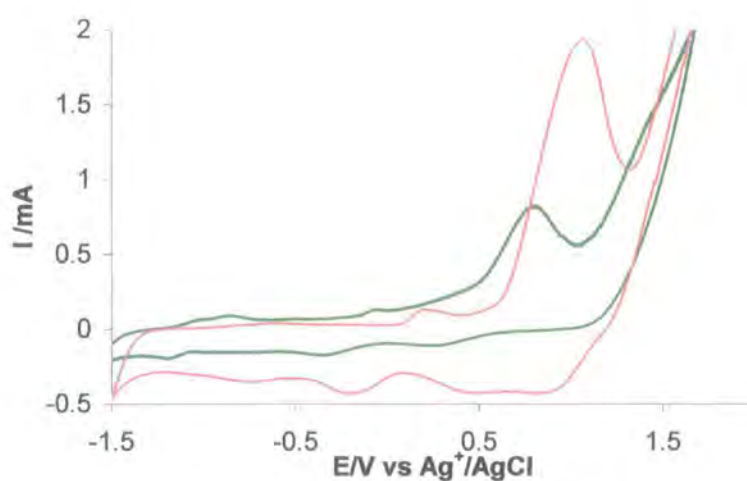
These data suggest that without a source of hydrogen in the system, the dechlorination of the TCE is not occurring. To correct this, the molasses substrate intended for use in bacteriological studies was introduced: this had the added advantage of allowing investigation of the carbohydrate's behaviour concurrent with the cobalt study. When molasses was added to a cobalt solution, a very different voltammogram was produced (Fig. 3.9).

CHAPTER 3
Corrinoids and cobalt:
a viable abiotic alternative?

Figure 3.9. Voltammogram of Co(II) chloride and molasses, at a platinum WE.
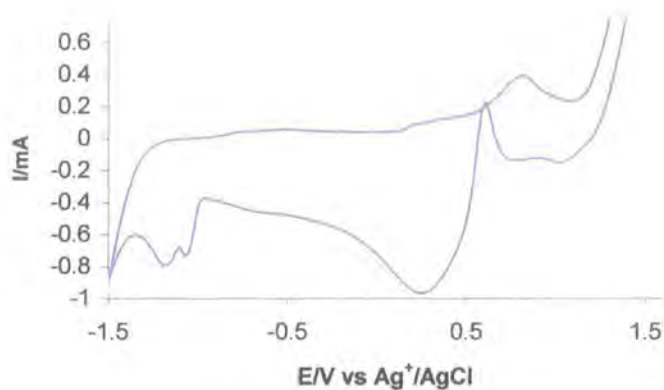
When molasses was added to the cobalt chloride solution, there was a decrease in the peak current, and a slight shift to lower oxidation potential, showing that Co(II) is involved in the redox process. The reverse sweep shows an oxidation at 0.58V, and two reductions are shown at −1.09V and −1.23V.

The oxidation on the reverse sweep is a phenomenon displayed by some carbohydrates. Ernst *et al.*[44] (Figure 3.10) demonstrated it with monosaccharide glucose.

CHAPTER 3
Corrinoids and cobalt:
a viable abiotic alternative?

Figure 3.10. Reverse sweep oxidation of 0.1 mol dm^{-3} glucose on a platinum electrode, as demonstrated by Ernst, Heitbaum, and Hamann[44].
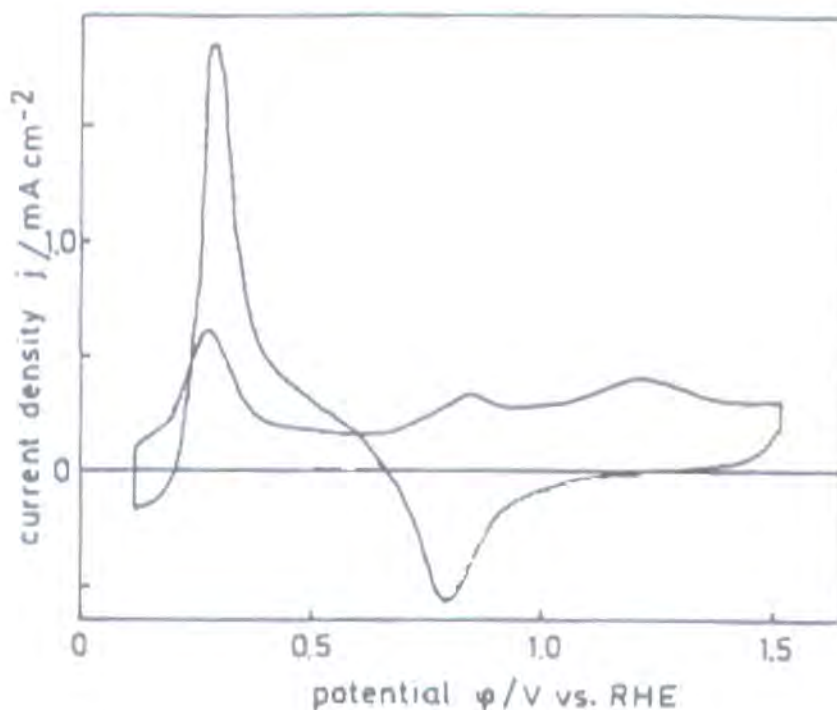
As a general case, electrochemical oxidation of organic compounds such as carbohydrates progresses by the following stages:

1. Adsorption
2. Associated deprotonation (producing dissociated, adsorbed hydrogen)
3. Subsequent oxidations of the carbon chain (steps 2 and 3 are considered to be rate limiting under steady state conditions)[45].

In this case we see the electro-oxidation of glucose, as demonstrated in Figure 3.11. The oxidation produces lactone and 2 H$^+$ [44, 45, 46, 47] (see Figure 3.12). The peak observed in Figure 3.9 shows the oxidation of the adsorbed hydrogen, releasing 2H$^+$. The two H$^+$ ions are then sequentially reduced at negative potentials (the reductions seen at –1.09V and –1.23V). Hence

CHAPTER 3
Corrinoids and cobalt:
a viable abiotic alternative?

molasses acts as a hydrogen source for the potential dechlorination reaction with the chlorinated ethenes.

Figure 3.11. Electrochemical oxidation of glucose at a platinum electrode (after ref.[45]).
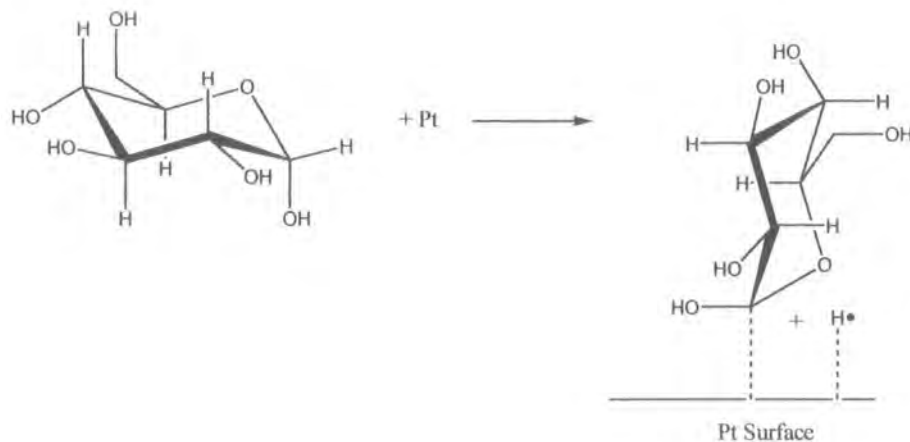
Figure 3.12. Oxidation of glucose to lactone.

100

CHAPTER 3
Corrinoids and cobalt:
a viable abiotic alternative?
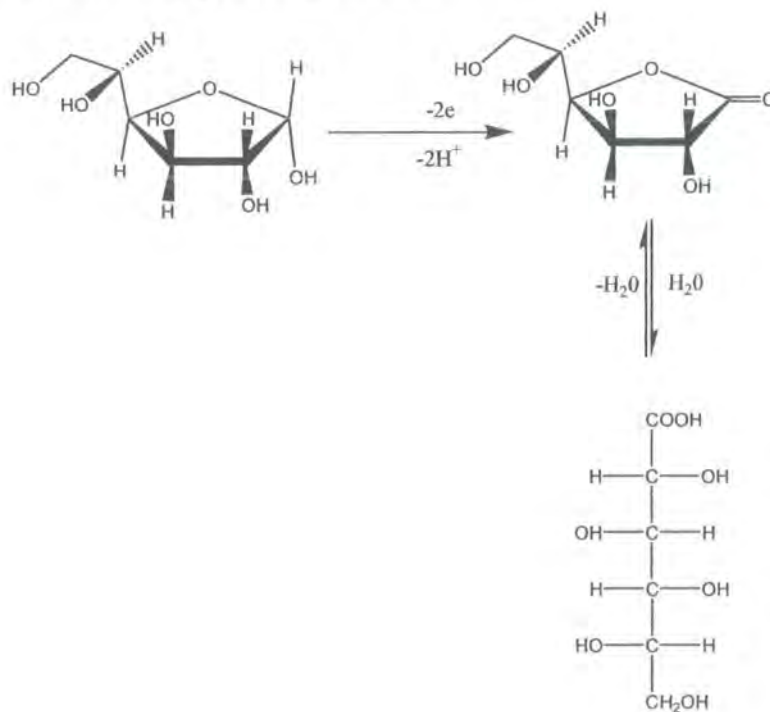
When a CV of molasses alone is taken (Fig. 3.13), we see that no oxidation occurs on the reductive sweep, suggesting that the Co (II) Cl$_2$ is catalysing the oxidation at 0.58V.

Figure 3.13. Cyclic Voltammogram of molasses, at a platinum WE.
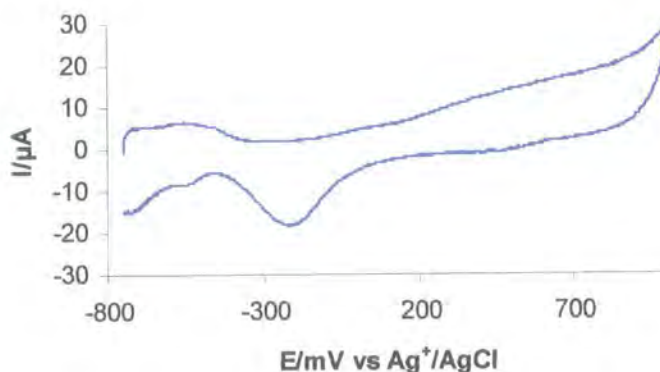
Once TCE is added to the solution, the hydrogen ions produced by the molasses are utilised to facilitate the dechlorination; reduction peaks are observed at 0.44V and −1.12V (I and II) (Fig. 3.14). If the voltammogram is compared to the reaction mechanism shown in Figure 3.1, the oxidation of Co^{2+} to Co^{3+} at 1.10V, the reduction of Co^{3+}/Co2$^+$ at 0.44V, and the reduction of Co^{2+}/Co$^+$ at 1.12V in the presence of the chlorinated ethene molecule demonstrate that the dechlorination process is indeed occurring as shown.

CHAPTER 3
Corrinoids and cobalt:
a viable abiotic alternative?

Figure 3.14. Voltammogram of Co(II) chloride, molasses and TCE, compared to Fig. 3.9, at a platinum WE.

Co(ii)Cl2/Molasses ——— Co(ii)Cl2/Molasses/TCE
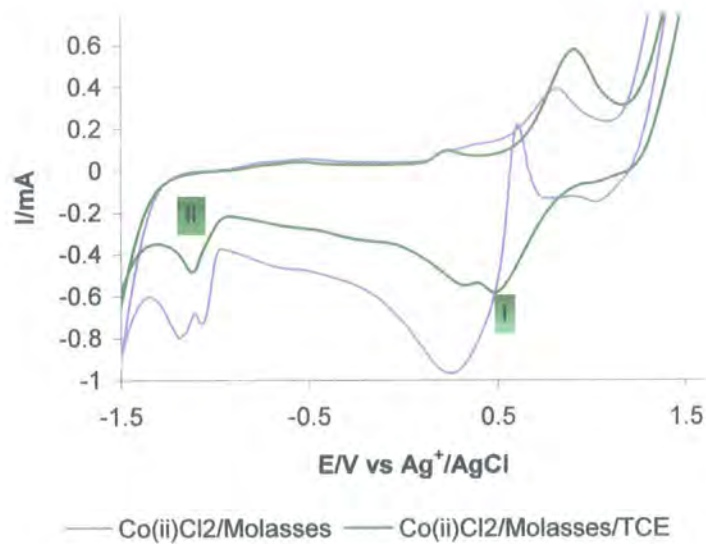
Addition of PCE to the Co (II) chloride/molasses mixture produced an initially eventless voltammogram (Fig.3.15), with a small oxidation peak at 0.38V. The peak attributed to the Co^{2+}/Co^{3+} couple reduced dramatically, and a very slight reduction is observed at 0.45V on the negative sweep. The presence of PCE appears to inhibit the oxidation of the cobalt to its 3^+ state, and there is no evidence of reduction which might suggest dechlorination.

CHAPTER 3
Corrinoids and cobalt:
a viable abiotic alternative?

Figure 3.15. Voltammogram of Co(II) chloride, molasses and PCE compared to Fig. 3.9, at a platinum WE.
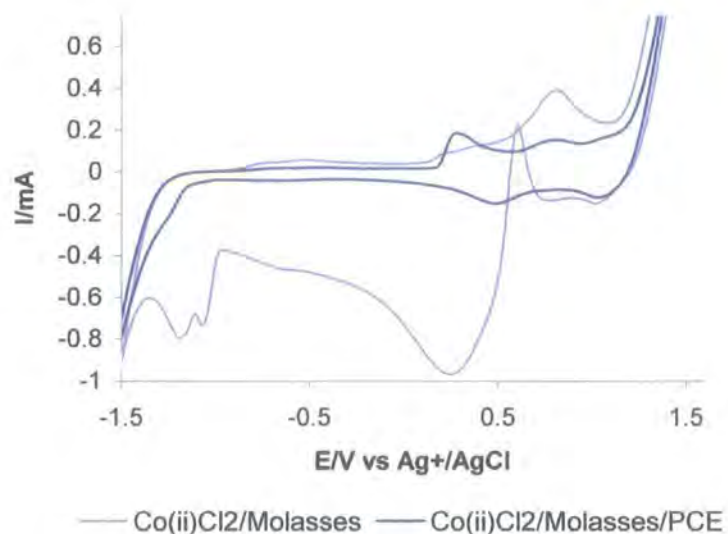
When c-DCE is added to the Co(II) chloride/molasses mixture, the $Co^{2+/3+}$ peak is enhanced, and two small reductions are seen at 0.10V and –1.10V (Fig. 3.16). In the presence of t-DCE, the cobalt oxidation peak is greatly enhanced, and there is a large reduction peak at 0.36V, as well as a small reduction at –1.10V, however neither voltammogram suggests that dechlorination has occurred.

CHAPTER 3
Corrinoids and cobalt:
a viable abiotic alternative?

Figure 3.16. Voltammogram of Co(II) chloride, molasses and *cis-/trans*-DCE compared to Fig. 3.7, at a platinum WE.
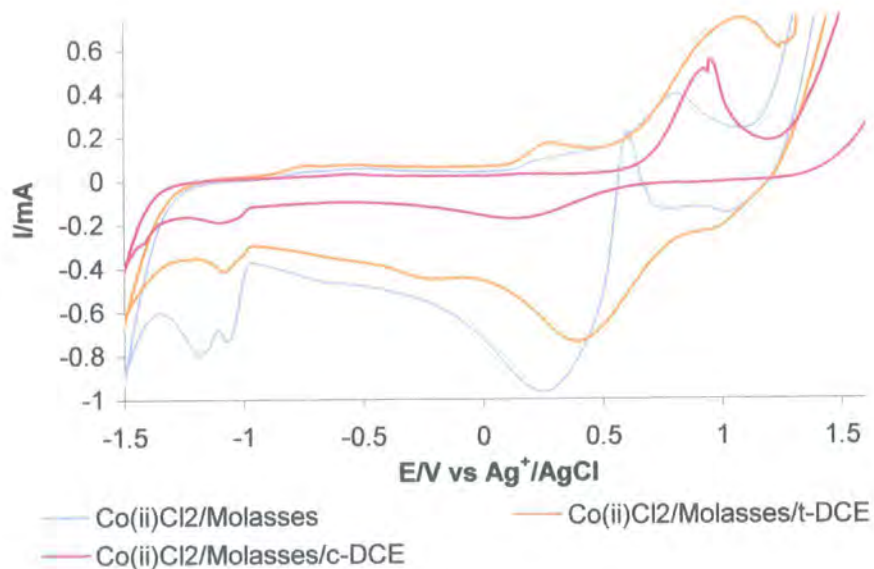
From these experiments we can conclude that Co (II) Cl_2 salt is capable of reductively dechlorinating trichloroethene in the presence of a hydrogen source. Tetrachloroethene and the dichloroethene isomers do not appear to be dechlorinated, as demonstrated by the absence of significant reduction peaks in their voltammograms.

CHAPTER 3
Corrinoids and cobalt:
a viable abiotic alternative?

3.4.2. Controlled potential electrolysis of Cobalt (II) Chloride and Vitamin B12 solutions for dechlorination.

Cyclic voltammetry of vitamin B_{12} was carried out to compare its electrochemical behaviour with that of Co(II) chloride (Fig. 3.17).

Figure 3.17. Cyclic voltammogram of Vitamin B_{12}.
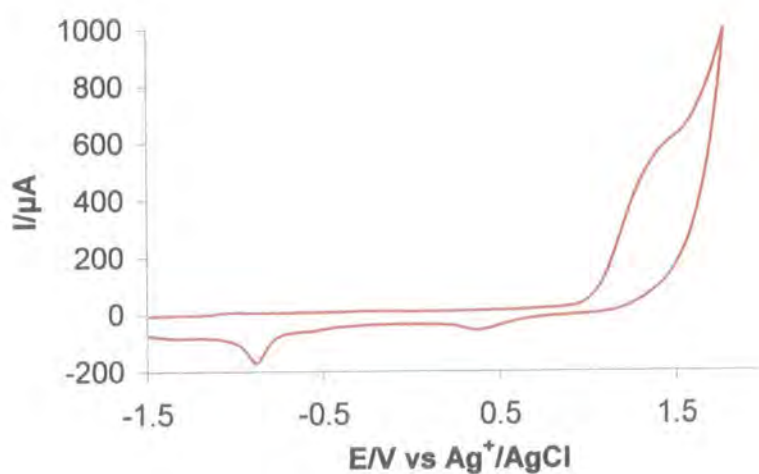
The oxidation at 1.50V is correspondent with oxidation of Co^{2+} to Co^{3+}. There is a minor reduction at 0.32V, and a more significant reduction at –0.90V, which represents the reduction of H^+. The voltammogram is very similar to that of cobalt chloride (Figure 3.18).

CHAPTER 3
Corrinoids and cobalt:
a viable abiotic alternative?

Figure 3.18. Cyclic Voltammogram of Cobalt (II) Chloride.
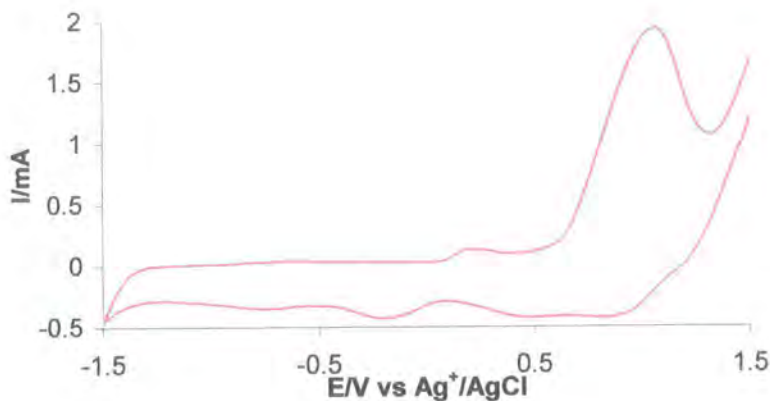
The similarity of behaviour shown by both cobalt complexes ($Co(II)Cl_2$ and Vitamin B_{12}) in their cyclic voltammetry studies is a significant indicator that simple cobalt salts might be capable of dechlorinating trichloroethene in extremely reducing conditions and the presence of a hydrogen source such as molasses. As a preliminary large-scale test of the hypothesis, controlled potential electrolysis was carried out.

Solutions of cobalt(II) chloride and Vitamin B_{12} were made up with a molasses substrate solution. TCE was introduced, and the solutions were subjected to controlled potential electrolysis experiments. The potential of the electrolysis cell was set extremely negative (-2V vs. Ag/AgCl) in order to ascertain if the reduced cobalt (I) would initiate dechlorination of the TCE. The solutions were submitted for anion exchange chromatography prior to electrolysis to determine baseline chloride concentrations. The initial concentrations of chloride in the Vitamin B_{12} system and the cobalt (II) chloride system were 29.05 ppm and 682 ppm respectively (see Table 3.2).

Samples of the solution from the cell were submitted for anion chromatography once the electrolysis was terminated, and re-analysed for chloride. In the case of B_{12} the chloride concentration was found to have increased to 102.60 ppm in

CHAPTER 3
Corrinoids and cobalt:
a viable abiotic alternative?

the cell solution. The change in [Cl$^-$] of 73.55ppm is 69.3% of the theoretical yield of chloride (106ppm) if the TCE had been completely dechlorinated; as a future consideration, the yield may prove to be higher in a cell with optimised conditions. The bulk electrolysis of the cobalt(II) chloride solution produced a slight increase in chloride concentration to 692.5 ppm, and UV monitoring proved inconclusive (data not shown).

Table 3.2. Chloride concentrations in bulk electrolysis experiments.

Experimental solution	[Cl$^-$] (ppm)	Δ [Cl$^-$] (ppm)
B$_{12}$ electrolysis initial solution	29.05	N/A
B$_{12}$ electrolysis final solution	102.60	73.55
Co(II)Cl$_2$ initial solution	682.00	N/A
Co(II)Cl$_2$ final solution	692.50	10.5

The initial UV-vis spectrum of the Vitamin B$_{12}$, molasses, and trichloroethene solution is shown in Fig. 3.19, compared to that of a solution of Vitamin B$_{12,}$ and a solution of molasses. The double peak at 521nm and 556 nm corresponds to published absorption wavelengths for Cob(III)alamin (520nm and 550nm), the stable state of the cobalamin molecule[19]. After electrolysis, this double peak was seen to have deteriorated (Fig. 3.20), suggesting a change in state of the cob(III)alamin molecule.

CHAPTER 3
Corrinoids and cobalt:
a viable abiotic alternative?

Figure 3.19. UV spectra of Vitamin B_{12}, molasses and TCE, compared to individual components.
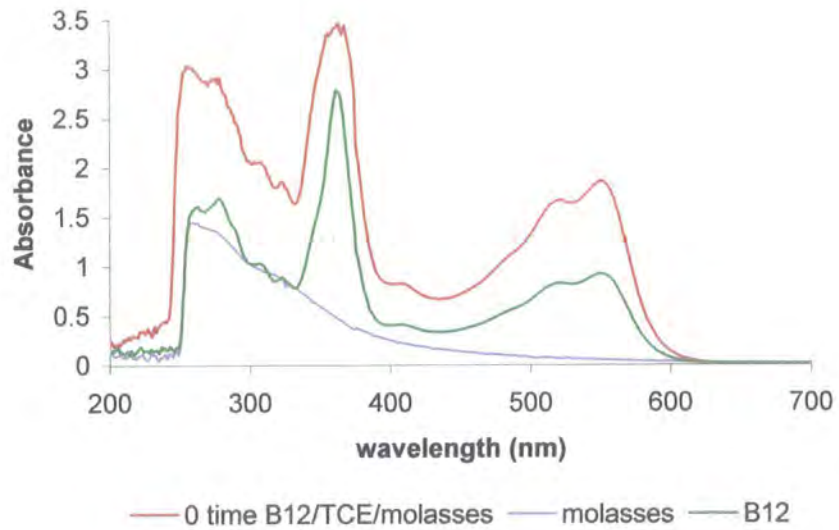
Figure 3.20. Deterioration of Vitamin B_{12} trace after electrolysis.

CHAPTER 3
Corrinoids and cobalt:
a viable abiotic alternative?
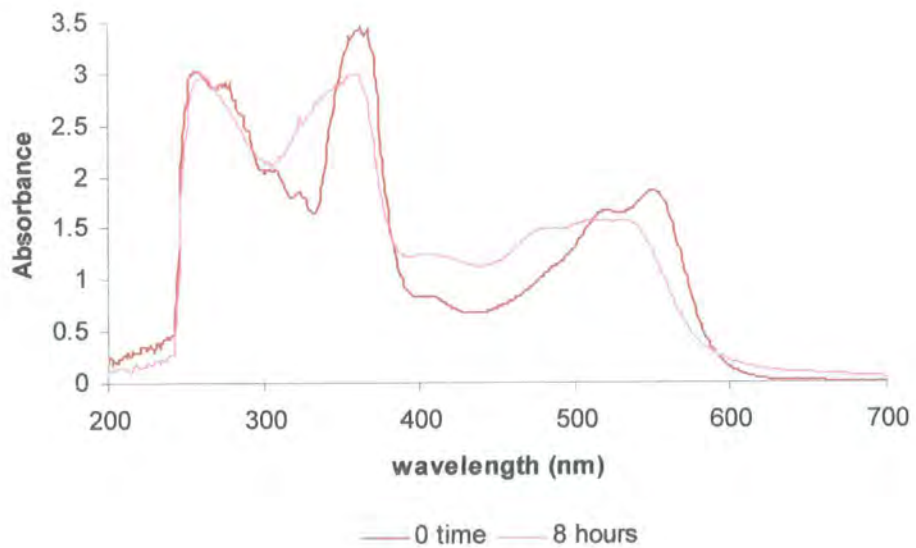
3.4.3. Continuous monitoring of artificial contaminated systems

3.4.3.1. Physical observations of systems

Physical changes in the cells over time are shown in the table below.

Table 3.3. Observed changes in the physical characteristics of the experimental cells.

Cell	Day	Colour	Texture
Control	1	Pale brown	-
	5	Pale brown	Mould
	14	Pale Brown	Mould
	16	Pale Brown	Mould
Co (II) Cl$_2$	1	Pale Brown	-
	5	Brown	-
	14	Brown	-
	16	Brown	-
Vitamin B$_{12}$	1	Red	-
	5	Red	-
	14	Red-Brown	Red plastic solid
	16	Red-Brown	Red plastic solid
Bacterial	1	Pale Brown	-
	5	Pale Brown	White biomass
	14	Pale Brown	> White biomass
	16	Pale Brown	> White biomass

Thereafter, no further physical changes were observed in the cells. Introduction of a second aliquot of PCE (0.01 mol dm^{-3}) on Day 39 failed to stimulate any further (visible) activity in the cells. From these data, the following observations concerning reactivity within the cells could be made:

CHAPTER 3
Corrinoids and cobalt:
a viable abiotic alternative?

1. The formation of biomass in the B_{12} and bacterial cells is indicative of reactions within these systems.

2. The reactions occurred on a short time-scale in an environmental sense (most remediation studies demonstrate reactions over a period of months[8]); within the first sixteen days.

3.4.3.2. Voltammetric measurements

Cyclic Voltammetry was carried out on each cell on a daily basis. A voltammogram of the control cell initially showed two oxidations, at –0.29V and 1.19V, and reductions at 0.10V and –0.39V (Fig 3.21). Two weeks after the experiment commenced (day 15), the voltammogram shows that the oxidations have persisted, but decreased in current, and no reduction is now observed.

Figure 3.21. Voltammetric response of the control cell, containing 0.01mol dm^{-3} PCE, and 0.01mol dm^{-3} molasses, in the background electrolyte (0.1mol dm^{-3} KNO$_3$). over two weeks.

CHAPTER 3
Corrinoids and cobalt:
a viable abiotic alternative?
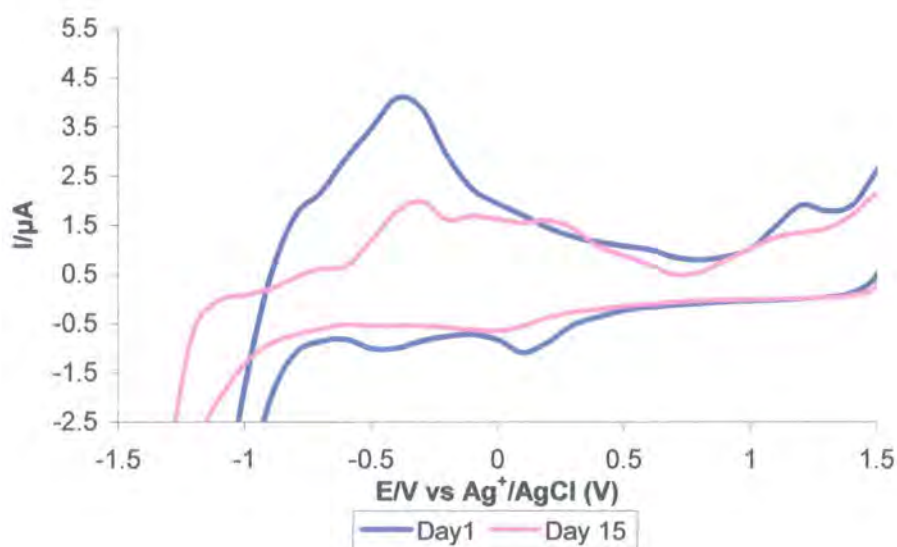
Figure 3.22. Voltammetric response of the Co (II) Cl$_2$ cell (control solution + 0.01mol dm^{-3} Co(II)Cl$_2$) over two weeks.
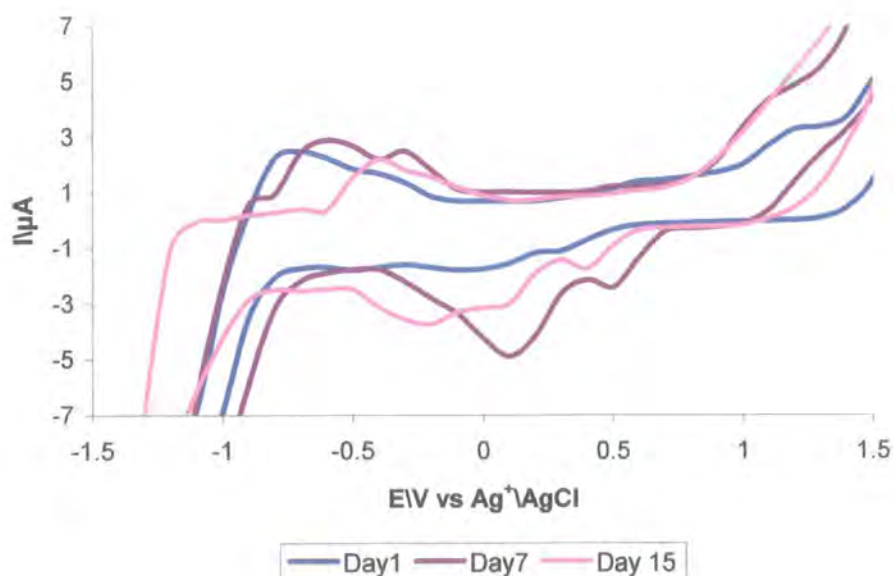
Voltammetric examination of the cobalt (II) chloride cell (Fig. 3.22) showed very slight initial reductions at 0.30V, and –0.49V. At day 7, reductions are clearly visible at 0.50V and –0.10V. After two weeks three reductions can be seen at 0.30V, 0.00V, and –0.29V, however these are much inhibited compared to those seen on Day 7. This demonstrates a lessening of the reaction taking place at the electrode surface.

When the Vitamin B$_{12}$ cell was subjected to cyclic voltammetry, oxidations were seen at –0.70V, -0.30V, and 1.29V. Three reductions occurred, at 0.40V, 0.10V (similar to those seen in the Co(II)Cl$_2$ cell, but with slightly different potentials), and –0.40V (Fig 3.23). At day 7, the first oxidation had reduced in current, and the second was no longer observed, however the third persisted. Only one

111

CHAPTER 3
Corrinoids and cobalt:
a viable abiotic alternative?

reduction was observed, at 0.10V. At day 15, there was a single oxidation peak at –0.30V, and a single reduction at –0.40V.

Figure 3.23. Voltammetric response of the Vitamin B_{12} cell (control solution + 0.001mol dm^{-3} Vitamin B_{12}) over two weeks.
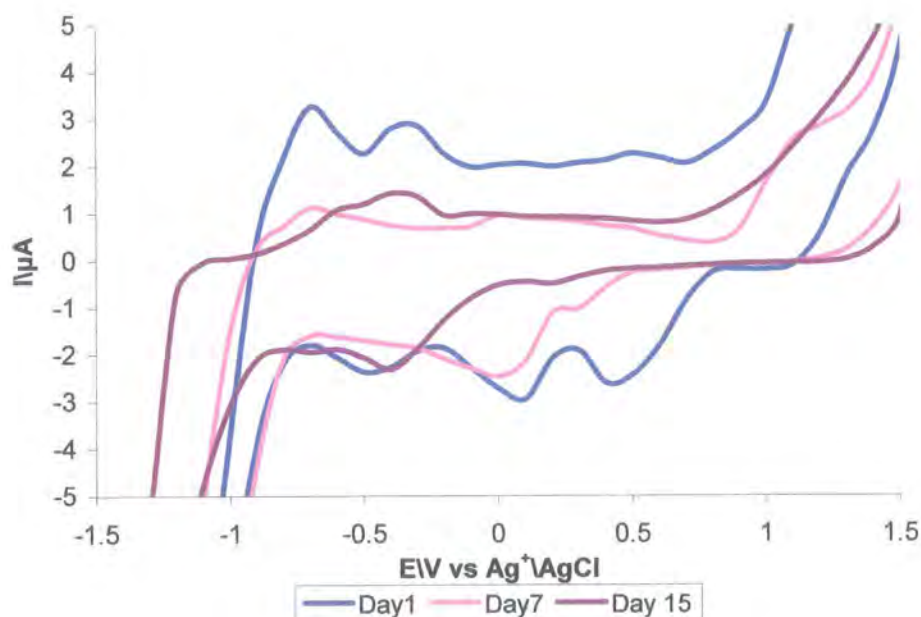
Cyclic voltammetry of the bacterial cell (Fig 3.24) showed two oxidations at –0.50V and 1.19V, and two reductions, one very slight, at 0V, the other at –0.49V. After one week the first oxidation was seen to decrease in peak current and shift slightly positive, to –0.30V. A second oxidation peak forms at 0.49V, and the higher oxidation sees a shift to a more negative potential of 1.10V. After two weeks, the initial and third oxidations continue to be inhibited; the second peak is no longer observed. No reductions are seen after two weeks.

CHAPTER 3
Corrinoids and cobalt:
a viable abiotic alternative?

Figure 3.24. Voltammetric response of the bacterial cell (control solution + 10ml bacterial culture) over two weeks.
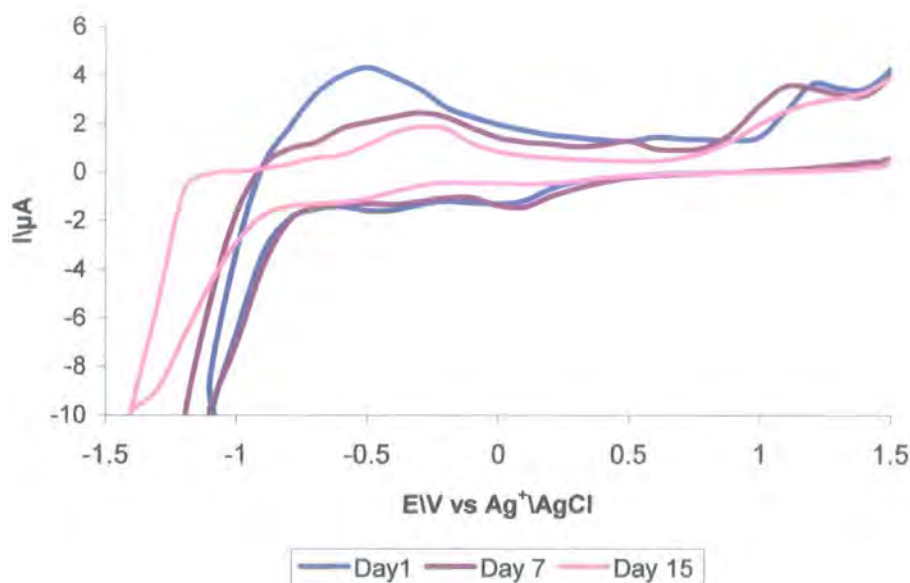
Further voltammograms produced no significant change in behaviour over the course of the remaining experimental time, even after the addition of a second dose of PCE.

All four cells in the experiment experience a decrease in signal with time, which is attributable to the exhaustion of any electroactive species within the vicinity of the electrode, and fouling of the electrode by adsorbed matter.

Comparison of the CVs of the control cell and the bacterial cell indicate that there is no reactivity in the bacterial cell. It is likely that the bacterial strain introduced to the cell died after a few days, either from the imposed electrical current or through exhaustion of nutrients; *dehalobacter restrictus* relies on H^+ as a substrate, and the production of H^+ from the molasses was probably insufficient to support culture growth.

113

CHAPTER 3
Corrinoids and cobalt:
a viable abiotic alternative?

The cobalt (II) chloride and Vitamin B_{12} cells show more promising results, in that reductions are clearly seen in both sets of voltammograms which are not present in the control cell. Two reduction peaks at 0.30V and 0.00V are observed similar to the reduction peaks in Figure 3.11, which indicate reductive dechlorination of PCE.

3.5.   Conclusions

From the evidence presented above, the following conclusions can be made concerning the dechlorination of chlorinated ethenes by cobalt and corrinoids:

1. In the presence of a source of hydrogen ions, a simple cobalt salt such as cobalt (II) chloride is capable of reductively dechlorinating trichloroethene in an electrochemical system. Tetrachloroethene and the dichloroethene stereoisomers, however, do not appear to be affected.

2. In a scaled-up system held at an extremely reducing potential, Vitamin B_{12} (cyanocobalamin) was shown to be much more effective at dechlorination than cobalt (II) chloride.

3. A preliminary experimental set-up of a dechlorination scheme suggested that use of Vitamin B_{12} or cobalt (II) chloride in an electrochemically-assisted PCE dechlorination system could potentially be an effective method of remediation. Further work on cell development would need to be undertaken, particularly with regard to cell design and coulometric parameters before any significant data can be produced; the addition of controlled convection and a method for cleaning the electrode surfaces to counter the effects of species exhaustion and electrode fouling are

CHAPTER 3
Corrinoids and cobalt:
a viable abiotic alternative?

an imperative first step to any further work on this system. A
reliable method of chloride detection, preferably *in situ*, would also
be beneficial.

In summation, cobalt (II) chloride, whilst effective in a small-scale
electrochemical study, is inferior to the corrinoid molecule Vitamin B_{12} as a
dechlorination agent. Any proposed biomimetic technique for reductive
dechlorination of chlorinated ethenes should focus on use of Vitamin B_{12} rather
than simple cobalt salts. There is potential for an electrochemically assisted
remediation system, but further study will be necessary to elucidate the most
effective method.

CHAPTER 3
Corrinoids and cobalt:
a viable abiotic alternative?

REFERENCES

1. Maymo-Gatell, X., Chien, Y., Gossett, J.M., and Zinder, S.H., *Science*, 1997, 276, 1568 – 1571.

2. Wiegel J., and Wu, Q., *FEMS Microbiol. Ecol.*, 2000, 32, 1 – 15.

3. El Fantroussi, S., Naveau, H., and Agathos, S.N., *Biotechnol. Prog.*, 1998, 14, 167 – 188.

4. Häggblom, M.M., *FEMS Microbiol. Ecol.*, 1998, 26, 35 – 41.

5. Häggblom, M.M., Knight, V.K., and Kerkhof, L.J., *Environmental Pollution*, 2000, 107, 199 – 207.

6. Boopathy, R., and Peters, R., *Curr. Microbiol.*, 2001, 42, 134 – 138.

7. Yang, Y. and McCarty, P.L., *Environ. Sci. Technol*, 1998, 32, 3591 – 3597.

8. Ferguson, J.F., and Pietari, J.M.H., *Environ. Pollut.*, 2000, 107, 209 – 215.

9. Holliger, C., Schraa, G., Stams, A.J.M., and Zehnder, A.J.B., *App. Env. Microbiol.*, 1993, 59, 2991 – 2997.

10. Mohn, W.W., and Tiedje, J.M., *Microbiol. Rev.*, 1992, 56, 482 – 507.

11. Freedman, D.L., and Gossett, J.M., *App. Env. Microbiol.*, 1991, 57, 2847 – 2857.

12. Holliger, C., and Schumacher, W., *Antonie van Leeuwenhoek*, 1994, 66, 239 – 246.

13. Schumacher, W., and Holliger, C., *J. Bacteriol.*, 1996, 178, 2328 – 2333.

14. Kao, C.M. and Prosser, J., *J. Hazard. Mat.*, 1999, B69, 67 – 79.

15. Ballapragada, B.S., Stensel, H.D, Puhakka, J.A., and Ferguson, J.F., *Environ. Sci. Technol*, 1997, 31, 1728 – 1734.

16. Smatlak,, C.R., and Gossett, J.M., *Environ. Sci. Technol.*, 1996, 30, 2850 – 2858.

17. Carr, C.S., and Hughes, J.B., *Environ. Sci. Technol.*, 1998, 32, 1817 – 1824.

18. Chappelle, F.H., Haack, S.K., Adriaens, P., Henry, M.A., and Bradley, P.M., *Environ. Sci. Technol.*, 1996, 30, 3565 – 3569.

CHAPTER 3
Corrinoids and cobalt:
a viable abiotic alternative?

19. Neumann, A., Wohlfarth, G., and Diekert, G., *Archives of Microbiology*, **1995**, 163, 276 – 281.

20. Van den Pas, B.A., Smidt, H., Hagen, W.R., Van der Oost, J., Schraa, G., Stams, A.J.M., and de Vos, W.M., *J. Biol. Chem.*, **1999**, 274, 20287 – 20292.

21. Magnuson, J.K., Stern, R.V., Gossett, J.M., Zinder, S.H., and Burris, D.R., *App. Env. Microbiol.*, **1998**, 64, 1270 – 1275.

22. Christiansen, N., Ahring, B.K., Wohlfarth, G., and Diekert, G., *FEBS Lett.*, **1998**, 436, 159 – 162.

23. Holliger, C., Wohlfarth, G., and Diekert, G., *FEMS Microbiol. Rev.*, **1999**, 22, 383 – 398.

24. Lewis, T.A., Morra, M.J., and Brown, P.D., *Environ. Sci. Technol.*, **1996**, 30, 292 – 300.

25. Krone, U.E., and Thauer, R.K., *Biochemistry*, **1989**, 28, 4908 – 4914.

26. Wohlfarth, G., and Diekert, G., *Curr. Opin. Biotechnol.*, **1997**, 8, 290 – 295.

27. Holliger, C., Hahn, D., Hansen, H., Ludwig, W., Schumacher, W., Tindall, B., Vazquez, F., Weiss, N. and Zehnder, A.J.B., *Arch Microbiol.*, **1998**, 169, 313 – 321.

28. Glod, G., Angst, W., Holliger, C., and Schwarzenbach, R.P., *Environ. Sci. Technol.*, **1997**, 31, 253 – 260.

29. Gantzer, C.J., and Wackett, L.P., *Environ. Sci. Technol.*, **1991**, 25, 715 – 722.

30. Shey, J. and Van der Donk, W.A., *J. Am. Chem. Soc.*, **2000**, 122, 12403 – 12404.

31. Norton, J.W. Jr., Suidan, M.T., and Acheson, C.M., *Proceedings of the 1994 Water Environment Federation Conference, Dallas*, **1994**, TX, 1, 13 – 21.

32. Geoly, S.L., Sangamali, V.E., and Flora, J.R.V., *Proceedings of the 1997 CSE/ASCE Environmental Engineering Conference*, 1997, Edmonton, Alta., Canada, 751 – 762.

33. Gliham, R.W., and O'Hannesin, S.F., *Ground Water*, **1994**, 32, 958 – 967.

34. Weathers, L.J., Parkin, G.F., and Alvarez, P.J., *Environ. Sci. Technol*, **1997**, 31, 880 –885.

CHAPTER 3
Corrinoids and cobalt:
a viable abiotic alternative?

35. Farrell, J., Melitas, N., Kason, M., and Li, T., *Environ. Sci. Technol*, **2000**, 34, 2459 – 2556.

36. Farrell, J., and Li, T., *Environ. Sci. Technol*, **2000**, 34, 172 – 179.

37. Lin, C., and Tseng, S., *Chemosphere,* **1999**, 39, 2375 – 2389.

38. Kulikov, S.M., Plekhanov, V.P., Tysganok, A.I., Schlimm, C., and Heitz, E., *Electrochim. Acta*, **1996**, 41, 527 – 531.

39. Cheng, I.F., Fernando, Q., and Korte, N., *Environ. Sci. Technol*, **1997**, 31, 1074 – 1078.

40. Tsyganok, A.I., Yamanaka, I., and Otsuka, K., *Chemosphere*, **1999**, 39, 1819 – 1831.

41. Dabo, P., Cyr, A., LaPlante, F., Jean, F., Menard, H., and Lessard, J., *Environ. Sci. Technol*, **2000**, 34, 1265 – 1268.

42. Boopathy, R., Kulpa, C.F., Manning, J., Montemagno, C.D., *Bioresource Technology*, 1994, **47**, 205 – 208.

43. Binkley, W.W., and Wolfrom, M.L., *Adv. Carb. Chem. Biochem.*, **1953**, 8, 291 – 314.

44. Ernst, S., Heitbaum, J., and Hamann, C.H., *J. Electroanal. Chem.*, **1979**, 100, 173 – 183.

45. Yao, S.J., Appleby, A.J., and Wolfson, S.K., *Zeit. Physik. Chem. Neue Folge Bd.*, **1972**, 82, 225 – 235.

46. Lei, H, Wu, B., Cha, C., and Kita, H., *J. Electroanal. Chem.*, **1995**, 382, 103 - 110

47. Lund and Baizer (eds.) *Organic Electrochemistry*, Dekker, New York, **1991**, 644 – 645.

CHAPTER 4

A biosensor for chlorinated ethene detection.

4.1. Introduction

As was mentioned in Chapter 1, the two main thrusts of research into chlorinated solvent remediation are enhancing dechlorination rates and improving detection methods for monitoring at contaminated sites. Chapters 2 and 3 have investigated the former; this chapter will address the problem of improving detection in the environment.

Current practice for detection relies almost exclusively on chromatographic techniques. The generally accepted method of detection is gas chromatography; the US Environmental Protection Agency has produced a set method for determination of halocarbons using purge-and-trap gas chromatography[1], and examples of its use appear in work in both laboratory[2,3] and field[4] investigations. Headspace gas chromatography for determination of chlorinated alkenes and other volatile organic carbons is another common practice[5,6,7,8]; occasionally, the techniques are used in conjunction with one another[9].

However this approach has drawbacks, since remediation engineering companies are required to have samples sent to laboratories for testing, which can take days or weeks. In such circumstances, whilst the use of headspace gas chromatography produces extremely accurate results in and of itself, time delays, temperature variations and the potential for handling errors all provide scope for inaccuracies to be introduced. Furthermore, most laboratory work is contracted, and therefore expensive. Use of an in situ, on line or disposable, sensor would save time and money and reduce the potential for inaccuracy implicit in sample handling.

Electrochemistry has a long history of use in the sensors discipline, particularly for medical assays (for example, test kits for diagnosing diabetes utilise an electrochemical biosensor which incorporates a glucose oxidase enzyme) and increasingly in the more specialised field of biosensors. The existing knowledge and technology base offers a solid platform from which to investigate the viability of developing an electrochemical sensor for chlorinated ethenes.

4.2. Literature review

4.2.1. Sensors

At its most basic, a sensor is defined as "anything... that receives a signal or stimulus and responds to it."[10] If applied to electrochemistry, this can be viewed as the function of an electrode. However, a simple working electrode by itself cannot be used as an electrochemical sensor; there are certain criteria which must be met, namely,

1) Redox behaviour which is modified by the target molecule (i.e. selectivity towards the target molecule)

2) A simple reaction system to allow the electrode to be as small as possible

3) Capability to detect environmental levels of concentration (usually ppb)

A standard platinum or carbon working electrode has no specificity for any chemical species, therefore to create a sensor, the behaviour of the system must be modified. The glucose oxidase based biosensor described above would be an example.

In terms of detection of chlorinated ethenes, relatively little research has been done in the field. Jakusch *et al.* developed molecularly imprinted IR fibre optic

sensors for the detection of a broad range of volatile organic compounds including TCE and PCE,[11] and ATR-FTIR optical sensors[12] have been reported.

However, since the first isolation of a bacterial species which was found to dechlorinate chlorinated hydrocarbons[13], work has been done on the development of biosensors. The field of bioelectronics, specifically biosensors, offers a much greater scope for chlorinated ethene detection. A biosensor is "A device incorporating a biological sensing element either intimately connected to or integrated within a transducer."[14] The transduction method varies, but most commonly involves current, potential, charge, capacitance, or impedance. Biological sensing elements include enzymes, whole cell microbes or bacteria, antibodies, oligonucleotides and DNA. An example is shown in the figure below (Fig. 4.1.). These biomaterials are immobilised at the conductive surface of the electrode by various methods such as sol-gel encapsulation, surface functionalisation and membranes to ensure good contact between the sensing element and the transducer. The choice of sensing element is defined by the target species, but generally must be capable of fast electron transfer with the electrode, such that, "...The resulting current corresponds to the turnover rate of the electron exchange between the substrate and the biocatalyst. Hence the transduced current reflects the substrate concentration in the system."[15]

Figure 4.1. An example of a biosensor with an enzyme as a sensing element. Adapted from Reference 15.
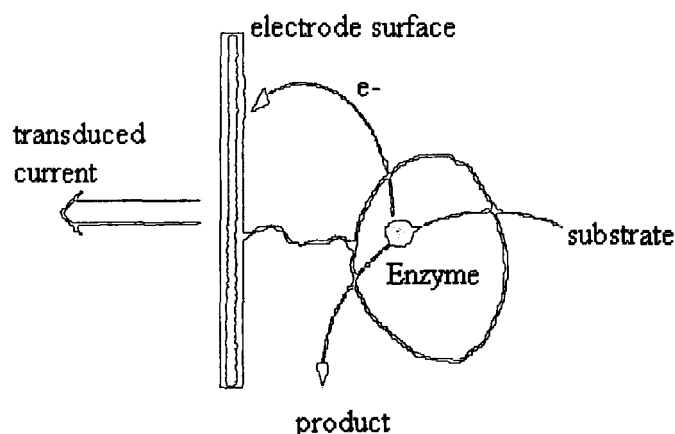
Biosensors are advantageous in that they couple the specificity of biological recognition systems with the high sensitivity of electrochemical techniques. The first biosensor was described by Clark and Lyons in 1962[16], and was an enzyme-based sensor for the detection of glucose. Enzyme based biosensors remain the most common, however there have been none developed for chlorinated ethenes. Three other types of biosensors have been reported. Xing *et al.*[17] constructed an evanescent field immunosensor for pesticide detection; tetrachloroethene was among its target analytes. Naessens et al developed a whole cell sensor for the determination of volatile organic compounds in aerosol[18]. Han *et al.* have recently reported a whole cell biosensor specifically for the determination of TCE levels in aqueous media[19].

Initially, it was envisaged that a whole-cell microbial biosensor could be developed for chlorinated ethenes, using the previously discussed *dehalobacter restrictus* strain of dehalorespiratory bacteria. This approach was appealing for several reasons:

    1) Microbes tend to be more stable than enzymes.

2) Microbes have a longer lifetime.

3) They are more robust than enzymes in terms of environmental variation (e.g. change in pH or temperature).

4) They tend to be cheaper than enzymes as they do not require isolation.

Specifically, it was also better to use microbes in this investigation as the dehalogenase enzyme has only been purified in a few laboratories and is not commercially available. These considerations outweighed the general drawbacks of slower response times and baseline equilibration than enzyme electrodes.

However, after several attempts to grow and maintain a culture of dehalobacter restrictus, it was found that the requirement for anoxic conditions essential for the bacteria's survival made the proposed system too delicate even for characterisation in the laboratory. Therefore it was necessary to rethink the strategy.

4.2.2. Glutathione and its biological role

Glutathione is a tripeptide molecule, molecular formula $C_{20}H_{32}N_6O_{12}S_2$, formed with the peptide residues Glutamyl, Cysteinyl, and Glycinyl (Fig. 4.2.). It is an intracellular compound in mammals, and its primary function is to protect cells from electrophilic damage.

Figure 4.2. The reduced form of glutathione (GSH), showing its component peptides.
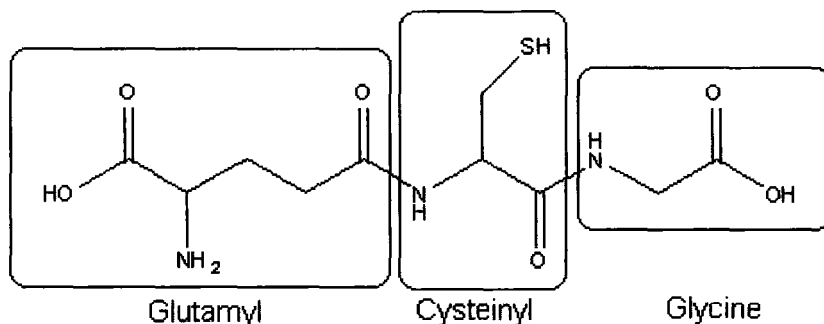
Any compound that does not take part in the natural metabolic processes of an organism is classified as *xenobiotic* (i.e. any compound not naturally present in the body). Many such compounds, which are generally hydrophobic, are reactive with or structurally complementary to molecules within living cells. This reactivity can result in cell damage by bursting due to over concentration, inhibition of enzyme active sites, or loss of structural complementarity (and hence molecular recognition) in key metabolic systems. Such effects are usually classified as *toxicity*.

Glutathione and other molecules like it are evolved to prevent such damage by altering the xenobiotics to more hydrophilic substances which can then be excreted into the body's waste systems. This process is referred to as xenobiotic metabolism. The most important part of the molecule is the thiol group. A strong nucleophile, it reacts with the electrophilic xenobiotics via direct substitution reactions (Figure 4.3)

Figure 4.3. Substitution reaction of a thiol with a chlorinated alkene.
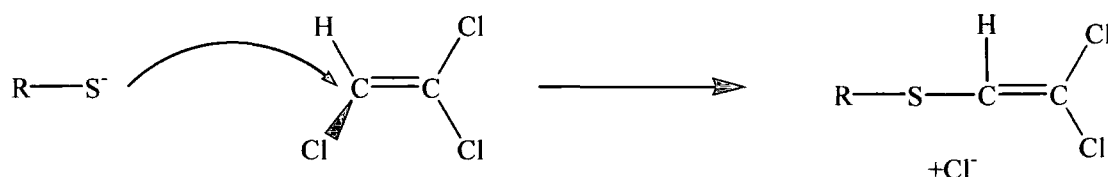
Further transformations are then carried out by other enzymes to make the xenobiotic hydrophilic, and thus, easily disposable.

Glutathione tends to exist as its oxidised dimer, and reduces according to the following reaction in the presence of the enzyme Glutathione Reductase (GR):

$$GSSG + 2H^+ + 2e^- \longrightarrow 2GSH \qquad (1)$$
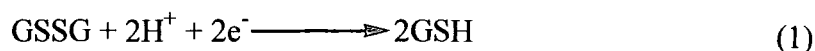
Glutathione Reductase requires the presence of reduced Nicotinamide Adenine Dinucleotide Phosphate (NADPH) as a co-factor. NADPH is a major electron source in biosynthesis, and provides the reducing equivalents for GSSG/2GSH, hence it is more accurate to say that GSH is generated through glutathione reductase via the reaction given below:

$$GSSG + NADPH + H^+ \xrightarrow{\text{GR}} 2GSH + NADP^+ \qquad (2)$$
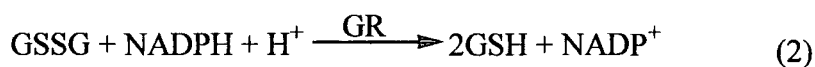
The nucleophilic thiol group of reduced glutathione is free to bind electrophilic molecules, and as thiols are known to react very strongly with alkyl halides, it was concluded that a glutathione system utilising glutathione reductase as the biosensing element would offer a more practical route to chlorinated ethene detection.

4.2.3. Literature precedent for a thiol sensor

A glutathione based system will rely upon the detection of a complexation between the reduced glutathione, GSH, and the target chlorinated ethene. Detection of simpler thiol molecules such as cysteine can provide insight into the system's requirements, as GSH should behave in a similar fashion.

Thiol detection at a normal, bare electrode is difficult to achieve[20]. Large anodic potentials are needed to oxidise them, which usually results in the oxidation of every reduced species in the solution, giving rise to interferent signals which can obscure the target. Separation methods are frequently used to improve resolution, but this approach is both time and equipment intensive, undesirable traits for a sensor system.

A better option is the use of an electrochemical mediator. A mediator is an alternative electron transfer acceptor which moves electrons between an electrode and a redox centre (Figure 4.4). Their diagnostic criteria are:

1) Rapid reaction with the redox centre.
2) Reversible heterogeneous kinetics.
3) A low overpotential for regeneration.
4) Stable with variable pH, temperature, redox state and $[O_2]$.

Figure 4.4. Schematic of a mediated enzyme sensing system.
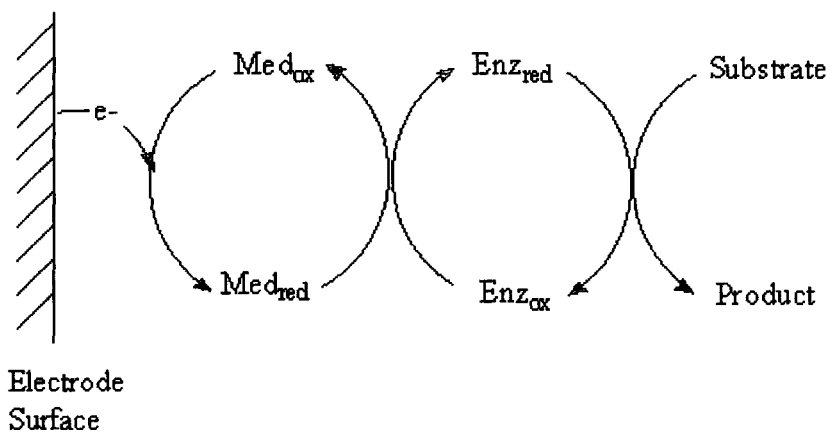
Metal complexes are the most common type of mediator, and conducting organic salts such as TTF:TCNQ (Tetrathiafulvalene: Tetracyanoquinodimethane) are good general mediators, however, in a recent publication, Lawrence *et al.*[20] utilised catechol as a successful mediator for cysteine (Fig.4.5), and other quinoid structures have since been reported by that group as being similarly successful[21]. An additional benefit is that the quinoid mediator is selective only for reduced sulfhydryl molecules, R-SH: RS-SR dimers do not elicit a response.

Figure 4.5. Reaction scheme for quinoid structure mediated thiol detection and improvement in signal response as demonstrated by White *et al.* (Reference 21).
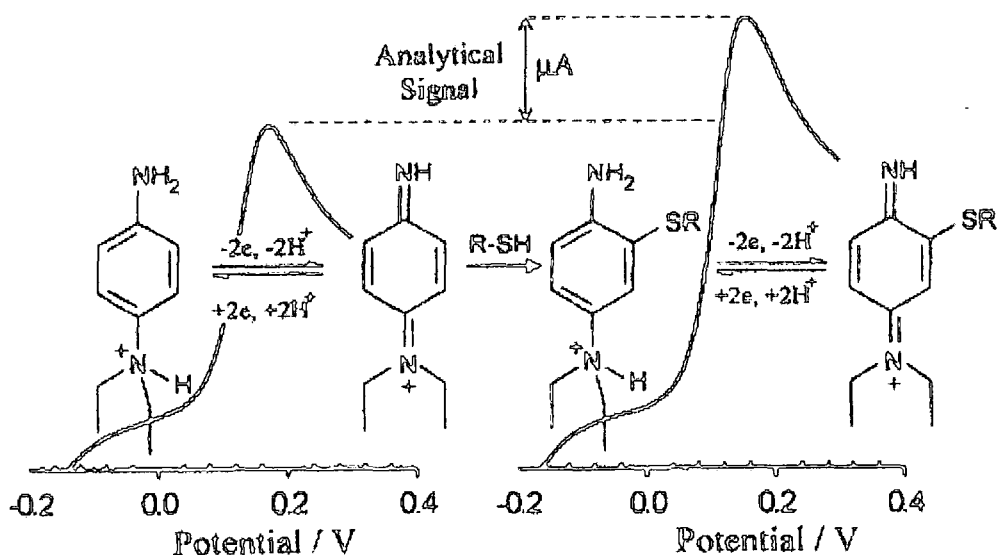
4.2.4. Strategy for development of a glutathione based biosensor

4.2.4.1. Potentiometric biosensor

Two forms of electrochemical sensor system utilising the redox properties of glutathione were developed. The first of these is a potentiometric sensor, where the detection is achieved by means of a Nernstian response at the electrode surface (see Chapter 1, section 1.10). This sensing method is based on the concept of the GSH 'pool' in biological systems, where the relative concentrations of GSH/GSSG are an important indicator of the systems' redox environment.

The term Redox Environment (E_{env}) is used to describe the state of redox couples within biological materials, and can be expressed mathematically as:

$$\text{Redox Environment } E_{Env} = \sum_{i=1}^{n(couple)} E_i \times \left[\text{reduced species}\right]_i \tag{3}$$

A redox couple can be considered as a half-cell, and is therefore subject to the Nernst Equation in the form:

$$\Delta E = \Delta E^0 - \frac{RT}{nF}\log\frac{[Red]}{[Ox]} \tag{4}$$

At 25°C:

$$\Delta E = \Delta E^0 - \frac{59.1}{n}\log\frac{[Red]}{[Ox]} \tag{5}$$

For the reduction of GSSG to GSH, two couples (GSSG/2GSH and NADPH/NADP) control the redox environment. At 25°C, pH7, the E^0 of NADPH/NADP is –315mV vs. NHE[22], hence:

$$E\left(NADP^+, H^+, NADPH\right) = -315 - \frac{59.1}{2}\log\left(\left[NADPH\right]/\left[NADP^+\right]\right) \tag{6}$$

Schafer and Buettner[23] give the E^0 of GSSG/2GSH as –240mV vs. NHE at 25°C, pH7, therefore:

$$E\left(GSSG/2GSH\right) = -240 - \frac{59.1}{2}\log\left(\left[GSH\right]^2/\left[GSSG\right]\right) \tag{7}$$

At the beginning of the experiment, in a system where only GSSG and NADPH are present, the concentrations of NADPH:NADP and GSSG:2GSH are both 100:1 mmol dm^{-3}. Therefore the E values of both couples can be calculated as:

E(NADPH/NADP$^+$) = -374mV

E(GSSG/2GSH) = -181mV

And the overall redox environment at the beginning of the experiment is:

$$E_{Env} = (2 \times -181) + (1 \times -374) = -736mV \qquad (8)$$

Conversely, if complete conversion of the GSSG to its reduced form is achieved, (i.e. the ratio of GSSG/2GSH is 1:100), then:

$$E_{Env} = (2 \times - -358) + (1 \times -374) = -1090mV \qquad (9)$$

Hence, any value of E_{Env}, as read by an electrode in a potentiometric cell, which is more positive than –1090mV, indicates a depletion of the concentration of GSH in the system. In this case, it would indicate reaction of the GSH with chlorinated ethenes, or autooxidation to GSSG.

4.2.4.2 Amperometric biosensor

An amperometric biosensor system utilising glutathione would operate on the same principles as the thiol sensors described above (see Section 4.2.3). An electrode with a suitable mediator would function in effect as a glutathione sensor. The redox reaction of GSSG and GSH produces a measurable amperometric response (registering a flow of current at a specific potential). Complexation of GSH with a target chlorinated ethene should change that response; the potential at which the current is seen to flow should be different. If all four chlorinated ethenes give a reproducible response at different (and unique) potentials, the basis of an extremely sensitive biosensor will have been achieved.

One potential drawback to the use of a mediated system is that retention of the mediating species on the electrode surface can be difficult, however techniques such as sol-gel encapsulation and membrane entrapment can be used to combat the loss of material.

4.3. Experimental

4.3.1. Potentiometry

4.3.1.1. Materials

Platinum ribbon, 2mm width was obtained from Goodfellow (Cambridge, Cambs., UK). Glutathione (oxidised and reduced forms), Glutathione s-transferase, $NADP^+$, NADPH, c-DCE and t-DCE were purchased from Sigma-Aldrich (Poole, Dorset, UK). PCE was obtained from Fluka (Gillingham, Dorset, UK). Sodium Phosphate buffer solution (pH 7, 0.05 mol dm^{-3}) and TCE were from BDH Laboratory supplies (Poole, Dorset, UK).

4.3.1.2. Methods

Four two-electrode cells consisting of the varying analyte solutions and two platinum ribbon electrodes were set up on stirring plates. Magnetic stirrer bars were introduced to keep the mass transport in the cells even.

The cell compositions were as follows:

Cell 1: GSSG/NADPH/Reductase   Cell 2: GSSG/NADPH/
                                                                        Reductase/ PCE

Cell 3: GSSG/NADPH/   Cell 4: GSSG/NADPH/
                Reductase/TCE

The GSSG/NADPH/Reductase/t-DCE experiment was run singly in a second experiment.

131

One electrode from each cell was connected to a common wire and then grounded to 0V. These electrodes acted as pseudo-reference electrodes. The remaining electrode in each cell was connected to the inputs of a Molspin (Newcastle-upon-Tyne, UK) multi-input pH/mV meter. Computer control was achieved using Molspin SP1NA potentiometry software, and a reading was taken on average once every 1.1 seconds.

All potentiometric experiments were carried out using 0.001mol dm^{-3} GSSG, GSH and chlorinated ethenes. Glutathione reductase, where used, was present in equivalent units to reduce 0.001mol dm^{-3} GSSG. All solutions were made up in aqueous phosphate buffer (pH 7, 0.05mol dm^{-3}). Concentration dependence experiments were carried out by adding a series of concentrated aliquots (10^{-7} mol $\text{dm}^{-3} - 10^{-1} \text{mol dm}^{-3}$) of chlorinated ethenes to GSH.

4.3.2. Amperometry

4.3.2.1. Materials

All solution chemicals (Glutathione, chlorinated ethenes, enzymes etc.) were obtained from the sources listed above. Screen-printed PVC electrode substrates, which comprise a platinised carbon working electrode and an $Ag^+/AgCl$ reference electrode, were purchased from Cambridge Life Sciences, (Ely, Cambs., UK). Polyurethane Tecoflex SG80 was obtained from Thermomedics (Woburn, MA, USA). Dopamine (3-Hydroxytyramine), TTF, TCNQ and Glutathione Reductase were from Sigma-Aldrich (Poole, Dorset, UK). The plasticiser bis-(1-butylpentyl)adipate (BBPA), and the lipophilic additive potassium tetrakis-3,5-bis(trifluoromethyl)phenyl borate (KTPB) were from Fluka (Gillingham, Dorset, UK).

The TTF:TCNQ conducting salt complex was prepared as follows:

1) Weigh out equivalent (1:1) quantities of TTF and TCNQ.

2) Dissolve the TTF and TCNQ in separate portions of hot spectroscopic grade acetonitrile.

3) Mix the solutions. A black precipitate should form immediately.

4) Cover and cool overnight whilst stirring.

5) Filter over a vacuum, and wash with cold acetonitrile then diethyl ether.

6) Dry under vacuum.

4.3.2.2. Preparation of Screen Printed Electrodes

The screen-printed electrodes constructed were produced in batches of three in order to allow reproducibility to be tested. The various electrodes that were made are listed in the table below.

Table 4.1. Background and analytical electrodes constructed for amperometric studies of glutathione and chlorinated ethenes.

Electrode Type	Electrode Type
1) Blank Substrate	2) Blank Substrate with membrane
3) Dopamine **or** TTF:TCNQ Mediated	4) Dopamine **or** TTF:TCNQ Mediated with membrane
5) 1×10^{-4} mol dm^{-3} GSSG Reductase + NADPH, Dopamine **or** TTF:TCNQ Mediated	6) 1×10^{-4} mol dm^{-3} GSSG Reductase + NADPH, Dopamine **or** TTF:TCNQ Mediated, with membrane
7) 1×10^{-3} mol dm^{-3} GSSG Reductase + NADPH, Dopamine **or** TTF:TCNQ Mediated	8) 1×10^{-3} mol dm^{-3} GSSG Reductase + NADPH, Dopamine **or** TTF:TCNQ Mediated, with membrane

The screen-printed electrodes were prepared in accordance with the procedure
previously described by Kataky et al.[24]

(1) The surfaces of the working electrodes were cleaned by gently wiping
them with a lens cloth damped with deionised water.

(2) A 0.1 mol dm^{-3} solution of mediator (dopamine or TTF:TCNQ) was
prepared in ethanol, and 2µl of this solution was deposited on the
working electrode surface of each screen-printed substrate. The
solvent was allowed to evaporate at room temperature.

(3) Two solutions of glutathione reductase and NADPH were prepared in
sodium phosphate buffer (pH 7, 0.05 mol dm^{-3}), one at 1 x 10^{-4} mol
dm^{-3} equivalent, and one at 1 x 10^{-3} mol dm^{-3} equivalent.
Approximately 2µl of these solutions were deposited on screen-printed
working electrodes to form two sets of electrodes with differing
concentrations. The electrodes were then left to dry in the refrigerator
overnight (4°C).

(4) A thin film (2µl of solution) comprised of 44.8% w/w Tecoflex SG80,
54.6% w/w BBPA and 0.6% w/w KTPB (total solids 180mg) dissolved
in 3ml dry THF was cast over the enzyme layer on those electrodes
which required it. The electrodes were left overnight to allow the
solvent to evaporate, and stored in the refrigerator when not in use.

4.3.2.3. Methods

Screen-printed working and reference electrodes were as described above. The
auxiliary electrode was a platinum plate electrode, as previously employed.
Experimental control and data recording were achieved using an EG&G Princeton

Applied Research model 273 Potentiostat/Galvanostat and Model 270 computer

software. Such stirring as was required was provided by a magnetic stirrer bar.

All measurements were carried out at room temperature and atmospheric pressure,

within a Faraday cage to eliminate interference.

4.3.3. HPLC

Samples of GSSG, GSH, and GSH/Chlorinated Ethenes were submitted to the

Departmental Chromatography service to investigate the formation of end

products. All samples were dissolved in a phosphate buffer (0.3 mol dm^{-3} sodium

phosphate in 10% methanol solution) and run through a C_{18} column.

4.3.4. Electrospray Ionisation Mass Spectrometry

Electrospray Ionisation is a technique used to achieve soft ionisation of samples

for mass spectrometric analysis. At the injection port, a high voltage (typically

between 0.5KV and 2KV is applied across the sample, causing it to charge. The

sample physically destabilises as the charged particles begin to repel one another.

Once a critical level of charge is reached, the ionised sample is rendered aerosol.

Thus the liquid being injected is transformed to a 'spray' of micrometric droplets

which are attracted to the spectrometer's counter electrode.

Electrospray Ionisation Mass Spectrometry may be run in either positive or

negative charge modes, depending on the sample composition. In this case it was

run in positive mode to identify negatively charged matter.

Samples of GSH/TCE and GSH/PCE were submitted to the Departmental Mass

Spectrometry service to identify end products. The samples were prepared as

follows. GSH was dissolved in deionised water at 0.1mol dm^{-3} concentration, and made up to pH 7 using sodium hydroxide, then stored in a refrigerator. A TRIS buffer solution, pH 8.5, was then prepared and 0.001mol GSH and chlorinated ethene (PCE and TCE) were added. The solution was left to react at room temperature for thirty minutes, then diluted 1:10 in a 1:1 methanol/water solution to give final analyte concentrations of 0.0001mol dm^{-3}.

4.4. Results and Discussion

4.4.1. Potentiometry

4.4.1.1. Response to changes in concentration of TCE.

To determine whether or not a quantitative discernment of the presence of chlorinated ethenes could be attained, a solution of 10^{-3} mol dm^{-3} GSH was prepared in phosphate buffer (pH 7). TCE was then added in aliquots of concentrated aqueous solution or neat liquid, to a final volume of 5ml, and the change in potential was recorded (Figure 4.6). Since:

$$\text{TCE} \longrightarrow \text{TCE}^{\bullet} + Cl^{-} \qquad E_0 = 0.64V \text{ vs NHE} \qquad (10)$$

and

$$\text{GSSG} \longrightarrow \text{GS}^{-} \qquad E_0 = -0.24V \text{ vs NHE} \qquad (11)$$
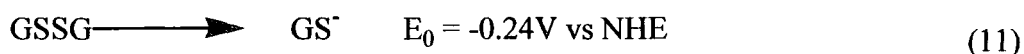
the reaction was expected to proceed very easily.

Figure 4.6. Response of the potentiometric system to TCE concentration.
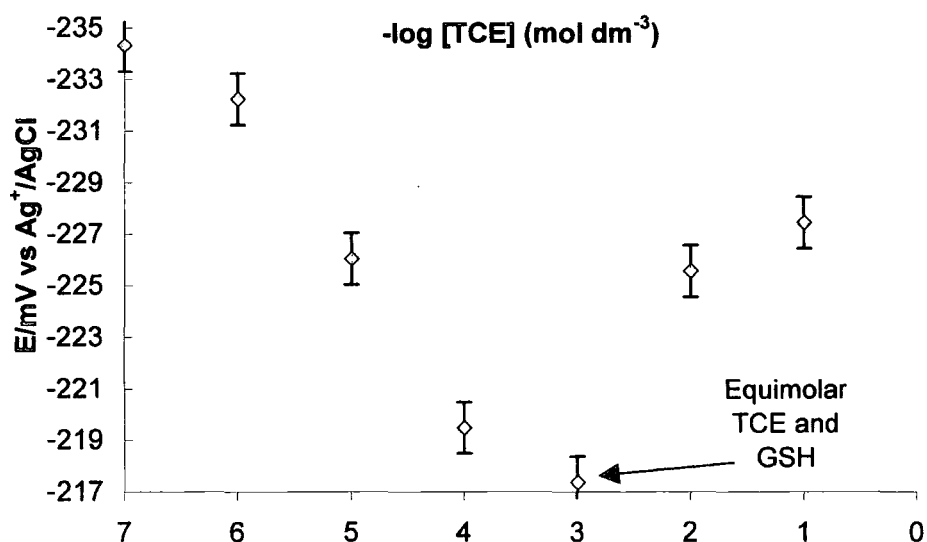
From the above graph, it can be seen that the response of the system alters with the change in TCE concentration. A titration end point is observed at equimolar concentrations, demonstrating that the reaction of GSH and TCE has a 1:1 stoichiometry. Where TCE is in excess, the response increases. This demonstrates that the sensitivity of such a system is well within the limits of detection required for environmental monitoring.

If $\Delta G = -nF\Delta E$ (see Chapter 1, Section 1.15.1), then the free energy of the reaction at equimolar concentrations is -20.93 KJ. Therefore the rate constant of the reaction ($\Delta G = -RT \ln K$) is approximately 2.182×10^{-4}.

4.4.1.2. Response of GSSG/Reductase to chlorinated ethenes.

The potential of cells containing solutions of GSSG, glutathione reductase and various chlorinated solvents at 10^{-3} mol dm^{-3} concentration was recorded over a period of time in ambient conditions until the readings stabilised to steady state, a process which took approximately twenty minutes (Figure 4.7).

The steady state potential of a GSSG/glutathione reductase solution was recorded as 47.4mV (Table 4.2). From the time plot and the steady state potentials it is immediately clear that reaction of the reduced glutathione with each chlorinated solvent produces a unique and reproducible reading (the experiment was repeated three times). This fulfils the basic aim of an online sensor system, in which the contaminant is extracted and separated on chromatography columns; the analytes are detectable, and differentiated, with a simple technique rather than utilising more complex methodologies such as electron capture detection.

Figure 4.7. Change in potential with time of solutions of GSSG and Glutathione Reductase with chlorinated solvents in equivalent concentrations.
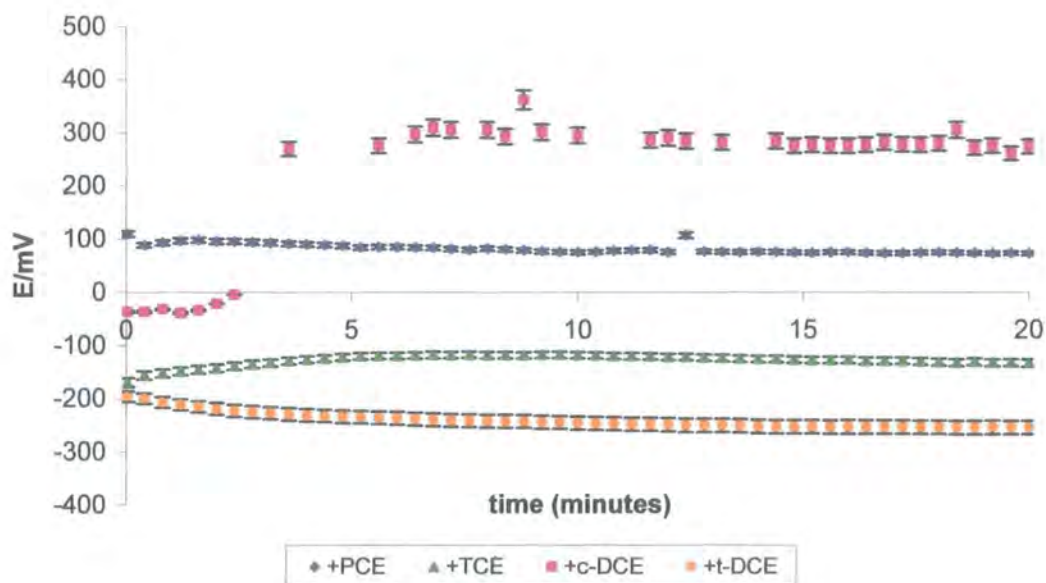
If we assume complete conversion of GSSG to GSH by the GSSG reductase enzyme, the absolute potentials reflect the depletion of the GSH concentration within the solutions. As was demonstrated in Section 4.2.4.1, the redox environment potential, E_{Env}, of a total conversion to GSH by the reductase would be -1090mV vs. NHE. A more positive potential than -1090mV therefore reflects a depletion in the quantity of GSH present.

Table 4.2. Steady state potentials for analyte solutions after 20 minutes.

Solution	Steady State Potential E (mV)
GSSG/reductase/NADPH	47.4 ± 1.1
GSSG/reductase/NADPH + PCE	88.5 ± 2.1
GSSG/reductase/NADPH + TCE	-155.8 ± 1.5
GSSG/reductase/NADPH + c-DCE	258.2 ± 1.2
GSSG/reductase/NADPH + t-DCE	-249.5 ± 1.5

From Table 4.2, we can see that the order of greatest change from the theoretical E_{Env} of -1090mV is as follows: + c-DCE > + PCE >GSSG/Reductase/NADPH > + TCE > + t-DCE.

Figure 4.8. Theoretical GSH plot showing % GSH present at a given potential.
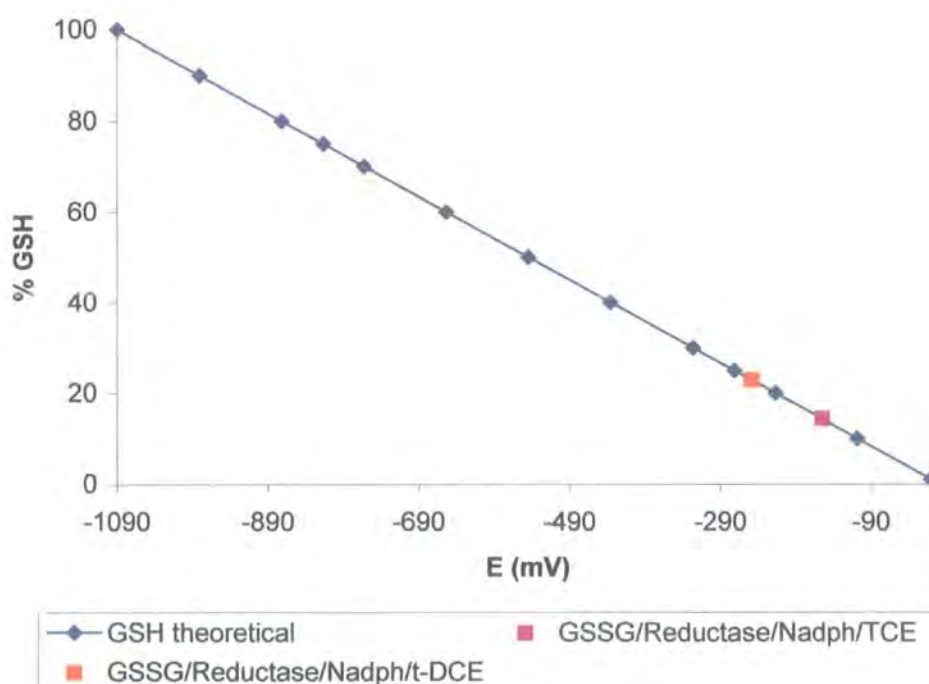
From figure 4.8, we see that the negative potentials of the TCE and t-DCE solutions reflect that 14% and 22% of available GSH remains in the respective

140

solutions. The more positive potentials of the PCE and c-DCE reflect absolute depletion of the GSH pool: the reaction in these cases has gone to completion. The fast reaction of c-DCE correlates well with the results shown in Chapter Two, where the c-DCE is seen to dechlorinate easily in the presence of the strong electron donor TDAE.

4.4.2 Amperometry

4.4.2.1. TTF:TCNQ electrodes

The initial set of SPE electrodes prepared utilised the conducting organic salt TTF:TCNQ as a mediator. The TTF:TCNQ donor-acceptor complex has a stable potential window of approximately 0.1V to 0.4V vs. SCE. Within this range it is capable of behaving as a conventional metallic electrode. Potentials negative of TCNQ's redox potential (0.13V vs SCE) cause the reduction of TCNQ$^-$ to TCNQ, an insoluble compound which fouls the electrode surface. Similarly, potentials positive of TTF's redox potential (0.3V vs. SCE) causes the oxidation of TTF$^+$, and again leads to electrode fouling, as well as the breakdown of charge transfer across the complex.

TTF:TCNQ was chosen initially as its behaviour is well documented and understood. It was expected that the salt would act as the electron mediator in the system (see Fig 4.4 above), allowing the transduction of charge between the electrode and the substrate, thereby enabling the sensor to function. However, when tested using Differential Pulse Voltammetry, the response of the TTF:TCNQ mediated electrodes was poor. Within the voltage window, no peaks were seen. A peak at –0.42V was observed, however the strongly negative potential cannot be accepted as valid data.

It is likely that the TTF:TCNQ failed as an electron mediator due to competition
to form donor-acceptor salts with TTF between TCNQ⁻ and GSH; since GSH has
a lower redox potential (-0.08V vs Ag/AgCl), its complexation with TTF is more
favourable. Also, no potential shift could be seen between a simple mediated
electrode and one with immobilised glutathione reductase (Fig. 4.9); such a
change in response is critical to the sensor function.

Figure 4.9. Response of two TTF:TCNQ modified electrodes (one with GSSG
reductase and GSSG s-transferase enzymes immobilised) to a solution of 0.1 mol
dm^{-3} GSSG.
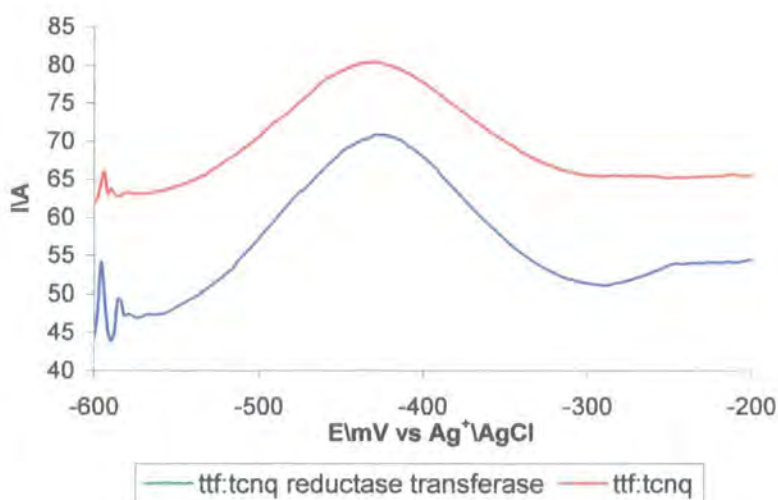
4.4.2.2. Dopamine mediated electrodes

The dopamine mediated electrodes proved to be much more successful. Figures
4.10 to 4.12 display differential pulse voltammograms detailing the background
stages of testing necessary for determination of response.

Figure 4.10. Voltammogram produced by a blank SPE substrate in phosphate buffer, displaying no response.
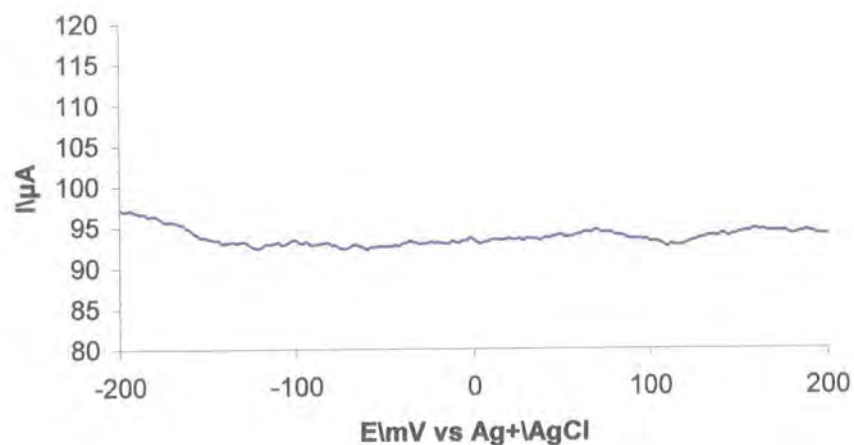
Figure 4.11 shows the peak given by a dopamine modified electrode, at an E_p of -224mV. This peak represents the transformation of dopamine to quinone, as shown in Figure 4.12.

Figure 4.11. Response of the dopamine modified electrode in phosphate buffer.
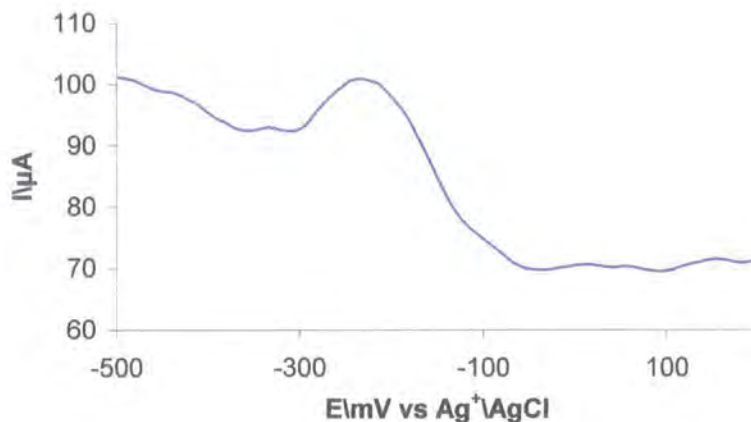
Figure 4.12. Oxidation of dopamine to quinone.
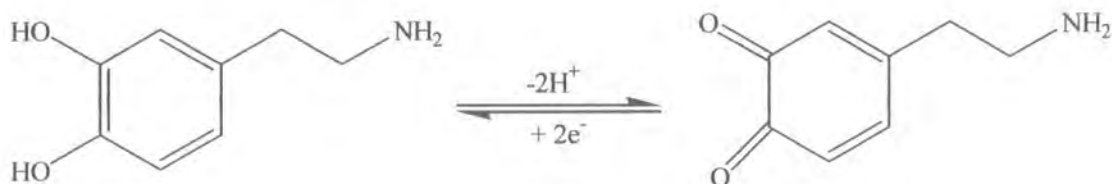
In Figure 4.13, after immobilisation of the GSSG reductase enzyme and the coenzyme NADPH, the background current becomes much higher and the peak due to the oxidation of dopamine has shifted marginally. The improved definition of the curve and peak show that the mediated system is functioning correctly, in accordance with the reaction scheme shown in Figure 4.14.

Figure 4.13. Dopamine/Reductase/NADPH electrode response in phosphate buffer.
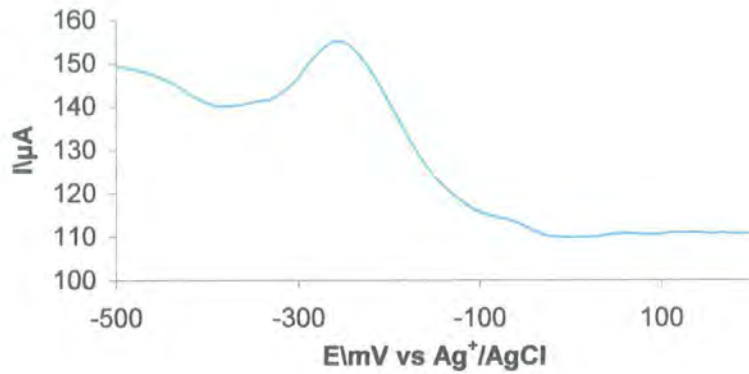
Figure 4.14. Mediated glutathione sensor reaction scheme.
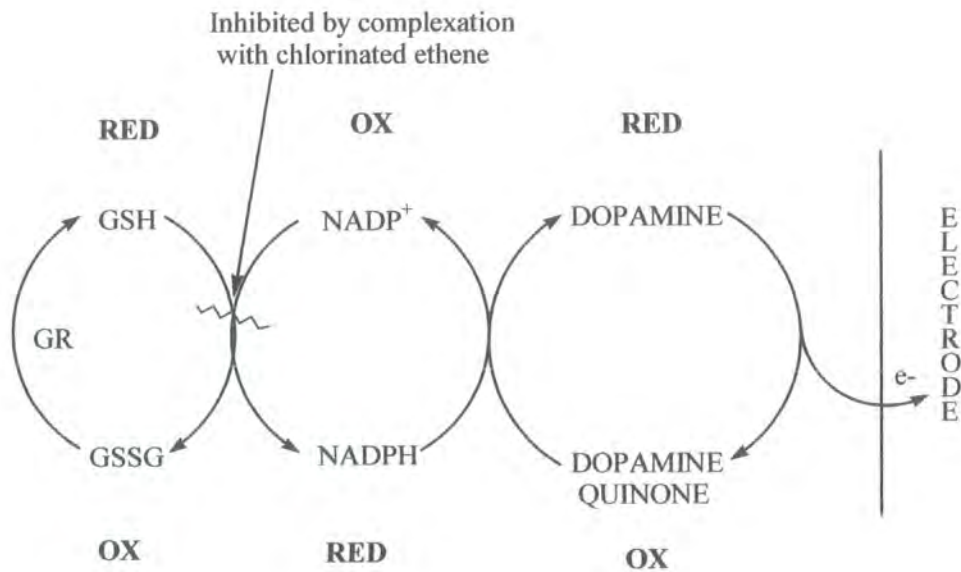
The electrodes were then tested in solutions containing GSSG and chlorinated ethenes. The results obtained are shown in Figure 4.15.

145

Figure 4.15. Response of a 10^{-3} mol dm^{-3} Dopamine/GSSG Reductase/NADPH electrode to analytes, 50 mV Pulse Height, 5mV s^{-1} Scan Rate.
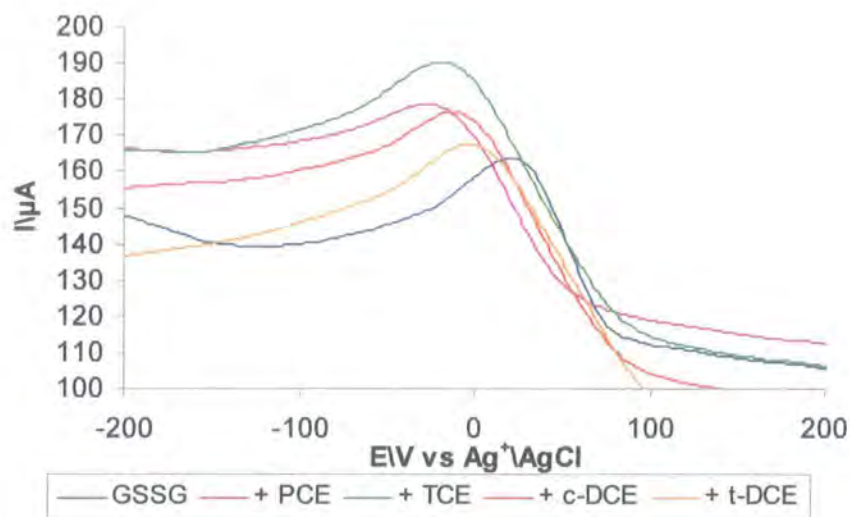
The peak potential displayed in the presence of GSSG alone is 23.99mV vs. Ag/AgCl, a considerably different response to that of the electrode in phosphate buffer. It is apparent from the voltammograms that each solution with chlorinated ethenes added also demonstrates a potential difference from the E_p of the GSSG solution. As complexation between GSH and the chlorinated ethenes occurs, the change in the system's chemistry results in a potential shift. These shifts are summarised in Table 4.3. These unique potential values demonstrate a clear selectivity for each individual chlorinated ethene.

The complexation gradually removes GSH from the reaction, resulting in the inhibition and eventual breakdown of the electrode response; this will reflect in decreased peak current with the passage of time.

Table 4.3. Potential shifts displayed by 10^{-3} mol dm^{-3} Dopamine/GSSG
Reductase/ NADPH electrode response to chlorinated ethenes.

Solution	Peak Potential E_p (mV vs. Ag^+/AgCl)	ΔE (mV)
GSSG	23.99 ± 1.19	
GSSG + PCE	-22.00 ± 1.10	-45.9
GSSG + TCE	-16.01 ± 0.8	-40.02
GSSG + c-DCE	-08.00 ± 0.4	-30.01
GSSG + t-DCE	1.99 ± 0.09	-22

Repetitive testing of the electrode batches found the potentials to be reproducible, and the current was found to decrease over time (data not shown). Although the electrodes modified with 10^{-4} mol dm^{-3} equivalent of GSSG reductase produced a response, the peak current was not high enough to give a clear indication of the presence of the chlorinated ethenes (data not shown).

Although the response of the electrodes modified with 10^{-3} mol dm^{-3} GSSG reductase was good, the issue of substrate leaching from the electrode (the loss of enzymes into solution, which destroys the sensor capability), was still to be investigated. The batches of electrodes covered with Tecoflex membranes were constructed and tested to ascertain whether or not a good response would be achieved through the membrane, which gives improved immobilisation of the substrate enzyme. The results of DPV carried out with Tecoflex membrane electrodes are shown in Figure 4.16.

Figure 4.16. Response of a 10^{-3} mol dm^{-3} Dopamine/GSSG Reductase/ NADPH/ Tecoflex membrane electrode to analytes, 50 mV Pulse Height, 5 mV Scan Rate.

Again, the GSSG alone displays the most positive shift, and the addition of chlorinated ethenes result in clearly discernible and individual changes in response. (Table 4.4.) The peak currents displayed are smaller than those of the electrodes with no Tecoflex membrane, indicating an inhibition of the reaction by the polymer film.

Table 4.4. Potential shifts displayed by 10^{-3} mol dm^{-3} Dopamine/GSSG Reductase /NADPH/ Tecoflex membrane electrode response to chlorinated ethenes.

Solution	Peak Potential E_p (mV vs. Ag$^+$/AgCl)	ΔE (mV)
GSSG	27.99 ± 1.19	
GSSG + PCE	-24.00 ± 1.2	-51.99
GSSG + TCE	-16.01 ± 0.8	-44.02
GSSG + c-DCE	-02.00 ± 0.01	-29.99
GSSG + t-DCE	-34.01 ± 1.70	-62.02

The addition of the glutathione s-transferase enzyme (an intracellular enzyme which facilitates the reaction of GSH with xenobiotic molecules) to the analyte solution was carried out to investigate if the response of the electrode could be further improved. However, DPV carried out with these electrodes elucidated that the additional enzyme only served to make the response less clear, as is evidenced in Table 4.5.
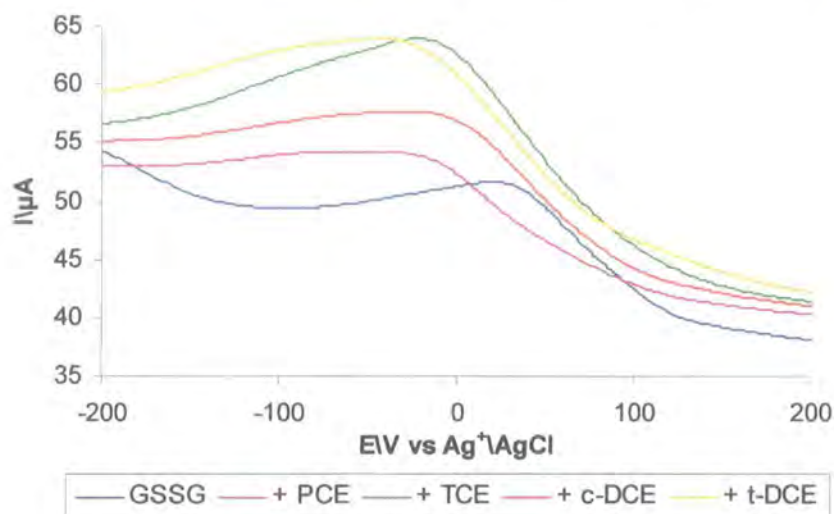
Table 4.5. Potential shifts displayed by 10^{-3} mol dm^{-3} Dopamine/GSSG Reductase/NADPH electrode response to chlorinated ethenes in the presence of glutathione s-transferase.

Solution	Peak Potential E_p (mV vs. Ag$^+$/AgCl)	ΔE (mV)
GSSG/Transferase	-6.00 ± 0.3	
GSSG/Transferase + PCE	-2.00 ± 0.1	-4
GSSG/Transferase + TCE	-2.00 ± 0.1	-4
GSSG/Transferase + c-DCE	-12.00 ± 0.6	-6
GSSG/Transferase + t-DCE	-16.01 ± 0.8	-10.01

As well as selectivity for the target compound, a viable biosensor must be able to detect at concentrations which are comparable to those found in the environment under study. Since chlorinated ethene concentrations in groundwater are typically between 10^{-3} mol dm^{-3} and 10^{-6} mol dm^{-3}, the electrodes' ability to sense PCE and TCE at these concentrations was investigated.

From the theory given in Chapter 1, Section 1.15.1, the concentration of a species in solution directly relates to the peak current, I_p, displayed in a voltammetric investigation; hence a change in concentration should be reflected as an increase or decrease of the peak current. Figure 4.17 shows the peak current readings obtained at varying concentrations for PCE.

Figure 4.17. Peak current vs. concentration of PCE, as measured by the 10^{-3} mol dm^{-3} Dopamine/GSSG Reductase/NADPH electrode.
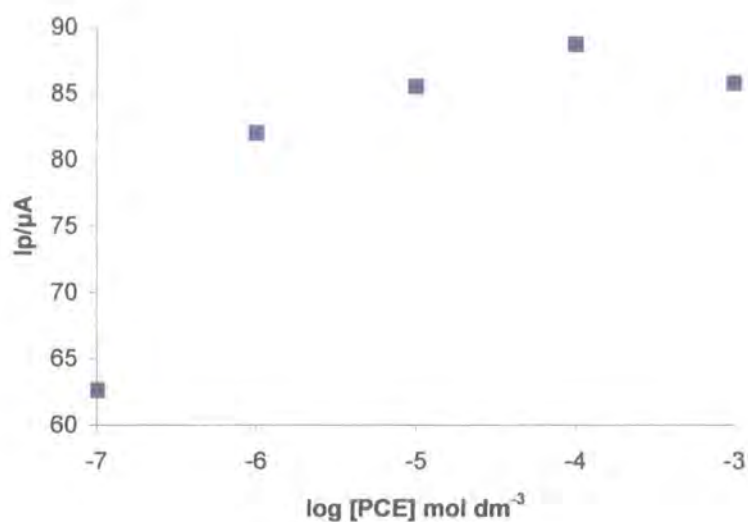
The graph shows that the electrode demonstrates an extremely sensitive response to the concentration of PCE present, particularly at lower concentrations. This is advantageous given that environmental pollution levels are most commonly measured in parts per billion (ppb), which equates to 10^{-6} mol dm^{-3} concentration. When tested against TCE, the electrode displayed a similar response, with greater sensitivity being displayed at low concentrations.

4. 4. 3. High Performance Liquid Chromatography

Samples of the oxidised and reduced forms of glutathione were submitted to the Departmental Chromatography service for HPLC analysis. Figures 4.18 and 4.19 show that GSH and its dimer have easily distinguishable retention times, 2.7 minutes and 3.6 minutes respectively.

Figure 4.18. HPLC trace of reduced glutathione (GSH), retention time 2.7 minutes.
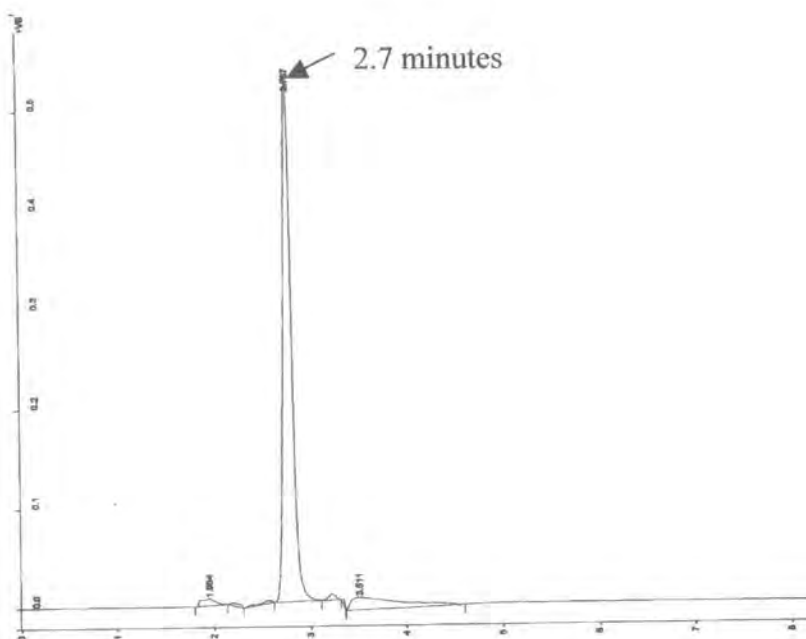
Figure 4.19. HPLC trace of oxidised glutathione (GSSG), retention time 3.626 minutes.
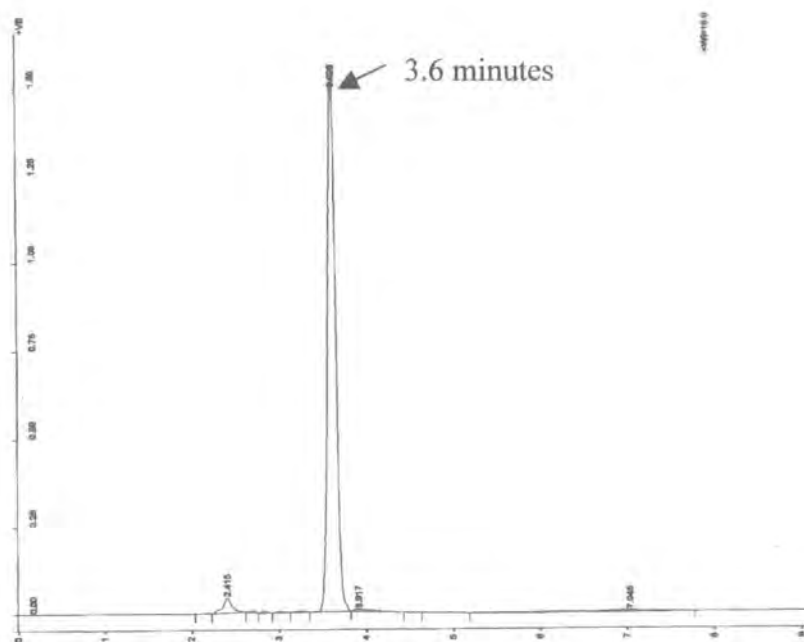
Samples of GSH with PCE and TCE were submitted to determine whether or not formation of an end product could be identified. In Figure 4.20, it can be seen that a peak with the retention time 3.2 minutes has formed, along with a second, smaller peak at 3.6 minutes. The latter corresponds to the presence of oxidised glutathione, which is unsurprising given that GSH is extremely unstable and tends to oxidise very quickly. The peak at 3.2 minutes presents the first evidence that adduct formation between the PCE and the GSH is occurring.

Figure 4.20. HPLC trace, GSH and PCE mixture.

3.2 minutes

3.6 minutes (GSSG)
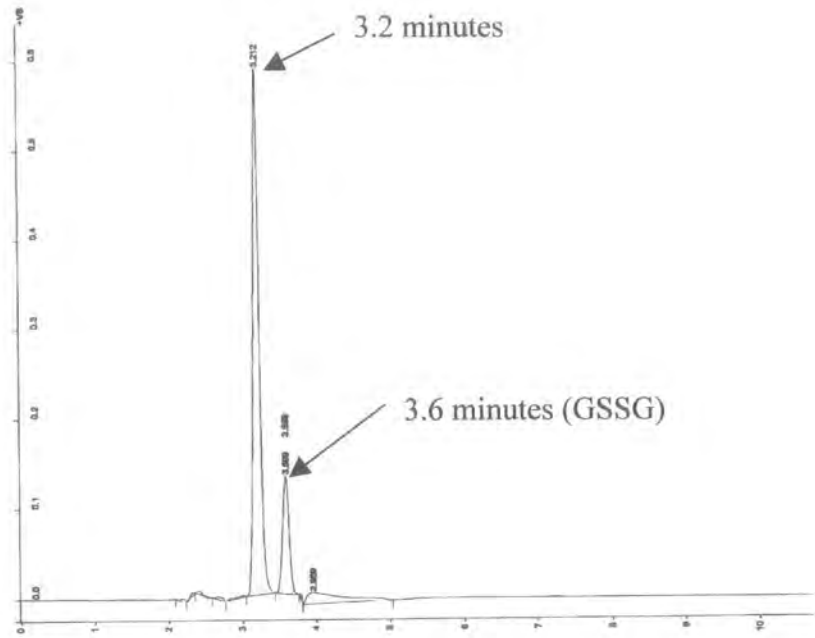
The mixture of GSH and TCE produced almost identical peaks (Figure 4.21) to those formed in the PCE/GSH solution, again indicating the formation of an adduct with residual GSH oxidising to GSSG.

Figure 4.21. HPLC trace of GSH and TCE mixture.
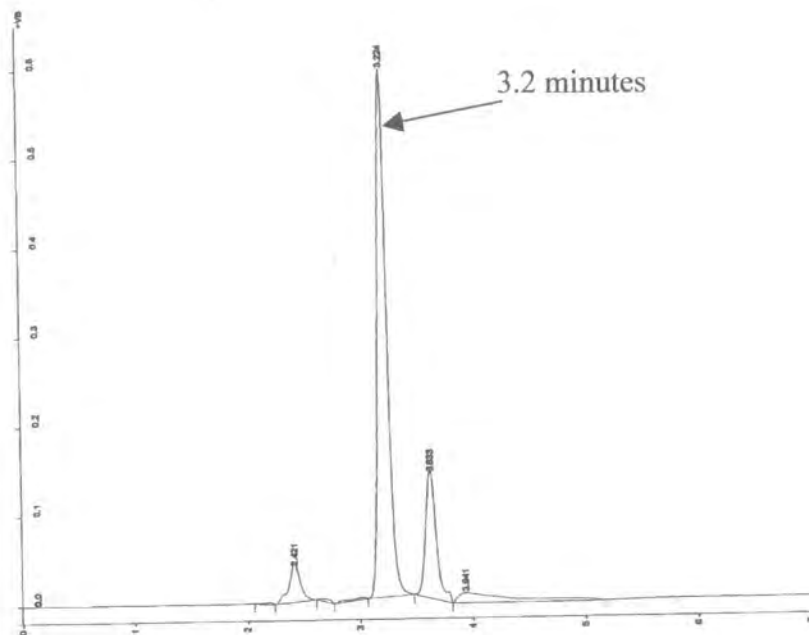
4.4.4 Electrospray Ionisation Mass Spectrometry

Positive mode Electrospray Ionisation Mass Spectrometry was carried out in conjunction with Liquid Chromatography in order to identify the adduct forming between GSH and the chlorinated ethenes as evidenced by the HPLC results. Samples of GSH/PCE and GSH/TCE were permitted time to react, and then analysed.

Figure 4.22 shows the mass spectra of an initial peak in the chromatographs of both the PCE/GSH and TCE/GSH solutions. The peak at 308.15 is GSH; 330.14 is GSH with Na attached. Similarly, 613.24 represents GSSG, where the GSH is oxidising in atmosphere, and 635.22 is the sodium salt of GSSG.

Figure 4.22. Mass spectra showing GSH, GSSG and their respective sodiated
forms.
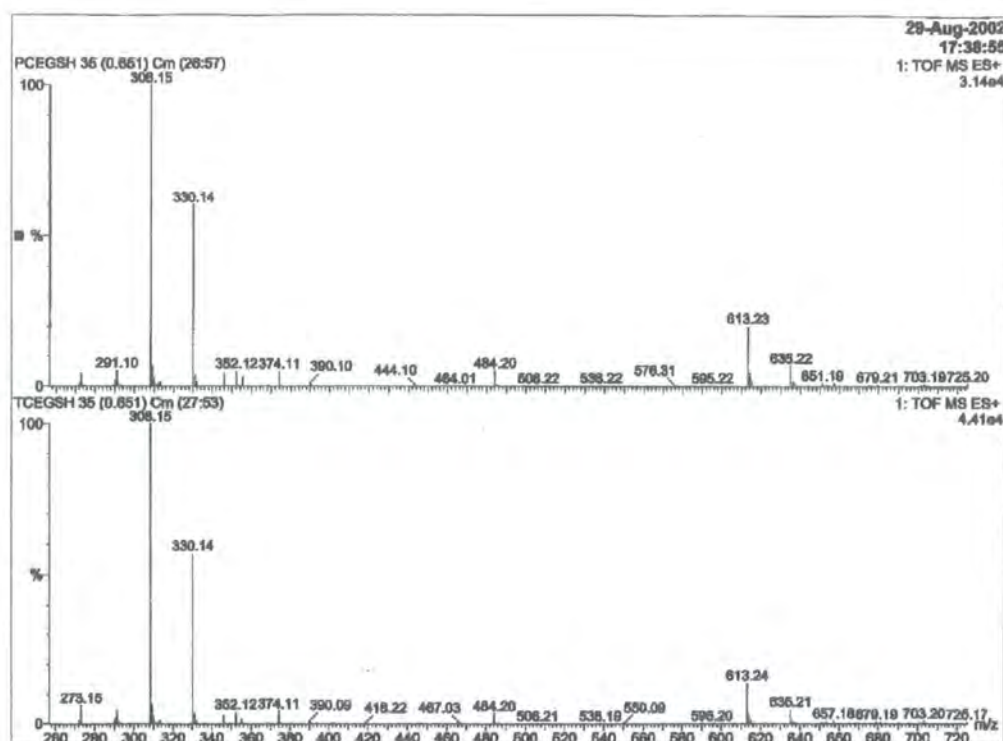
A second significant peak in the chromatograph at 4.15 minutes shows the
presence of two chlorinated compounds, characterised by the two atomic mass
unit separation of its isotopes. Both mass more than GSH (Figure 4.23). The mass
peak at 345.20 is GS-Cl (if the m/z of GSH is subtracted (308.15) the difference is
approximately 36, which can be accounted for by the presence of chloride (35.5)
and the loss of one H$^+$). Due to time constraints further analysis was not
undertaken.

Figure 4.23. Complexation between GSH and components of chlorinated ethenes.
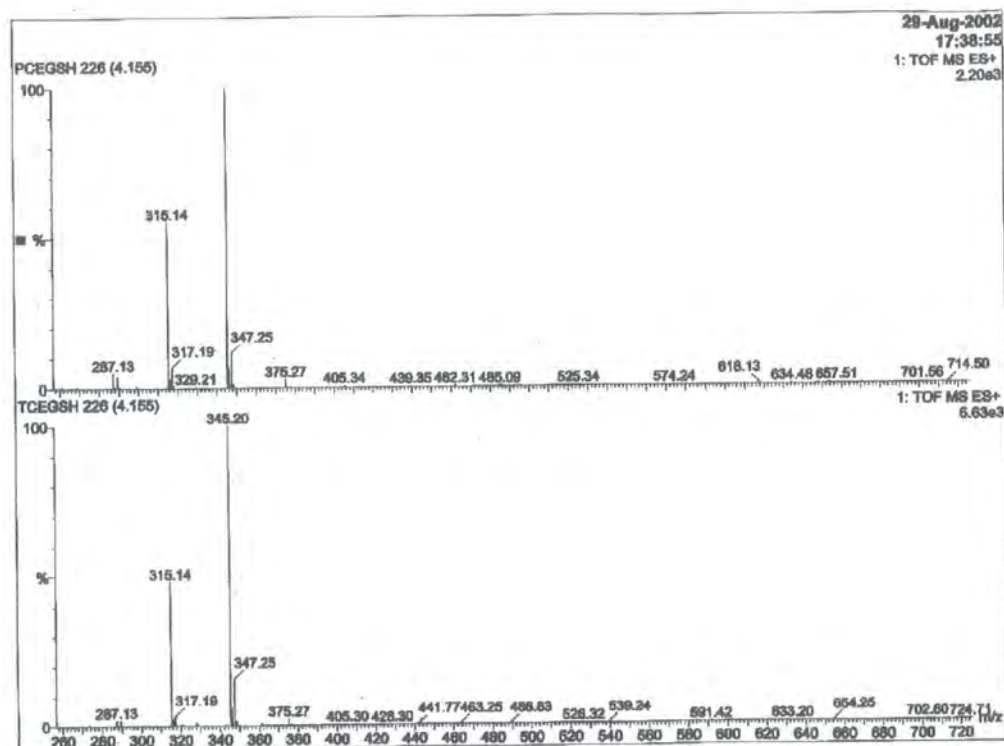
4.5. Conclusions

The objective of this research was to devise a preliminary sensor for the detection of chlorinated ethenes. Literature study suggested that the intracellular molecule glutathione, with its fundamental thiol functional behaviour, presented an attractive basis for the development of a biosensor capable of identifying individual chlorinated ethenes.

Potentiometric and amperometric systems were examined, and the following results were elucidated:

o   Based on calculation of the redox environment of the GSH/GSSG –

NADPH/NADP$^+$ redox couples, potentiometric differentiation of PCE,

TCE, c-DCE and t-DCE reacting with GSH could be achieved.

o   An amperometric system mediated by the conducting organic salt

TTF:TCNQ could not be used in conjunction with GSH.

o   Dopamine was found to be a suitable mediator, via its oxidation to

quinone.

⊕   An amperometric electrode with Glutathione reductase as the biosensing

element and NADPH as a cofactor was capable of being selective towards

each different chlorinated ethene, and operable at concentrations down to

10^{-6} mol dm^{-3}.

⊕   A Tecoflex membrane introduced to improve the immobilisation of the

enzyme substrate did not significantly impede the signal.

⊕   HPLC and mass spectrometric analysis showed that complexation between

GSH and chlorinated ethenes was occurring.

On this evidence, the glutathione redox system offers an excellent basis for the

development of a commercially viable sensor system for *in situ* chlorinated ethene

monitoring, an advance which could be of critical importance in devising more

efficient and cost-effective methods of pollution remediation.

REFERENCES

1. US Environmental Protection Agency, 40 CFR Part 136 Appendix A, Method 601 – Purgeable Halocarbons. http://www.epa.gov/OST/Tools/guide/601.pdf, accessed 24/06/01.

2. Schollhorn, A., Savary, C., Stucki, G., and Hanselmann, K.W., *Wat. Res.*, **1997**, 31, 1275 – 1282.

3. Ballapragada, B.S., Stensel, H.D, Puhakka, J.A., and Ferguson, J.F., *Environ. Sci. Technol*, **1997**, 31, 1728 – 1734.

4. Kao, C.M. and Prosser, J., *J. Hazard. Mat.*, **1999**, B69, 67 – 79.

5. Kuivenen, J., and Johnsson, H., *Wat. Res.*, **1999**, 33, 1201 – 1208.

6. O'Loughlin, E.J., Burris, D.R., and Delcomyn, C.A., *Environ. Sci. Technol.*, **1999**, 33, 1145 – 1147.

7. Leahy, J.G., and Shreve, G.S., *Wat. Res.*, **2000**, 34, 2390 – 2396.

8. Smatlak,, C.R., and Gossett, J.M., *Environ. Sci. Technol.*, **1996**, 30, 2850 – 2858.

9. Carr, C.S., and Hughes, J.B., *Environ. Sci. Technol.*, **1998**, 32, 1817 – 1824.

10. *Collins Concise Dictionary* (4th Ed.), **1999**, HarperCollins Publishers, Glasgow, 1351.

11. Jakusch, M., Mizaikoff, B, Kellner, R., and Katzir, A., *Sens. Actuators, B*, **1997**, 38-39, 83 – 87.

12. Acha, V., Meurens, M., Naveau, H., and Agathos, S.N., *Biotechnol. Bioeng.*, **2000**, 68, 473 – 487.

13. Maymo-Gatell, X., Chien, Y., Gossett, J.M., and Zinder, S.H., *Science*, **1997**, 276, 1568 – 1571.

14. Turner, A.P.F., Karube, I., and Wilson, G.S. (eds.), *Biosensors,* **1989**, Oxford Science Publications, Oxford, v.

15. Willner, I., and Katz, E., *Angew. Chem. Int. Ed.*, **2000**, 39, 1180 – 1218.

16. Clark, L.C. Jr., and Lyons, C., *Ann. N.Y. Acad. Sci.*, **1962**, 102, 29.

17. Xing, W., Ou, G.R., Jiang, Z.H., Ma, L.R.R., and Chao, F.H., *Anal.Lett.*, **2000**, 33, 1071 – 1078.

18. Naessens, M., Tran-Minh, C., *Anal. Chim. Acta*, **1998**, 364, 153 – 158.

19. Han, T-S, Kim, Y-C, Sasaki, S., Yano, K., Ikebukuro, K., Kitayama, A., Nagamune, T., and Karube, I., *Anal. Chim. Acta*, **2001**, 431, 225 – 230.

20. Lawrence, N.S., Davis, J., and Compton, R.G., *Talanta*, **2001**, 53, 1089-1094.

21. White, P. C., Lawrence, N.S., Davis, J., and Compton, R.G., *Electroanalysis*, **2002**, 14, 89 – 98.

22. Rodkey, F.L., *J. Biol. Chem.*, **1955**, 213, 777 – 786.

23. Schafer, F.Q., and Buettner, G.R., *Free. Radic. Biol. Med.*, **2001**, 30, 1191 – 1212.

24. Kataky, R., Dell, R., and Senanayake, P.K., *Analyst*, **2001**, 126, 2015 – 2019.

CHAPTER 5

Associated Studies and Further Work

5.1. Introduction

Not all investigation carried out over the course of the research period directly
relate to the main studies detailed in the preceding three chapters. However, these
additional experiments provided insight and evidences which are relevant to the
processes of dechlorination and detection of chlorinated ethenes, and will be
discussed below.

The further work described below is suggested as a means of advancing the
studies described in previous chapters towards the ultimate goal of the research
undertaken; the development of successful dechlorination and detection methods
for the remediation of chlorinated ethene pollution.

5.2. Associated studies

5.2.1. High Performance Capillary Electrophoresis

5.2.1.1. Theory of High Performance Capillary Electrophoresis

High Performance Capillary Electrophoresis (HPCE) is a separation technique based on the differences in solute velocities when they are exposed to an electric field as a solution is passed through a narrow capillary (usually less than 100µm in diameter). The driving force of the technique is the electroosmotic flow.

Electroosmotic flow (or EOF) is the bulk flow of the solution in the capillary: a result of the surface charge on the interior capillary wall, it is an outcome of the applied electric field on the solution's electrical double layer. In aqueous conditions, the walls of the capillary are negatively charged. In the instance of a fused silica capillary, anionic silanol groups form the capillary wall, and cations in the solution build up a diffuse double layer to maintain a neutral charge balance. This creates a potential difference at the capillary wall, termed the zeta potential. When a voltage is applied across a capillary, the cations in the double layer are attracted to the cathode; since the cations are solvated, they drag the bulk solution with them.

EOF can be expressed either in terms of velocity or mobility:

$$v_{EOF} = (\varepsilon\zeta / \eta)E$$

(1)

162

$$\mu_{EOF} = \left(\varepsilon \zeta / \eta \right)$$

(2)

Where V_{EOF} = velocity (m s^{-1})

    μ_{EOF} = EOF mobility (unit)

    ζ = zeta potential (V)

    ε = dielectric constant

The zeta potential is determined by the surface charge at the capillary wall. Since
the other variables in the equations are constant, it can be said that the zeta
potential governs the velocity of the EOF. The surface charge, in turn, is pH
dependent, therefore it can be seen that the simplest way to control the EOF of a
given electrolyte is to alter the pH. At high pH, the silanol groups in silica
become predominantly deprotonated, thus increasing the surface charge and zeta
potential, resulting in an increased EOF. Other methods of adjusting the EOF
include altering the ionic strength (i.e. the electrolyte concentration), varying the
applied electric field, or using buffer additives to coat the capillary walls; adding
cyclodextrins to achieve enantiomeric separation is an example of the latter.

The above discussion shows that EOF causes movement of species in a solution;
this effect is not selective. EOF will cause all species solvated in a given sample
to move towards a cathode, regardless of their charge. Separation in the system is
achieved by the relative migration velocities generated by EOF and the species'
electrophoretic mobility. Cations will travel at the combined velocity of their
electrophoretic attraction and the EOF; neutral particles at the EOF velocity;
anions at EOF minus their electrophoretic attraction.

5.2.1.2. Experimental materials and methods

The work was carried out using a Waters Quanta 4000 Capillary Electrophoresis system. The detector was an ultraviolet fluorescence lamp, set to detect inverse signals at either 214nm or 284nm. The system was manually controlled, and output was registered on a Perkin Elmer (Wellesley, MA, USA) R50 recorder, driving at 10mm/min.

The capillary was made of fused silica, with an internal diameter of 75μm and a total length of 60cm.

All samples were made up in MilliQ deionised water. C-DCE and t-DCE were purchased from Sigma-Aldrich (Poole, Dorset, UK). All other chemicals were stocked in the laboratory in Warsaw.

The electrolyte used for separation was 50ml (aq), 0.02 mol dm^{-3} $Na_2B_4O_7$, 0.02 mol dm^{-3} Carboxymethyl-β-cyclodextrin, pH 7.5. Experimental parameters were varied to elucidate optimum separation conditions.

5.2.1.3. Results

Initial separation of a mixed sample of the *cis-* and *trans-* isomers was achieved,
and calibrated by running separate samples of c-DCE and t-DCE. A successful
separation is shown in Figure 5.1. C-DCE's initial retention time was 7.85
minutes, and t-DCE's 7.35 minutes. Parameter variation to find optimum
conditions is detailed in Table 5.1. Optimum conditions were found to be; 15s
injection, 15KV voltage, 0.01mol dm^{-3} sample concentration, at instrument
sensitivity 0.02.

Table 5.1. Optimisation of *cis-/trans-*dce separation using HPCE

Injection time (s)	Concentration (mM)	Voltage (KV)	Sensitivity	Retention time (trans/cis) (mins)
5	5	15	0.02	7.35/7.85
10	10	15	0.02	7.20/7.85
5	10	15	0.01	7.10/7.70
5	10	20	0.01	3.75/4.10
5	10	10	0.01	13.25/14.50
15	*10*	*15*	*0.02*	*7.10/7.65*

Figure 5.1. *Cis/trans*-DCE isomer separation by capillary electrophoresis.
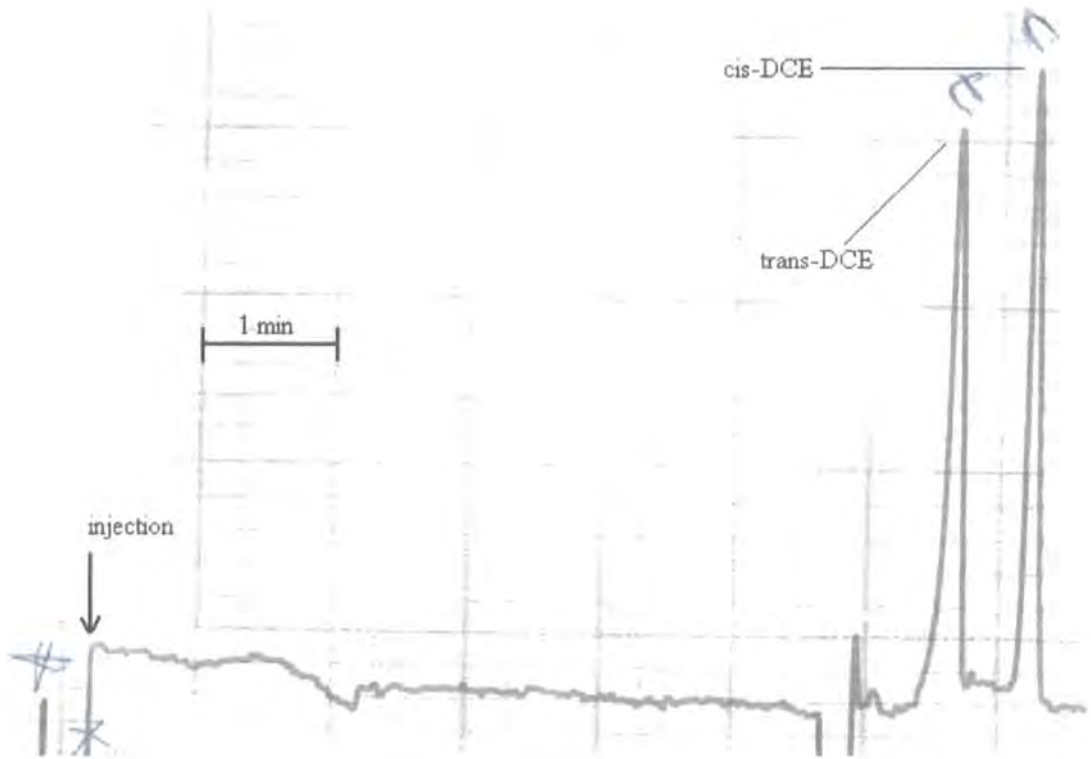
Due to time constraints, further experimentation on the potential use of HPCE as a detection technique for Chlorinated Ethenes was not possible. However, given the ease with which separation of the Dichloroethene isomers was achieved, it is likely that distinguishing the more highly chlorinated molecules PCE and TCE would be relatively simple. Thus, HPCE could prove to be a valuable tool in the development of in-situ sensor systems, in particular those microfluidic systems such as Lab-on-a-Chip. Or, with its lack of requirement for sample pre-treatment, HPCE could offer an attractive alternative to Headspace Gas Chromatography as a laboratory-based identification technique.

5.2.2. Dechlorination by a Sulphate Reducing Bacterial Consortium

5.2.2.1. Introduction

As was described in Chapter 3, sulphate reducing bacteria are capable of dechlorinating chlorinated ethenes under anoxic conditions in the environment[1,2,3], as a fortunate side-effect of their metabolic systems[4]. A preliminary experiment to investigate the possibility of utilising bacteria in a remediation system was undertaken, to determine if environmental conditions could be simulated in the laboratory.

Four sets of batch samples (PCE, TCE, *cis*-DCE and *trans*-DCE) were set up in serum bottles to simulate environments with five differing substrate compositions under sulphate reducing conditions. Each sample was made up according to the following format:

- 100ml MilliQ water
- 13mmol dm^{-3} Na_2SO_4(aq) solution
- 5x10^{-3}mmol dm^{-3} Chlorinated ethene
- 2.5mmol dm^{-3} Organic substrate (as detailed below)
- 10ml Bacterial culture

The recipe for the bacterial culture, which was obtained from L.A. Mason of the School of Engineering, is shown in the table below.

Table 5.2. Constituents of nutrient media for sulphate reducing bacterial culture.

Constituent	Concentration (mol dm^{-3} unless stated)
KH_2PO_4	3.6×10^{-3}
NH_4Cl	18×10^{-3}
Na_2SO_4	31×10^{-3}
$CaCl_2.6H_2O$	2×10^{-4}
$MgSO_4.7H_2O$	2×10^{-4}
Yeast (Marmite ™)	1g/l
$FeSO_4.7H_2O$	1.4×10^{-5}
$HOC(CO_2Na)(CH_2CO_2Na)_2.2H_2O$	1×10^{-3}
Methanol	0.2
Groundwater	500ml/L

The bacteria in the culture were primarily sulphate reducing species, but since the culture was grown from a real environmental source rather than under laboratory conditions, other unidentified strains of bacteria may have been present.

Sodium sulphate, a redox-sensitive compound, was added in solution to the batch samples to simulate sulphate reducing conditions. To determine whether or not this was successful, a control bottle with no sodium sulphate (other than that present in the bacterial culture) was also prepared.

The five different substrates chosen for use were TDAE, Na DL-Lactate, Molasses, methanol, and methanol with alcohol dehydrogenase (ADH) (in 1:1 ratio). TDAE was chosen in keeping with the work reported in Chapter 2. Molasses, Na DL-Lactate and methanol were selected as they have been utilised in other studies[5, 6]. The addition of ADH, along with a coenzyme, NAD$^+$, to the second methanol bottle was intended to facilitate the release of molecular hydrogen, as shown in the diagram below (Fig 5.2).

Figure 5.2. Reaction mechanism of alcohol dehydrogenase, for ethanol.

$$H_3C-\underset{\underset{H}{|}}{\overset{\overset{H}{|}}{C}}-OH \ + NAD^+ \xrightarrow[]{\begin{array}{c}\text{Alcohol}\\\text{Dehydrogenase}\end{array}} H_3C-\overset{\overset{O}{\|}}{CH} \ + NADH$$

$$H^+$$
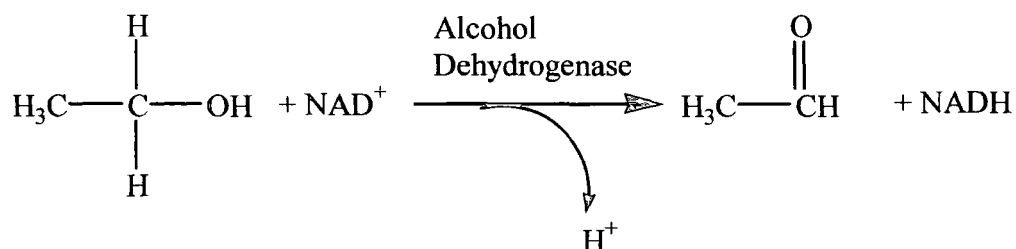
5.2.2.2. Experimental materials and methods

PCE, c-DCE t-DCE, Na DL-Lactate, NAD^+, Alcohol dehydrogenase and TDAE were purchased from Sigma-Aldrich (Poole, Dorset, UK). TCE was from BDH (Lutterworth, Leics, UK). All other chemicals were taken from pre-existing laboratory stocks. Bacterial culture was supplied by the School of Engineering, University of Durham.

The batch samples were mixed together and then purged for 15 minutes with nitrogen to remove all oxygen, before being sealed with rubber septa and aluminium crimp caps. The bacterial culture was then injected with a syringe, and the bottles were stored in the dark at room temperature, and left to develop.

Chloride and sulphate ion analysis was carried out on a Dionex (Sunnyvale, CA, USA) DX-120 Ion Chromatograph with an electron capture detector. The eluent was 3mmol dm^{-3} NaOH.

5.2.3. Results

5.2.3.1. Physical Observations

After four days, all batch samples showed visual evidence that reactions had taken place. Black precipitate had formed in varying quantities in all bottles containing TDAE, methanol, methanol/ADH, and Na DL-Lactate as substrates. The bottles utilising a molasses substrate had precipitated a white solid (Fig. 5.3.).

Figure 5.3. Photograph of t-DCE batch samples displaying precipitation of matter.

Visual inspection of the sample bottles showed the most precipitation of solids under all substrate conditions occurred in batch order TCE >*trans*-DCE > *cis*-DCE> PCE. The control bottle, where no sodium sulphate solution was present, showed no precipitation at all.

In terms of electron donor type, the sample bottles containing TDAE consistently produced the greatest quantity of black precipitate, again determined by visual inspection. The order of effectiveness of the electron donors in producing black precipitate was as follows: TDAE > Na DL-Lactate > Methanol/ADH > Methanol.

The molasses substrate produced an apparently consistent amount of white precipitate regardless of the type of chlorinated solvent present.

5.2.3.2. Ion Exchange Analysis

Aliquots of analyte mixture from each batch sample were analysed for both chloride and sulphate content. The results are shown in the tables below.

Table 5.3. PCE batch samples: chloride and sulphate content

Substrate	[Cl⁻] (mmol dm⁻³)	[SO₄²⁻] (mmol dm⁻³)
PCE/Methanol	1.72	3.26
PCE/Methanol/AdH*	2.34	4.36
PCE/Na DL-Lactate	2.59	4.45
PCE/TDAE	2.70	15.46
PCE/Molasses	3.63	11.97

---

* Alcohol Dehydrogenase Enzyme

Table 5.4. TCE batch samples: chloride and sulphate content

Substrate	[Cl⁻] (mmol dm⁻³)	[SO₄²⁻] (mmol dm⁻³)
TCE/Methanol	1.80	2.10
TCE/Methanol/AdH	1.57	2.64
TCE/Na DL-Lactate	1.55	5.27
TCE/TDAE	1.77	12.67
TCE/Molasses	3.09	12.77

Table 5.5. c-DCE batch samples: chloride and sulphate content

Substrate	[Cl⁻] (mmol dm⁻³)	[SO₄²⁻] (mmol dm⁻³)
c-DCE/Methanol	1.55	3.14
c-DCE/Methanol/AdH	1.86	4.13
c-DCE/Na DL-Lactate	1.60	6.09
c-DCE/TDAE	1.72	12.21
c-DCE/Molasses	2.98	11.93

Table 5.6. t-DCE batch samples: chloride and sulphate content

Substrate	[Cl⁻] (mmol dm⁻³)	[SO₄²⁻] (mmol dm⁻³)
t-DCE/Methanol	1.49	3.06
t-DCE/Methanol/AdH	1.55	2.40
t-DCE/Na DL-Lactate	1.80	5.73
t-DCE/TDAE	1.72	12.50
t-DCE/Molasses	3.27	12.93

It can be seen from the data that the production of sulphate by the bacteria is, in all cases, at least twice that of chloride, and is especially prolific in samples where TDAE and molasses are the substrates. For a sulphate-metabolising bacterial species, these results are not unexpected, however the concentration of chloride produced is significant. Again, this is especially the case in the presence of molasses. The chloride concentrations show that the sulphate-reducing bacterial consortium is capable of dechlorinating the target compounds PCE, TCE, c-DCE and t-DCE.

The results of the batch sample tests show that environmental redox conditions can be successfully simulated in the laboratory. Sulphate-reducing bacteria were found to dechlorinate chlorinated ethenes, but not to a degree great enough to be a viable base system for an enhanced dechlorination or detection system. Molasses was shown to be an effective substrate for bacterial processes.

5.3 Future Work

Further work on various aspects of the research presented in this and previous chapters would allow further progress towards optimised techniques for both remediation and dechlorination of chlorinated ethenes.

5.3.1. Vitamin B_{12} as an aid to remediation

Vitamin B_{12} was shown to be capable of significant levels of dechlorination (circa 70%) in preliminary electrochemical experiments. Further work to optimise cell parameters, electrochemical conditions and monitoring techniques could render an efficient, cheap and sustainable method for abiotic dechlorination.

5.3.2. Glutathione sensor systems

The glutathione based sensor systems described in Chapter 4 offer excellent scope for a reliable and cheap biosensor for on site use. The potentiometric system could be of potential use as a sensing component if integrated into a flow injection analysis system, particularly in microfluidic systems such as Lab-on-a-Chip. The amperometric system requires further work to elucidate the optimum electrode substrate and enzyme immobilisation in order to be developed into a viable disposable electrode for *in situ* detection and monitoring systems. Tests on real-life contaminated samples are also a requisite study prior to any field deployment of such a system.

5.3.3. HPCE detection of chlorinated ethenes

Separation of the cis-/trans- DCE isomers was achieved with relative ease. If PCE and TCE were to prove similarly distinguishable, High Performance Capillary

174

Electrophoresis would offer a fast, cost-effective alternative to Headspace Gas Chromatography, requiring little if any sample pre-treatment.

REFERENCES

1. El Fantroussi, S., Naveau, H., and Agathos, S.N., *Biotechnol. Prog.*, **1998**, 14, 167 – 188.

2. Häggblom, M.M., *FEMS Microbiol. Ecol.*, **1998**, 26, 35 – 41.

3. Häggblom, M.M., Knight, V.K., and Kerkhof, L.J., *Environmental Pollution*, **2000**, 107, 199 – 207.

4. Holliger, C., Wohlfarth, G., and Diekert, G., *FEMS Microbiol. Rev.*, **1999**, 22, 383 – 398.

5. Ferguson, J.F., and Pietari, J.M.H., *Environ. Pollut.*, **2000**, 107, 209 – 215.

6. Boopathy, R., Kulpa, C.F., Manning, J., Montemagno, C.D., *Bioresource Technology*, 1994, **47**, 205 – 208

Conclusions

The purpose of this research was to investigate the possibility of development of remediation and detection systems for chlorinated ethene pollution in the environment utilising electrochemical techniques.

Optimisation of existing remediation technology requires advancement in the fields of detection and abiotically enhanced dechlorination. It was postulated that in order to achieve such advances, understanding of the mechanisms of dechlorination would be required.

An electrochemical study utilising tetrakis(dimethylamino)ethylene (TDAE) as an electron donor confirmed that a donor-acceptor complex forms between TDAE and tetrachloroethene. It also showed that trichloroethene and *cis*-dichloroethene can be dechlorinated by accepting electrons from a donor such as TDAE, resulting in the removal of their chlorines, with the most positive halogen being removed first.

Once the mechanistic study was complete, and investigation of a potential abiotic dechlorination method was undertaken. Vitamin B_{12} (cyanocobalamin) and cobalt chloride ($Co(II)Cl_2$) were chosen due to the active role of superreduced cobalt (I) in the dehalorespiratory bacterial dehalogenase enzyme.

$Co(II)Cl_2$ was seen to dechlorinate trichloroethene in the presence of a hydrogen source (in this case molasses) when interrogated electrochemically. However, in a scaled-up bulk electrolysis, Vitamin B_{12} was found to be approximately ten times as effective as $Co(II)Cl_2$, achieving circa 70% dechlorination of trichloroethene in an un-optimised system. With further study, an environmentally acceptable remediation system could be developed from this data.

177

In order to investigate the furtherance of chlorinated ethene detection, it was deemed that a form of *in situ* sensor would be most beneficial to remediation strategy, as current practice involves sample removal for laboratory-based analysis. The thiol functionality and redox properties of the intracellular molecule glutathione and its reductase enzyme offered scope for the formulation of a biosensor which could fulfil the requisite criteria for a simple, accurate detection system.

Potentiometric strategy based on Nernstian response and redox environment calculations demonstrated successful detection of all four chlorinated ethenes under study. Each chlorinated ethene responded with a differentiated and unique value which allows for immediate identification. The potentiometric data also provided evidence of depletion of the GSH concentration in the solution, indicating complexation with the chlorinated ethenes was occurring: this was confirmed by HPLC and Mass Spectrometry.

An amperometric system employing dopamine as an electron mediator (via its oxidation to quinone) and glutathione reductase (co-factor NADPH) as its biosensing element demonstrated detection and species selectivity for the chlorinated ethenes under study at concentrations ranging from 10^{-3} mol dm^{-3} to 10^{-6} mol dm^{-3}. These concentrations cover the typical range of environmental pollution levels, hence it can be concluded that this biosensing system presents an extremely attractive option for the design of a practical field-capable detection system. Optimisation of the enzyme substrate immobilisation by application of a protective membrane did not significantly inhibit the sensor's response, but further optimisation of materials and transduction will be critical steps in any further development.

In conclusion, the results summarised above should provide a sound basis of mechanistic understanding of chlorinated ethene dechlorination. A rudimentary remediation method has been hypothesised and tested with a 70% degree of

success, and a sensor system capable of detecting chlorinated ethenes has been successfully designed and tested, demonstrating selectivity for its target analytes at concentrations relevant to environmental pollution levels. Electrochemical methods for the dechlorination and detection of chlorinated ethenes offer an attractive alternative to existing methodologies of environmental remediation.

APPENDIX 1: Biological Methods

Preparation of plates for bacterial count

Solidified media in a Petri dish is a widely used method of culturing organisms for growth counts in biological sciences.

1) Prepare Media as recommended for the species, then add agar as a gelling agent. Heat until the agar is dissolved.

2) Cool the molten media to between 45°C and 60°C to decrease the amount of water vapour condensation that will occur in the Petri dishes.

3) Open the media container, sterilising the neck with a Bunsen flame; keep hold of the cap.

4) Lift the cover of the Petri dish with the hand holding the cap. Keep the cover as close to the dish as you can, tilted away from the media container mouth.

5) Pour about 20ml (a bit more than you need to cover the bottom of the dish) into the dish, replace the cover and swirl the dish on the bench to give an even distribution.

6) Disperse any air bubbles on the surface of the plate by passing a Bunsen burner over it.

7) Allow to harden on a level surface, with the cover on.

8) Store inverted (to prevent contamination form water vapour) in a cool, dark place.

Preparation of plate cultures for cell counts

1) Sterilise eight 10ml vials, ten pipettes, and a culture loop, and prepare eight agar plates as described above.

2) Fill each vial with 9ml of recommended bacterial nutrient media.

3) From the original culture, take a 1ml aliquot and dilute it in the first vial. This will dilute the culture by a factor of ten.

4) Using a fresh pipette, transfer 1ml from vial one into vial 2, achieving a further x10 dilution. Repeat for each vial, remembering to use a fresh pipette each time, until the desired number of dilutions (typically between six and eight) have been carried out.

5) Beginning with the most diluted vial, take a 1ml aliquot and deposit it onto an agar plate. Spread the solution over the agar surface and then cap the Petri dish. Repeat with increasingly concentrated solutions, until a plate has been prepared for each dilution.

6) Incubate the plates in darkness for 24 hours at 25°C

7) Open the plates, and choose the one which has a countable number of colonies (between 20 and 200). Note its dilution, and calculate from the colonies present the growth rate of the bacteria.

APPENDIX 2: List of Conferences and Lecture Courses attended

CONFERENCES

Europt(r)ode V – Opt(r)ode 2000. 5th European Conference on Optical Chemical Sensors and Biosensors. Lyon Villurbane, 16th –19th April, 2000.

RSC New Directions in Electroanalysis. Salford University, 10th – 15th April 2001.

LECTURE COURSES

Separation Methods. Oct – Dec 1999. Dr. G. Sandford.

Electrochemical Methods. Jan – Mar 2000. Dr. R. Kataky

Hydrology (Dept of Engineering). Oct 1999 – Mar 2000. Dr. S. White.